White Volta Water Retention

Thesis on the Impact of Constructing Multiple Small Dams on Floods and Sedimentation in Northern Ghana

V. Kingma

Witteveen+Bos
TU Delft
African Water Corridor

Cover photo: the White Volta River near Daboya. As there is no bridge to connect the two roads, people and products cross the river using canoes. The picture was taken during a field visit by Jasper Schakel.

White Volta Water Retention

thesis on the impact of constructing multiple small dams on floods and sedimentation in northern Ghana

by

Vera Kingma

to obtain the degree of Master of Science
at the Delft University of Technology

Student number:	4411722	
Project duration:	Februari, 2021 – November, 2021	
Thesis committee:	Prof. dr. ir. Nick van de Giesen	TU Delft, chair
	Dr. ir. Olivier Hoes	TU Delft
	Dr. Markus Hrachowitz	TU Delft
	Prof. Dr. ir. Susan Steele-Dunne	TU Delft
	Ir. Michel Zuijderwijk	Witteveen+Bos
	Ir. Jasper Schakel	African Water Corridor

TU Delft

Preface

This thesis is the final work to obtain my Master of Science in Civil Engineering at Delft University of Technology. During the last three years, I have specialised in both Water Management and Environmental Science. Within these tracks, I have explored the fields of water resources management, modelling techniques, meteorology and climate change. Together, the tracks formed a good basis on which I was able to perform this research. Besides the help from my supervisors at Delft University of Technolgy, I collaborated with the African Water Corridor and Witteveen+Bos. The research explores the impact of constructing multiple small dams in the White Volta River on flood risk and sedimentation. This subject was proposed by the African Water Corridor as a potential project. My interest in environmental modelling and development projects made that I was excited to dedicate the last eight months to this research.

During this research, I was supported by a lot of different people. I would like to acknowledge those who have helped me improve and finish this research. First of all, I would like to thank Jasper Schakel from the African Water Corridor for setting up the project, helping me define the research and connecting me to Witteveen+Bos. And later, as project coordinator, for helping me collect data from different institutions in Ghana. Secondly, I would like to thank Witteveen+Bos, and especially Michel Zuijderwijk for supervising me during this thesis. Our weekly meetings helped me a lot in overcoming the difficulties of the modelling process, and your expertise on morphology helped me to improve my physical understanding of the subject. Besides that, the days working at the office with the whole team and getting insight into some of the aspects of the projects that the group does at Witteveen+Bos made graduating a lot more fun. Thirdly, I want to express my gratitude to the rest of the members of my graduation committee; Nick van de Giessen, Markus Hrachowitz, Susan Steele-Dunne, and especially to Olivier Hoes, for helping me closely during the whole research. I have enjoyed our meetings and whenever I thought I had hit a dead-end, or when I was stressed about the imperfectness of my model, Olivier set me back on track and made me remember no model is perfect.

Multiple organisations have helped me by providing data and software. First of all, I would like to thank the RiverLab community of Deltares for answering all my questions on their forum. Especially Victor Chavarrias has helped me a lot in solving the problems I faced with the D-HYDRO 1D2D software. Furthermore, I want to thank Job Udo from HKV, the Hydrological Service Department and the Volta River Authority for sharing the morphological and hydraulic data that I needed for my model.

Finally, I would like to thank all of my close friends and family for helping me to write, and sometimes not to write, this thesis. First of all, my roommates, for making something fun out of a long period of quarantine. Furthermore, my fellow master students for all of our study days on campus. And most importantly, my family, for supporting me morally and financially during all of my studies, and letting me free to make every decision and detour needed to find my way.

Vera Kingma
Rotterdam, 2021

Executive Summary

Human interventions in the White Volta River in Ghana increase the flood risk in living spaces of the local communities, causing great challenges in the area. Burkina Faso has built a hydropower dam near the border with Ghana which has a large impact on the discharge extremes of the White Volta River. As a result of poor water management of this dam, water is spilled during the wet season, causing more floods in northern Ghana. Several communities, living near the White Volta River, depend on the river water for their drinking water demand and use the sand in the river bed as construction material. This puts them in a vulnerable position when changes in the natural flow regime of the river occur.

This thesis studies the impact of constructing multiple small dams in the White Volta river in order to decrease the flood risk in villages located close to the river and create an opportunity for controlled sand mining as a result of sedimentation.

Tamale is, with 672.000 inhabitants, the largest city in this area and struggles with the consequences of the floods as well. The drinking water company has trouble meeting the drinking water demand during both the wet and the dry season. When the area is flooded, the water intake point shuts down, and during low water levels, the pumps can get clogged. This clogging occurs even more often as a result of increased illegal sand mining from the river banks by the local communities. This has broadened the river, resulting in lower water levels and a higher turbidity.

A possible solution to ensure the water intake in Tamale and reduce the flood risk in northern Ghana is the construction of multiple small dams in the river bed to flatten the discharge peaks and slow down the water in the White Volta River. At the same time, these dams can create an additional advantage by causing upstream sedimentation that provides a possibility for controlled sand mining in the river bed. To research the effectiveness of this solution, the impact of the dams on flood risk and sedimentation, near seven villages in northern Ghana, was modelled.

A base case of the flood of 2003 was compared to a scenario in which seven dams were implemented at locations close to villages that are often exposed to floods. This was done by building a hydromorphological model of the White Volta River, using the D-HYDRO 1D2D software.
First, a 1D hydraulic model was built to simulate the water levels in the river and investigate the impact of different crest heights of the weirs. After finding the optimal weir design, the morphological changes in the bed level as a result of the dams where simulated. The results show that upstream of each dam, sedimentation occurs as a consequence of the decreasing flow velocity and the subsequent decrease in sediment transport capacity of the water. And downstream of the dam, the river bed erodes, as a result of an increasing flow velocity in combination with an unfulfilled sediment transport capacity.
Next, to simulate the flood extent and the inundation depths, the model was extended with 2D grids covering seven villages near the White Volta River. Using QGIS, the model results were compared to exposure maps, showing agricultural areas, population density and two types of houses. The total value loss of these elements as a result of the flood hazard was quantified.

The results of the morphological simulation show that in total, the sedimentation upstream of the dams can fill 81 trucks with sand per day. However, extracting the sediment at the most upstream dams decreases the possibilities for sedimentation near the downstream dams. The results of the 1D2D hydraulic model show that the proposed dams are not able to reduce the flood extent in villages and can even increase inundation depths, resulting in more flood damage.

For future research, it is recommended to perform more field work in order to improve the data and gain better understanding of the project area. Furthermore, implementing floodplains in the hydraulic model would improve the model results and provide more realistic backwater curves.

Contents

List of Figures

List of Tables

1 Introduction

1.1. Challenges of the White Volta Basin

The Volta Basin can be introduced as one of the largest water systems of the African West Coast. It is the main river system of Ghana, consisting of the White Volta, the Black Volta and the Oti River. The White Volta, having the largest discharge of the three, enters Ghana at the border with Burkina Faso. From there, the river flows through the savanna of northern Ghana, towards Lake Volta in the South, as shown in figure 1.1. In its natural flow regime, the river often causes floods during the rain season after which it returns to a smaller discharge during the dry season. Discharges range between 100 m^3/s and 2000 m^3/s during the dry and the wet season.

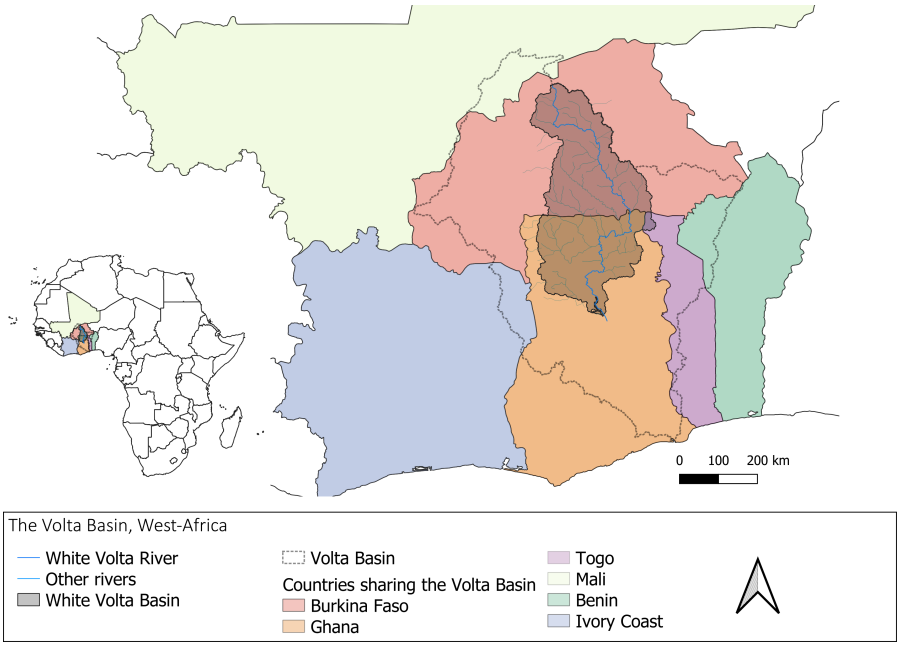

Figure 1.1: Map of the Volta Basin and its surrounding countries. As shown in the left corner, the basin is located in West Africa. The dotted line shows how the Volta Basin is spread over six different countries. The darker grey area shows the part of the Volta Basin that belongs to the sub-basin of the White Volta River.

Multiple factors have disrupted the natural flow regime, increasing the problems caused by the seasonal floods. First, in 1992, Burkina Faso (shown in pink in figure 1.1) build a large hydropower dam, with a capacity of 16 MW, near the border with Ghana. The reservoir behind this dam has a storage capacity of 7.000.000.000 m^3 and was supposed to decrease the discharge extremes. However, poor management of this dam has increased the magnitude and the number of flood events in Ghana

during the wet season. Secondly, climate change has an impact on the weather in Ghana, causing more extreme precipitation peaks and longer periods of drought. The third cause of disruption of the flow regime is illegal sand mining in the river bed. Due to urbanisation and population growth, the demand for construction materials increases. The river bed is the main supplier of clean, easy accessible sand, which is needed for the production of mortar and concrete. The Ghana Water Company Limited (GWCL) expects that the widening of the river, as a result of the sand mining, is the cause for further decrease in the water level during the dry season and an increase of the turbidity of the river water.

Tamale is the largest city in northern Ghana and is one of the cities that has to deal with the challenges described above. As the city depends on the White Volta river for its drinking water supply, the quality and quantity of the river water are of high importance. In 2019, the GWCL already struggled to meet the drinking water demand in both the dry season, due to the limited water level and high turbidity, and the rain season, due to heavy flooding of the river at the intake point of the GWCL.

The consequences of floods and drought on the communities living near the riverbed are widespread. Often, the floods cause damage to crops, housing, bridges, schools, fertile farmlands, animals, health facilities, water supply systems that use river water, irrigation systems, food storage and processing facilities (Musah & Oloruntoba, 2013). Furthermore, fatalities as a result of the floods occur. In less developed countries, these fatalities tend to impact the most vulnerable groups as they have limited options for settling in safe places or taking measurements to protect themselves (Abass, Dumedah, & Frempong, 2019). This group needs and deserves to be protected from climate hazards and therefore, research and action are needed to find the right solutions.

One solution to prevent the city of Tamale from floods and droughts as a result of discharge extremes is sustainable water storage in the river. The government of Ghana is planning on building a large dam, the Pwalugu Dam, near the border of Burkina Faso that can play a big role in achieving this. If the dam is going to be realised and managed in a proper way, it can positively influence the streamflow peaks near Tamale. Complementary to this dam, constructing multiple small dams near villages located close to the White Volta river, might help to store the river water upstream to reduce the discharge peaks. This can have a positive impact on the lives of the people living near the White Volta river.

1.2. Research Objective

The complementary solution of building multiple small dams to reduce the discharge extremes in northern Ghana was explored in this research. The research focuses on the scenario in which the dams are located near inhabited areas between Yarugu, some kilometers upstream of the planned location of the Pwalugu dam, and the planned drinking water intake point of Tamale.

The hypothesis of this research is that the dams will add multiple benefits for communities along the White Volta River. First of all, it is expected that the dams increase the upstream water storage in the river and reduce the downstream river flow. This will decrease the flood extent in inhabited areas. Secondly, upstream of the dams, sedimentation will occur which can be used for controlled sand mining in the nearby communities. Politicians promised to provide each community with a small hydropower dam, which will create income and give the community control of the river flow. As this solution is in line with the political promises that are already made, political support for this plan can be expected. Lastly, due to its simplicity, this solution is flexible which makes it easy to adjust or remove the construction. The simplicity also causes the construction to be inexpensive which makes it more realistic that the implementation will be financially possible.

This research aims to find out whether the expected benefits are possible results of the construction of the small dams in the river stream. The impact of different dam dimensions will be tested to understand the impact of the dams on this river stream.

The main research question is:

How will the construction of multiple small dams in the White Volta river impact the magnitude and occurrence of discharge extremes, sedimentation and flood risks in northern Ghana?

The following sub-questions were formulated to answer the main research question:

1. What influences the streamflow in the White Volta river and what is the current streamflow of the river?
    - How do the tributaries contribute to the streamflow?
    - What is the impact of the current and future structures in the river stream?
2. What is the impact of constructing dams on river characteristics?
    - What is the most effective dam design?
    - What is the effect of a dam on the backwater curve?
    - What is the effect of a dam on sedimentation and erosion?
3. How do multiple small dams in the White Volta river change the flood risk?
    - Which villages should be included in the flood risk simulation?
    - How can flood risk be quantified?

1.3. Methodology

The methodology of this research is based on literature study and modelling. The literature is used in order to gain knowledge on the problem and the case study. Parameters are selected based on satellite data and field study reports. These parameters are used in order to create the models.

1.3.1. Literature

In appendix A, a short literature review on the subject can be found. Most research agrees that the floods increase as a result of climate change and spilling of the Bagre Dam in Burkina Faso. Water storage in reservoirs is mentioned as a solution for similar problems. The studies from this literature review that use modelling methods, proved that parameters, meteorological data and land cover information are often accessible by literature, public data banks and remote sensing. Therefore, it was decided that data collection could be possible without doing actual fieldwork.

By looking into the different studies in the Volta Basin, it became clear that different Dutch engineering companies and the TU Delft have performed research in the study area. Some of these organisations were willing to share their data, which was used to define the model parameters. Other organisations, like the UN and NASA, have large open-source platforms with (satellite) data. With remote sensing, information was collected on the geographical characteristics of the basin, like the shape and the slope of the landscape. In combination with field reports, this was enough to create a rough bathymetry of the river. Mainly Sentinel-2 satellite data was used for this part of the research.

1.3.2. Modelling

The second part of the research is model-based. Two different models were used: a hydrological model and a hydraulic model.

The hydrological model was created by another master student (te Witt, 2021), using the software W-Flow. The model was used to add the lateral inflow from tributaries of the White Volta river into the hydraulic model. To come to the best results for the White Volta river, the model, that was originally calibrated to give the best results for the whole Volta Basin, was now calibrated on the discharge stations in the White Volta River.

The hydraulic model was created using a new software: D-HYDRO 1D2D. By using this software, the river hydraulics of a large river segment could be modelled in a one-dimensional way, while locally, the flood characteristics could be modelled in a two-dimensional way. The software was still under development by Deltares and the licence for the beta version was provided by Witteveen+Bos. The RiverLab community of Deltares was consulted for errors and difficulties in the modelling process.

1.4. Thesis Outline

This thesis starts with an in-depth description of the White Volta River Basin in chapter 2 which will focus on the location, the climate and the river stream characteristics from which also the current problems concerning floods will follow. Chapter 3 shows the theoretical framework of the research. In this chapter, three different theories will be explained that are needed to understand the model outcomes. The first theory describes the impact of dams on the river stream by discussing the Saint-Venant equation to calculate backwater effects. Then, the impact of dams on river morphology is described using the Exner principle. To conclude the third chapter, the theory on mapping and quantifying flood risk is explained. Then, the fourth chapter elaborates on the data needed to perform this research. Whenever data is manipulated, this process is explained. After that, the models are described in the fifth chapter from which, in chapter six, the model results follow. Finally, the results are discussed and the research questions are answered in the conclusions.

2

Case Study: White Volta River

In this chapter, the characteristics of the White Volta River basin are discussed. As the river spreads out over different countries in a dry climate, too many people have to compete for the water resources of the river. Burkina Faso built a hydropower dam, the Bagre Dam, to generate hydropower and store water for irrigation during the dry season. Poor water management of this dam causes spillage during the wet season, resulting in major floods of the White Volta River in Ghana. A combination of improved integrated water resources management and water retaining structures in Ghana is needed to reduce the damage that is caused by these floods.

2.1. Location

As shown in figure 1.1, the Volta Basin is a large river system in West Africa. The basin covers a total area of more than 400000 km^2 (10 times the Netherlands), of which more than 40% is located on Ghanaian grounds (Amisigo, McCluskey, & Swanson, 2015). The other five countries it touches are Burkina Faso, Togo, Mali, Benin and Ivory Coast. This part of Africa is characterised by the savannah climate (Van de Giesen, Andreini, Van Edig, & Vlek, 2001). In the North, the basin almost reaches the equator, where the desert begins and the landscape consists of sand and short grass.

The White Volta River basin is a large sub-basin of the Volta Basin. The White Volta river, locally called Nakambé river, starts in Burkina Faso, East of the city Ouahigouya. From there, it flows towards the South where, in 1993, about 50 km upstream of the border with Ghana, in Bagre, a hydropower dam was constructed. This dam, called the Bagre Dam, is from that point on the largest influencer of the downstream discharge. The river passes the border and then flows through the North of Ghana where, after 120 km, the Red Volta contributes to the river stream.

Besides the White Volta river, the Black Volta River in the West of Ghana and the Oti river in East Ghana, are large tributaries of the Volta Basin. Before 1960, the Black Volta and the White Volta would merge in central Ghana and form the Volta river all the way towards the coast. However, in 1960, the Akosombo hydropower dam was built, creating the largest artificial lake in the world: Lake Volta. South of Lake Volta, the Akosombo hydropower dam creates a turbine outflow that forms the Volta River and ends up in the Gulf of Guinea. The White Volta Basin is, besides this turbine outflow, the sub-basin with the largest mean discharge.

Along the river, multiple cities, towns, villages and hamlets are located. Hamlets are smaller than villages and from origin without a church. Figure 2.1 shows where these are located. As can be seen in this figure, Tamale is the only large city in this area. Around Tamale, a lot of suburbs and small villages are located. Villages and hamlets can be found near the river bed as well, experiencing the high flood risk of the White Volta River.

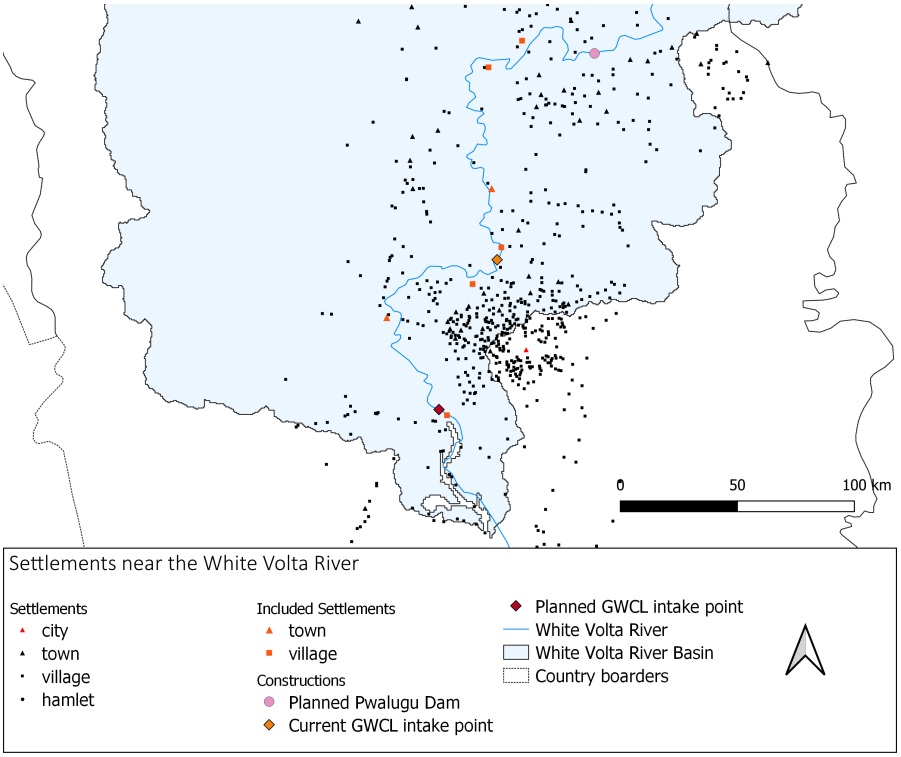

Figure 2.1: Settlements in a range of 50 km from the White Volta River in the Ghanaian part of the basin and constructions in the White Volta River. At the top, the planned Pwalugu Dam is shown in the pink dot. Moving downstream, the current intake point of the GWCL and the planned intake point of the GWCL follow. The orange settlements are included in the flood risk simulations of this research.

2.2. Climatology and the Impact of Climate Change

Ghana is a country that consists of three different hydro-climatic zones called the Volta basin system, the South-Western basin system and the Coastal basin system. The White Volta River basin is part of the Volta basin system. The rainfall in this area is characterised by the intertropical conversion zone (ITCZ) causing a mean annual rainfall of 1000 mm (The World Bank, 2011). However, even within the northern region, these rainfall amounts vary substantially depending on the specific location (Laube, Schraven, & Awo, 2012). The West African Monsoon brings a rain season in the North of Ghana that starts in May and stops in October. Furthermore, the El Nino Southern Oscillation (ENSO) causes variability in the onset and duration of the monsoon season. The events are associated with long periods of drought and high temperatures in the North (The World Bank, 2011).

The drylands in the North were always prone to climate difficulties. Due to the strong distinction between wet and dry seasons and the lack of knowledge on sustainable agriculture, desertification takes place in the area. As a result, the economical growth is limited and the agricultural areas are not able to develop as fast as the regions in the South. The North is also threatened when it comes to water scarcity and droughts, and land degradation increases the impact of the dry season even more (Armah et al., 2011). In the 20th century, the Sahara desert has already expanded by 10%, and this process is still ongoing (The World Bank, 2011), causing a threat for northern Ghana.

The Impact of Climate Change

Climate change makes the dry periods longer and the rainfall peaks more intense. The problems described in the previous paragraph will therefore be even harder to overcome when climate change continues (Niang et al., 2014).

The northern part of Ghana is the poorest region of the country. Although the area is not densely populated, the fertility rates are a lot higher than the natural average, 3.6% compared to 2.7%. This

causes concern as the poverty levels range between 69% and 88% and the prospects for development are small (Armah et al., 2011).

In qualitative interviews with farmers became clear that already for 20 years, delayed onset of the monsoon season was experienced. Furthermore, the natural signs of the onset have become less reliable (Laube et al., 2012). This is a problem as rainfed agriculture is the main source of income in Ghana (Armah et al., 2011).

2.3. Flood Occurrence and Flood Protection

In its natural flow regime, the White Volta river causes floods as a result of the extreme discharge peaks. It seems like poor water management of the Bagre Dam in Burkina Faso has caused an increase in these peaks. As a result, the periods of drought are longer and floods are more extreme.

From the start of this century, scientists began to address their concerns about water resource management in the Volta Basin (Van De Giesen et al., 2002). The need to identify the causes of floods grew throughout the years (Di Baldassarre et al., 2010) as the flood fatalities kept increasing (Komi, Amisigo, Diekkrüger, & Hountondji, 2016). During the last decade, floods and periods of drought are yearly occurring features in parts of northern Ghana (Musah & Oloruntoba, 2013) (Yiran & Stringer, 2016). Not only near the largest rivers but also more inland, people struggle with floods (Abass et al., 2019). At the same time, there is strong competition for water resources in the Volta Basin (Van de Giesen et al., 2001). The Volta Basin already lacks the surface water quantity to satisfy the three main water demands: hydropower, agriculture and municipal, while the population keeps increasing (Amisigo et al., 2015).

The nature of the problems that cause the floods have received limited attention (Abass, 2020). Only since 2013, the spilling of the excess water by the Bagre Dam was included in the literature (Musah & Oloruntoba, 2013). From then, it was concluded that this is the main cause of floods in the White Volta River. Musah and Oloruntoba even claimed that 75% of these floods were caused by the Bagre dam and that only 25% occur as the result of excessive rainfall events. He found that floods occur mainly in August en September and points at poor water management of the Bagre dam in Burkina Faso as the main problem. He states that as the intensity of the rain season increases southwards, Burkina Faso already experiences less extreme rain events during the rain season and therefore should make sure they manage their dam properly instead of spilling excess water during these months. Abass et al., agree on the reasoning that a combination of heavy rainfall and opening of the Bagre Dam are the main triggers of the flood events.

While research into the floods lacks for most cities of northern Ghana, Kumasi has been studied more often. Reasons for the flooding of the city come down to the rapid expansion of the city with poor spatial planning. As a result, the development of watercourses and wetland takes place which is dangerous and disrupts the natural flow regime (Abass, 2020). Kumasi is not located near the White Volta river, but it does show the possible risks that occur when poor water resources management and rapid urbanisation are combined.

Impact of the Future Pwalugu Dam

The government has made promises to provide long term solutions (Udo et al., 2011). One of the solutions that the government proposes is a multipurpose dam. This dam will be constructed near the city of Pwalugu and should store water for hydropower, irrigation and flood protection. The reservoir created by the dam will have a 350 km^2 water holding capacity, twice the size of the Bagre Dam. The turbines of the power station are planned to have a total capacity of 60MW, and besides that, the solar panel system in the reservoir will generate another 16.5 MW (Takouleu, 2020). This is a large amount in perspective with the 16 MW capacity of the Bagre Dam. Water storage in the reservoir upstream of the Pwalugu Dam is supposed to decrease the flood risk in the downstream areas.

2.4. Integrated Water Resources Management

Integrated Water Resources Management (IWRM) is a process in which all the parties that share a water source have coordinated development and water management. This includes both water quantity and water quality aspects. In the White Volta Basin, good IWRM is hard to reach as not only different organisations and companies share an interest in the river water but also different countries have to be on the same page managing the water resources.

Burkina Faso stores water for hydropower and irrigation by creating a reservoir upstream of the Bagre Dam. As explained before, this water is managed poorly during the wet season, creating floods downstream. As the downstream part is located in Ghana, Burkina Faso has no direct benefit to change the management of the dam.

The Water Resources Commission (WRC) is responsible for the Water Resource Management in Ghana. They have the mission to regulate and manage the sustainable utilisation of water resources. They try to coordinate policies made by the government in order to come to sustainable use of the water sources. The commission consists of 15 members and different institutions of which the Volta River Authority (VRA), the Hydrological Service Department (HSD) and the Ghana Water Company Limited (GWCL).

The VRA was established in 1961 with the function to manage and distribute electricity generated by dams in the Volta Basin. The Akosombo dam is the largest dam they manage and has the capacity to generate 1020 MW. Nowadays, the VRA also generates electricity with other techniques, like solar and wind. They have the mission to raise the living standards of people in Ghana by supplying electricity from renewable energy sources. Besides energy production, they are also concerned with river water quality and restoration of the ecosystem in Ghana at places where (illegal) dredging occurs (VRA, 2021).

HSD is part of the Ministry of Works and Housing at the government of Ghana. The ministry is responsible for the maintenance and monitoring of waterworks over the country. They are important for this research as they provide most of the gauge data.

The GWCL is a state-owned company that is responsible for the water supply to all urban communities in Ghana (GWCL, 2019). The extraction point of the drinking water for Tamale is located near Nawuni. Therefore, the GWCL has an interest in high-quality river water and reliable discharge.

3

Theoretical Framework

In this chapter, different theories are explored in order to answer the research question:

*How will the construction of multiple small dams in the White Volta river impact the magnitude and occurrence of **discharge extremes**, **sedimentation** and **flood risks** near Tamale, Ghana?*

The research question consists of three different parts and therefore this chapter follows the same structure. First, the theory to describe discharge extremes is explored by using the Saint-Venant equations to calculate backwater effects. Then, the impact of these dams on sedimentation and erosion will be explained by using the Exner principle. And finally, the method to quantify and map flood risk is defined by separating the hazard, exposure and consequences.

3.1. The Impact of Dams on River Hydraulics

In this section, the construction of a dam and the effects of the dam on the river flow are discussed. The design is a simple accumulation of large rocks that can be found within the area. In order to maintain the base flow at all times, pipes are added near the river bed to prevent dry spells. The dam is simplified as a broad crested weir of 3 meters long. The crest height is adjusted to assure free-flow conditions during the dry season and submerged flow during the peak discharge. By rewriting the Saint-Venant equations for the adjusted river and combining them with the continuity equation, a formula was found to calculate the 1-dimensional backwater effects of the river stream.

3.1.1. Dam Design and Function

The proposed dam has a very basic design consisting of large rocks build up together in the riverbed approximately as high as the mean water level. This robust design will be easy to install with natural building materials present in the region. Pipes will be installed near the river bed to maintain the base flow during the whole year.

The dams will cover the entire river section and have a width of 3 meters in order to create a robust structure. Therefore, it can be approximated as a broad-crested weir. In figure 3.1, an example is shown of a similar construction. These types of simple constructions have multiple benefits. First of all, they are cheap which is important in developing countries where governments have little money to invest. Secondly, the construction is simple so it is not necessary to hire an expensive company for the instalment of the dam but instead, it can be done locally. Besides, if an adjustment is needed, it is easy to adjust or maintain the structure.

When constructing a dam in a river, its function is to reduce peak discharges downstream by storing water in an upstream reservoir. As clearly shown in figure 3.1, the result will be a higher water level upstream and a lower water level immediately downstream. The effects of a dam on the water level height can be visible at meters or even kilometers upstream and downstream. The upstream effects are called the backwater effects. These are important to calculate as the backwater effects might also

Figure 3.1: The picture shows an example of an existing small dam (or free-flowing weir). This dam is comparable to the small dams that are explored in this research. The simple design makes it possible to remain low in price and easy to adjust.

increase the flood risk in upstream villages.

Understanding these backwater effects starts by understanding the basic equations for long waves: the Saint-Venant equations. When applying these equations to a specific case, the extend of the backwater curve can be determined.

3.1.2. Saint-Venant Equations

Long waves are defined as unsteady free-surface flows with a length scale that is far greater than the depth. Flood waves in rivers are good examples of these long waves as the river depth is small compared to the longitudinal shape.

As this research considers a long river reach with a small depth, the flow and the morphology can be approached as one-dimensional features. To do this, some important assumptions have to be made.

First of all, by analysing one-dimensional long waves, the streamlines in the river are almost parallel in the longitudinal direction, and therefore, negligible in the vertical plane. This assumption makes that hydrostatic pressure distribution can be assumed over the depth of the river.

Secondly, the lateral variations in surface elevation are neglected. In practice, when the river bends, the water level in the outer bend will be higher than in the inner bend but this effect is small on the large scale and is therefore ignored. The water level is thus assumed to be constant within the cross-section, and therefore, the pressure gradient is also constant over the cross-section. This pressure gradient determines the flow velocity, and the cross-sectional area determines the discharge, therefore, the discharge and the water height are both only dependent on the time and the longitudinal location (eq 3.1).

$$\begin{aligned} h &= h(s,t) \\ Q &= Q(s,t) \end{aligned} \tag{3.1}$$

Continuity equation

When applying these assumptions to the situation of river flow, the continuity equation can be derived (eq 3.2). This equation is based on the mass balance of incompressible water systems. The derivation of the continuity equation from this mass balance is shown in appendix E.1.

$$B\frac{\partial h}{\partial t} + \frac{\partial Q}{\partial s} = 0 \tag{3.2}$$

Momentum Balance
Momentum is defined as mass times the velocity of that mass (eq 3.3) and plays an important role in the flow of liquids.

$$\vec{p} = m * v \tag{3.3}$$

Using the second law of Newton in combination with the transformed Euler equation for one-dimensional flow, the momentum balance can be derived (eq 3.3). This derivation is given in appendix E.2.

$$\frac{\partial Q}{\partial t} + \frac{\partial}{\partial s}\left(\frac{Q^2}{A_c}\right) + gA_c\frac{\partial h}{\partial s} + c_f\frac{|Q|Q}{A_c R} = 0 \tag{3.4}$$

in which the unknowns are:
$Q =$ the discharge $[m^2/s]$
$h =$ the water level height above the reference plane z_0 $[m]$
and the known parameters for every location s, water level h and discharge Q are:
$t =$ time $[s]$
$s =$ distance $[m]$
$\alpha =$ the variation of particle velocity over the cross-section
$A_c =$ the conveyance cross-section $[m^2]$
$g =$ the gravitational acceleration $[m/s^2]$
$c_f =$ the resistance coefficient $[-]$
$R =$ the hydraulic radius (which is equal to the depth for large rivers)

Together, the continuity equation (eq 3.2) and the momentum equation (eq 3.4) are called the Saint-Venant equations, or the 1D shallow-water equations (Battjes & Labeur, 2017).

Physically, the resistance coefficient is a dimensionless parameter that depends on the type of riverbed and vegetation. In this research, the Chézy values were used to represent the roughness of the river bed. However, the parameters were used for calibration purposes and therefore represents not only the roughness of the river bed but also other shortcomings of the data and the model. The parameter will be further elaborated on in section 3.2.2.

3.1.3. Calculating the Backwater Effects Using the Saint-Venant Equations

The backwater effects can be calculated using the Saint-Venant equations. When the river has adjusted its stream after the dam is constructed, steady flow occurs. This means the discharge does not change over time and space, and the water height does not change over time. As a result, the surface elevation $h = h(s)$ is the only unknown in the momentum balance. This reduces the complexity of the equation, shown in equation 3.5. This equation can now be used to calculate the backwater curve upstream of the dam.

$$Q^2\frac{\mathrm{d}A_c^{-1}}{\mathrm{d}s} + gA_c\frac{\mathrm{d}h}{\mathrm{d}s} + c_f\frac{|Q|Q}{A_c R} = 0 \tag{3.5}$$

Here, h is measured with respect to the sloping bed level: $h = z_b + d$ and the depth d is used as the unknown that defines the backwater curve. When rewriting equation 3.5 explicitly in terms of discharge, it can be written as shown in equation 3.6.

$$\frac{\mathrm{d}d}{\mathrm{d}s} = \frac{i_b - c_f Q^2 P/gA_c^3}{1 - Q^2 B_c/gA_c^3} \tag{3.6}$$

3.1.4. Different Flow Types as a Result of the dams

Discharge in the White Volta river changes a lot over the different seasons. Therefore, the impact of the dams on the river hydraulics differentiates as well. The flow types can roughly be divided into two categories: free flow and submerged flow.

During the dry season, the dam will have little impact on the water levels in the river as most of the water flows through the pipes near the bottom of the river bed. When the discharge starts to increase, the backwater curve develops. After some time, the upstream water level exceeds the crest height of the dam. At this stage, the downward water level has no impact on the upstream flow conditions. This is called free flow. These flow types are visualised in figure 3.2

During the rain season, discharge increases a lot and the water levels rise further above the crest height of the dam. Submerged flow conditions occur when these downstream water levels become so high that the upstream flow velocity is reduced.

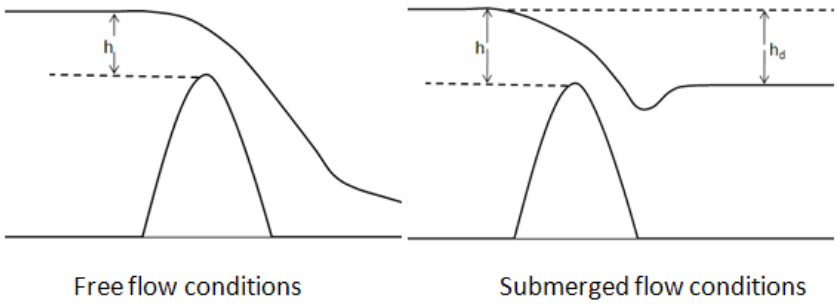

Figure 3.2: The left figure shows an example of a free flow over a dam and on the right, submerged flow is shown. During submerged flow conditions, the downstream water levels have increased so much, that the flow velocity over the dam reduces.

3.2. The Impact of Dams on River Morphology

River morphology describes the way that the shape and direction of the river bed change over time. A river in which the river bed and the banks are made of mobile sand is called an alluvial river. In alluvial rivers, the morphology is described by the entertainment, the transport and the deposition of sediment caused by water in the river channel. These three processes together determine and change the shape over time (Crosato, 2007). As a result, alluvial rivers often have a meandering shape.

Constructing a dam in an alluvial river has an impact on the mobility of the sand. The Exner principle can be used to assess the river response to human interventions. First, it is explained how a perturbation leads to a new equilibrium, and then a situation of continuous sediment extraction is described. By applying the Engelund & Hansen method, the total transport of sediment, consisting of erosion, storage and sedimentation, can be calculated.

3.2.1. The Exner Principle

The immediate effects of an intervention can be approached with the sediment balance. The volume of sediment entering and leaving a control volume ($q_{s1}\Delta t$ and $q_{s2}\Delta t$), can be calculated using the mass balance, see figure 3.3.

The amount of transported sediment q_s depends on the transport capacity and the velocity of the water, therefore $q_s = q_s(u)$. When water accelerates, its capacity to transport sediment increases and therefore, more sediment is able to suspend and erosion takes place. During decelerating flow, this capacity decreases, which causes sedimentation. When the velocity gradients in a stream are known, the Exner principle can be used to determine the sediment transport. Equation 3.7 shows the definition of the Exner principle. Besides the transport capacity of the water, it is also important that the threshold for initiation of motion of the sediment particles is above the critical values. When velocities are low, a situation might occur that the water is not able to lift the particle from the river bed. In this research, it is assumed that during the peak discharges, this threshold for initiation of motion is far exceeded. The model makes these calculations based on the grain sizes and sediment density.

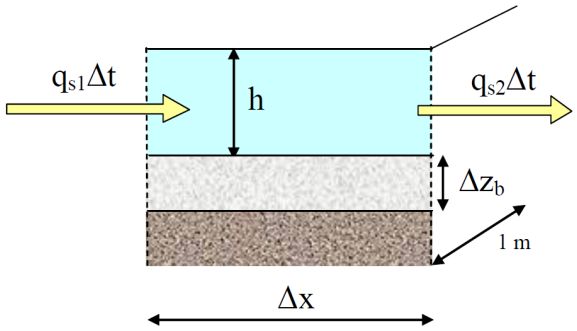

Figure 3.3: Control volume showing the sediment mass balance (Crosato, 2007)

$$\frac{\partial z_b}{\partial t} + \left[\frac{\mathrm{d}q_S}{\mathrm{d}u}\right]\frac{\partial u}{\partial x} = 0 \tag{3.7}$$

In this formula, the term $\frac{\partial z_b}{\partial t}$ shows the changing river bed height over time. This term is weighted by the change in sediment transport over the flow velocity, $\frac{\mathrm{d}q_S}{\mathrm{d}u}$, as the sediment transport determines in what way the river bed is effected over time. The third term, $\frac{\partial u}{\partial x}$, is the changing flow velocity over the river segment x. The sign of this term determines whether erosion or sedimentation occurs, and thus, whether the bed height increases or decreases over time. This term is often considered to be constant when the flow velocity does not change a lot and the conditions in the river have a high level of non-linearity in the sediment transport formula.

Equation 3.7 shows the relation between the velocity gradient and the morphological changes in a one-dimensional system. The next step is to quantify the sediment transport from the Exner principle. To do so, the power-law can be used. The power law describes the relation between two different quantities. It assumes that the relative change in one of the quantities has a proportional relative relation towards the other quantity. In the case of sediment transport, this means that the sediment transport q_s is related to the flow velocity of the river u as shown in equation 3.8.

$$q_s = mu^b \tag{3.8}$$

The two constants m and b can be determined by using the the Engelund & Hansen method. In equation 3.9, this method is shown (Crosato, 2007). The D-HYDRO software uses this method in order to calculate the sedimentation amounts.

$$\begin{aligned} m &= \frac{1}{\left(12C^3\frac{\rho_S-\rho_W}{\rho_W}D_{50}\sqrt{g}\right)} \\ b &= 5 \\ q_S &= \frac{1}{\left(12C^3\frac{\rho_S-\rho_W}{\rho_W}D_{50}\sqrt{g}\right)}u^5 \end{aligned} \tag{3.9}$$

in which:
ρ_S = sediment density $[\mathrm{kg/m^3}]$;
ρ_W = water density $[\mathrm{kg/m^3}]$
D_{50} = mean sediment grain-size $[\mathrm{m}]$
g = acceleration due to gravity $[\mathrm{m/s^2}]$

C = Chézy roughness coefficient $[m^{0.5}/s]$

When using equation 3.9, the total transport of sediment is calculated. This consists of both the bed load and the suspended load. It is important to differentiate between the two because the suspended particles will be less affected by the construction of a dam, as it will flow over or through the pipes installed in the dams, suspended in the water. The bedload, however, is the part of the sediment that will settle and cause sedimentation upstream of the dam.

3.2.2. Roughness Coefficient

As can be easily imagined, the roughness of the riverbed material has a distinct influence on the velocity of the river water. A riverbed full of rocks and vegetation reduces the flow velocity, while in the case of a smooth concrete channel, the flow velocity is higher.

A French engineer, called Antoine de Chézy, studied this phenomenon and found a relation between the resistance to uniform turbulent flow (τ) with the velocity of the water (u), as well as, to the wetted perimeter of the riverbed (P, which relates to the hydraulic radius by $\frac{A}{P} = R$). At the same time, it is known that the driving force (F) is proportional to the product of the area of the conveyance cross-section (A_c) and the slope of the riverbed (i_b). Due to the fact that resistance in uniform flow is in balance with the driving force of this flow, a relation can be found between the flow velocity and these river characteristics (Battjes & Labeur, 2017). This step-by-step derivation is shown in equation 3.10.

$$\begin{aligned} \tau &\propto \sqrt{u} \propto P \\ F &\propto A_c i_b \\ \tau &= F \\ A_c i &\propto \sqrt{u} \propto P \\ u &\propto \sqrt{\frac{A_c i}{P}} \\ u &= C\sqrt{R i_b} \end{aligned} \tag{3.10}$$

The coefficient C is called the Chézy roughness coefficient and is used in this research to represent the roughness of the riverbed. In practice, the value is unknown and the parameter is used for calibration purposes. The values should be in the order of 30 $[m^{0.5}/s]$ for a rocky riverbed up to 100 $[m^{0.5}/s]$ for a concrete-lined channel.

3.2.3. Impact of the Current Sand Mining

When no interventions take place in the river bed, the morphological processes find a long term dynamic equilibrium, within the seasonal variations. This means that over the years, the processes of erosion and sedimentation have shaped the river bed in a way that the movement of the river water does not have long term effects on the river bed anymore. Considering the control volume of figure 3.3, this leads to a situation in which the rate of sediment entrainment is equal to the rate of sediment deposition. Therefore, the sediment transport per unit width does not change.

However, in the case of the White Volta river, sand mining disrupts this balance. The extraction of sediment has no impact on the sediment entrainment but reduces the sediment deposition, as less sediment is available to settle. The continuous extraction of sand in the White Volta river creates a new equilibrium, where the available transport capacity downstream of the extraction point is equal to the reduced sediment load after extraction. An erosion expansion wave will cause erosion in the river bed up to the lake. This process is visualised in Appendix B.

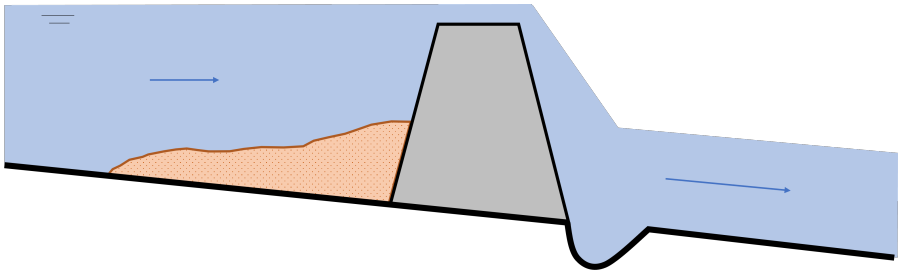

Figure 3.4: The Exner principle: sedimentation and erosion as a result of the dam. The water flows from the left to the right. It has to slow down upstream of the dams which causes particles to settle with sedimentation as a result. Downstream of the dams, turbulence and acceleration of the water causes the soil to erode.

3.2.4. Impact of Sand Mining Upstream of the Dams

As explained in section 3.1, constructing a dam has an impact on the velocity gradients in the river stream. Upstream of the dams, the water has to slow down as the riverbed is blocked. This decreasing velocity will reduce the sediment transport capacity and cause, in combination with blockage of bed-load, sedimentation upstream of the dam. A downstream effect of the dam is, that the water has a high velocity and will cause turbulence. The turbulence, together with the unutilised sediment transport capacity of the water, will result in erosion downstream of the dam, see figure 3.4. These morphological changes follow the profile of the backwater effects in the river, as the backwater effects occur where velocities changes. Similar to this pattern, the morphological effects will be most visible during the peak discharges in the rain season and minimal during the dry season.

So, constructing a dam has an impact on the sedimentation and erosion in the river bed. The sedimentation upstream of the dam will continue up to the point that a new equilibrium is found. However, this research evaluates the situation in which continuous extraction of sediment upstream of the dam will occur. Similar to the current situation, this means the sediment transport load is reduced and downstream of the dam, the water is able to transport more sediment than it does at that point. The equilibrium state will never be reached, leading to more erosion downstream of the river (Crosato, 2007).

3.3. The Impact of Dams on Flood Risk

"Disaster risk is the potential loss of life, injury, or destroyed or damaged assets which could occur to a system, society or a community in a specific period of time, determined probabilistically as a function of hazard, exposure, vulnerability and capacity" (UNDRR, 2020).

In order to know the impact of a flood on the people and the environment, the flood risk must be mapped. In this section, the definition and quantification methods used for flood risks are explained. By making a flood map of the base case, scenario's in which dams are constructed in the river can be compared to the original situation.

Flood risk is the product of hazard, exposure and vulnerability (Kron, 2005). Each of these three components can be mapped in a different layer but together they can visualize the areas prone to flood risk. Hazard is quantified using the intensity of the threatening event itself. The exposure counts people and properties in the by the hazard affected area. Within this research, a distinction is made between population, buildings and agricultural areas. Finally, the exposed elements all have their own level of vulnerability. This vulnerability includes the capacity of the elements to cope with the hazard.

3.3.1. Hazard

"A process, phenomenon or human activity that may cause loss of life, injury or other health impacts, property damage, social and economic disruption or environmental degradation" (UNDRR, 2020).

The hazard analyzed in this research is the river flood of the White Volta. To quantify the hazard of a flood event, the probability of occurrence and the extent of the flood are often taken into account

(Kron, 2005).

Flood hazards at a certain location can change as a result of different things. For example, urbanisation can often require channelising the river and construction of dikes near the city. This reduces the probability of the occurrence of a flood in that area. However, downstream, the flood peaks become higher which can cause floods of a larger extent that occur more often.

The same can happen when dams are constructed. When the retention volume in the river is large compared to the volume of the flood peak, the water can be stored upstream, which lowers the probability of occurrence of a flood downstream. At the same time, the backwater curve upstream of the dam can increase the flood hazard in upstream villages. It is important to map this shift and research the exposure and vulnerability in these flood-prone areas in order to know whether the shift will cause problems.

3.3.2. Exposure

"The situation of people, infrastructure, housing, production capacities and other tangible human assets located in hazard-prone areas" (UNDRR, 2020).

In this research, elements exposed to the floods in the White Volta basin are quantified. These elements can, for example, be humans, crops, time, environment and so on. To be able to map the exposure, elements have to be categorized based on similar economic values or vulnerability. For example, a differentiation can be made between urban and rural areas as the values of houses and landscapes differ. The type of income on which people depend also differs for urban and rural areas. In regions where a lot of farmers live, a flood can create income loss by flooding the farmland and destroying the crops (Widiarto, 2013).

In this research, due to scarce data availability, only three types of exposed elements were considered: population, buildings and agricultural land. Buildings include houses and industrial buildings like factories. The buildings are subdivided into two types: self-made wooden houses and stone houses. This will be elaborated on in section 4.4. On top of the hazard map now builds the exposure map that defines how many people live in an area, how many houses are built in that area and how many hectares of agricultural land use there is.

3.3.3. Vulnerability

"The conditions determined by physical, social, economic and environmental factors or processes which increase the susceptibility of an individual, a community, assets or systems to the impacts of hazards" (UNDRR, 2020).

In the context of this research, vulnerability is the chance of losing value of the exposed elements due to river floods. This depends on the distance to the river and the ability to cope with the hazard. When elements are resilient against floods, or people have the ability to move their properties in time, the vulnerability decreases. In developing countries, this coping mechanism is often limited by information access and resources. The possibility of adaptation against floods depends mainly on money or governments interest. This is hard to quantify, especially in data-scarce areas like northern Ghana. For each of the defined exposed elements, the vulnerability depends on another aspect of the flood.

The vulnerability of inhabitants living near the river is among other things related to the risk of drowning or hypothermia as a consequence of the flood. This can happen when the rising velocity of the water is too high and people cannot evacuate in time to a safer place. For children, the fast-rising water can even reach heights at which swimming techniques are needed to survive. Places, where a lot of people live near the river bed, will be the most vulnerable when it comes to loss of human lives as they have the least time to evacuate.

For buildings, the vulnerability depends on the maximum reached water depth of the flood. When the water level becomes too high, the water will enter houses and damage, for example, the floor or furniture. The value decrease per inundation range is determined using depth-damage functions specified

on different elements, these functions are elaborated on in appendix I. In some research, inundation depth is also taken into account as a cause for traffic delays when infrastructure becomes impassible. In this research, it is assumed that the economical value of time has a far lower impact than the damage that floods can cause on houses and crops. However, when it comes to industry, for example, the drinking water intake point in Tamale, the inundation depth can have a large economic impact in case the plant has to close down for some days and drinking water facilities become scarce (Kron, 2005).

Finally, for agricultural areas, the vulnerability mainly depends on the duration of the flood. Most crops can handle being flooded with water for some hours. But when the flood duration is larger than one day, many crops will drown as they do not receive oxygen anymore (Widiarto, 2013).

3.3.4. Flood Risk Quantification

As described at the beginning of this paragraph, the total flood risk can be quantified according to equation 3.11 (Kron, 2005):

$$\text{Flood risk} = \text{Hazard} * \text{Exposure} * \text{Vulnerability} \tag{3.11}$$

The exposure and vulnerability are combined in categories in a map where different threshold values define the level of exposure or level of vulnerability. That map is then covered with hazard maps, showing which places will experience the highest flood risk. Defining this map for a historical flood, in the case of this research the 2003 flood, gives the possibility to compare different scenarios including multiple small dams to the original situation. Comparing the maps visualises the shift in flood risk which helps to determine which possible dam locations or dimensions are the most effective in reducing flood risk.

4

Data Collection

In order to build the hydraulic model, different types of input data were required. In this section, the data sets used to set up the model are described. First, geographical data was collected in order to get insight into the shape of the river and the surrounding area. By using QGIS and satellite data, it was possible to locate open waters and create maps showing the land elevation in the surrounding area.

Besides the shape of the river, it was also important to know how the water and the sediment in the riverbed behave. Therefore, discharge data at three different stations in the White Volta river was analysed in Python and converted back to water level date after which it was used as input for the hydraulic model. Also, the characteristics of the sediment were collected by using research performed by HKV in 2011 (Udo & Termes, 2011). This provided the grain size in the river bed which was important for calculations on the morphology of the river.

Finally, QGIS was used again in order to quantify the flood risks. To do so, population, houses and agricultural areas that are affected by floods were mapped and their vulnerability against floods was researched.

4.1. Geographical Data

Different maps of the project area were created using QGIS. It was important to know the shape of the river for understanding the hydraulics of the river. And the shape of the landscape near the river was needed to model the flood development.

4.1.1. Remote Sensing for Open Water Detection

Remote sensing can be used to accurately detect water bodies from space. Satellites that orbit around the Earth carry different sensors that can be used in order to detect and monitor changes at the Earth's surface. The basis lies in the unique interaction of natural elements with light. Using the knowledge on these interactions can, for example, help distinguish between different types of vegetation, soils and open water bodies. Here, this principle was used in order to make accurate maps on the White Volta river stream by detecting open water with satellite data.

Light is a series of photons that follow a certain path, send by the sun or by an artificial light source. When the photons reach a water surface, they can either be absorbed by the water (or particles in the water) or they are reflected. Reflection is called scattering and can occur in the forward direction or in the backward direction. Backward scattering is detected by the satellite and provides information on the scattering surface.

Different types of satellites can be used to detect water in this way, but they all have a unique spatial, temporal and spectral resolution. Spatial resolution determines the pixel size of your output, temporal

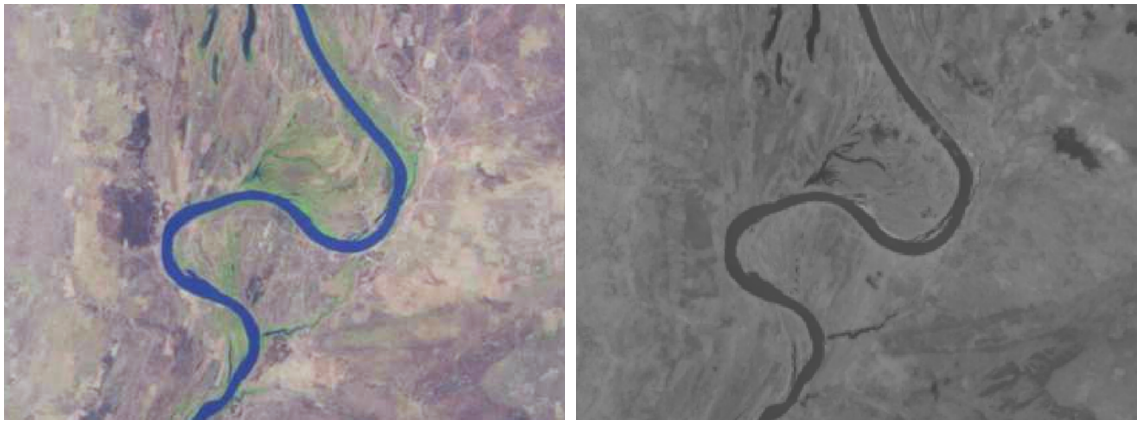

Figure 4.1: Comparison between SWIR sentinel data on the right and NIR Landsat data on the left. Both are able to detect the river shape in a good way but the smaller resolution of the sentinel data causes the shape to be slightly more clear.

resolution determines the time interval at which measurements are taken for one location and spectral resolution is the wavelength interval at which a sensor can make measurements. Therefore, the needed outcome determines the type of satellite that should be used. For instance, when determining the location of a river, a small spatial resolution is best. However, for data on the flood extent, a small temporal resolution is desirable, as you need information at the moment that the water still covers the floodplain. When a satellite measures once every two weeks, a flood can easily have been missed.

Two satellite missions that can be used in determining the river shape are Sentinel-2 and Landsat-8. Both satellites have sensors to send out different bandwidths of which: blue, green, red, near-infrared and short wave infrared (SWIR). These are often the bands used to detect water. The data of these satellites differ in resolution. Figure 4.1 shows the different raster files from the SWIR sentinel data and the NIR Landsat data. Both figures are detailed and are able to detect the river well. However, the spatial resolution of the Sentinel data is 20 meters while the spatial resolution of the Landsat data is 30 meters. Also, the available Landsat data of the basin was not completely cloud-free which made it harder to receive clear figures for some parts of the river. For these reasons, it was decided to continue with Sentinel raster data.

The sentinel-2 mission was started in 2015 by the European Space Agency (ESA). Two exactly similar satellites (Sentinel-2A and Sentinel-2B) occupy the same orbit, 180 degrees apart. Their satellite revisit period is 10 days, generating two types of products: level-C Top of the Atmosphere reluctance data and level-2A bottom of the Atmosphere reluctance data (ESA, n.d.). From the EartExplorer tool of USGS, three different bands of the level-2A sentinel data are available: SWIR, vegetation red edge and red. In figure 4.1 it is shown that only the SWIR band can already detect the open water detailed enough to make a correct shapefile of the White Volta River.

In Appendix C, the conversion from sentinel data to a shapefile is shown. This is needed as the hydraulic model takes vector as input and adds the cross-sections and bed level per created node.

4.1.2. Digital Elevation Model

A Digital Elevation Model (DEM) is a data map that shows the elevation of the landscape. This data is important, first of all, because the river runoff characteristics depend largely on the slope of the landscape, and secondly because the river slope has an influence on the flow velocity of the water in the river. The Japan Aerospace Exploration Agency (JAXA) supplies open-source DEM data of floating values with a spatial resolution of 30 m, measured by the Advanced Land Observing Satellite (ALOS) (Japan Aerospace Exploration Agency, 2021). In figure 4.4, the DEM, based on this satellite data, is shown. The heights are based on the height above sea level in meters. The figure shows no extreme height differences within and around the river stream.

4.1.3. Bathymetry

A bathymetry is similar to a DEM but specified on underwater surfaces. However, a bathymetric survey can not be performed by satellite missions. Instead, the shape of a river bed is often measured by echo soundings. To perform such surveys, a boat with the right measuring equipment has to make measurements along the whole river reach. Therefore, making a bathymetry costs a lot of time and there is little open-source data available.

Even though there have been projects for which bathymetries were made, the data was not available for this research. Therefore, the bathymetry was created based on a combination of the DEM, five measured cross-sections from a previous project (Udo & Termes, 2011) and Google satellite images. An important assumption that was made in this determination of the bathymetry, is that the Google Satellite images are taken at a bank-full situation. This assumption is based on a field visit to Yapei, by Jasper Schakel. Using this assumption, the river width on these satellite images was measured in QGIS at every kilometer on the shapefile of the river. These measured widths were then interpolated over the whole river to create a value for the width at each cross-section (node) in the hydraulic model.

The bed height was determined based on the DEM. By using the profile tool in QGIS, the DEM values underneath the shapefile of the river could be determined. The DEM values at the place of the river do not represent the river bed because the light beam of the satellite is not able to penetrate through the water. Therefore, in the best case, the water level is measured. But in a more realistic case, the beams are absorbed or scattered away at the places where water was found, which makes the DEM value an interpolation of the nearest surface. This value was used as the top of the riverbank. To know the level at which the river depth is located, these DEM values were lowered with the interpolated values from the known cross-sections at Yarugu, Pwalugu, Nawuni, Daboya and Yapei. As the original data is affected by landscape interruptions like trees, buildings or hills, the data is not as smooth as you would expect from a riverbed. Therefore, the moving average of the data was calculated and used instead. In this case, that means that for every group of 300 connected data points, the average is taken. Figure 4.2 shows the riverbed data from the DEM compared to the moving average of this data. An important limitation of this method is, that at places where the beam does scatter back on the water surface, the water level is measured, which is not necessarily a bank-full water level. As a result, the river bank will come out lower than is the case, in reality, creating a mismatch between the river shape and the floodplain. To minimise this problem, the 2D grids were adjusted to fit on the 1D bathymetry. This procedure is explained in appendix D.4.

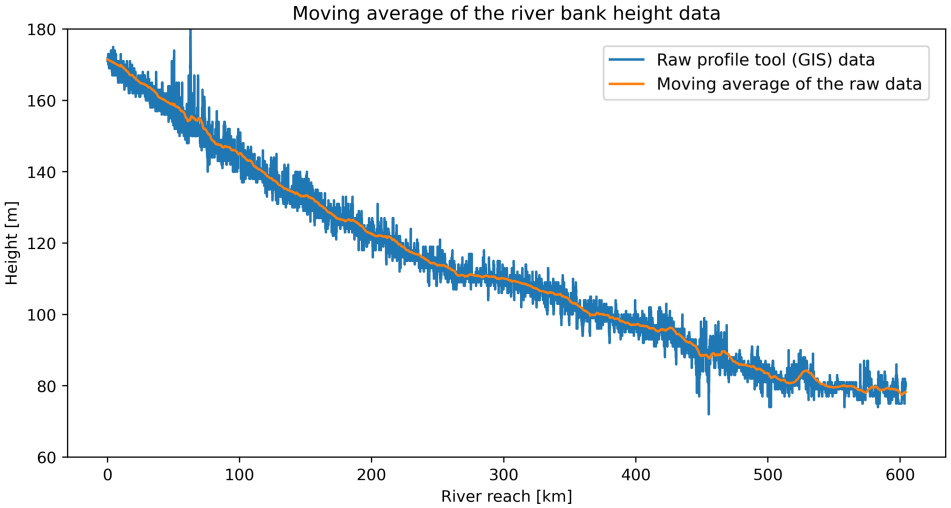

Figure 4.2: The riverbed height over the river reach of the White Volta. The figure shows both the data before the moving average was used (blue) and after the moving average was taken (orange).

4.2. Hydrological and Hydraulic data

In this section, the hydrological and hydraulic data are explored. Hydrological data is the data that results directly from rainfall and evaporation amounts, the discharge data. Hydraulic data is related to both the hydrological events as well as the river characteristics. In this research that is the water level data.

4.2.1. Discharge Data

Discharge data is available at three different stations in the river. The data is converted from water level measurements to discharge by rating curves before sharing.

The measurements in Yarugu are almost continuous between 1992 and 2007, in the other locations there are large gaps. Therefore, only the data from the years 2000 up to 2007 was used in this research. Figure 4.3 shows the plots of the discharges during these years. In figure 4.4, the locations where these measurements were taken are shown. The discharge data was interpolated to create a continuous dataset. The interpolation was done by using the mean discharge ratio with Nawuni, as that is the most complete dataset.

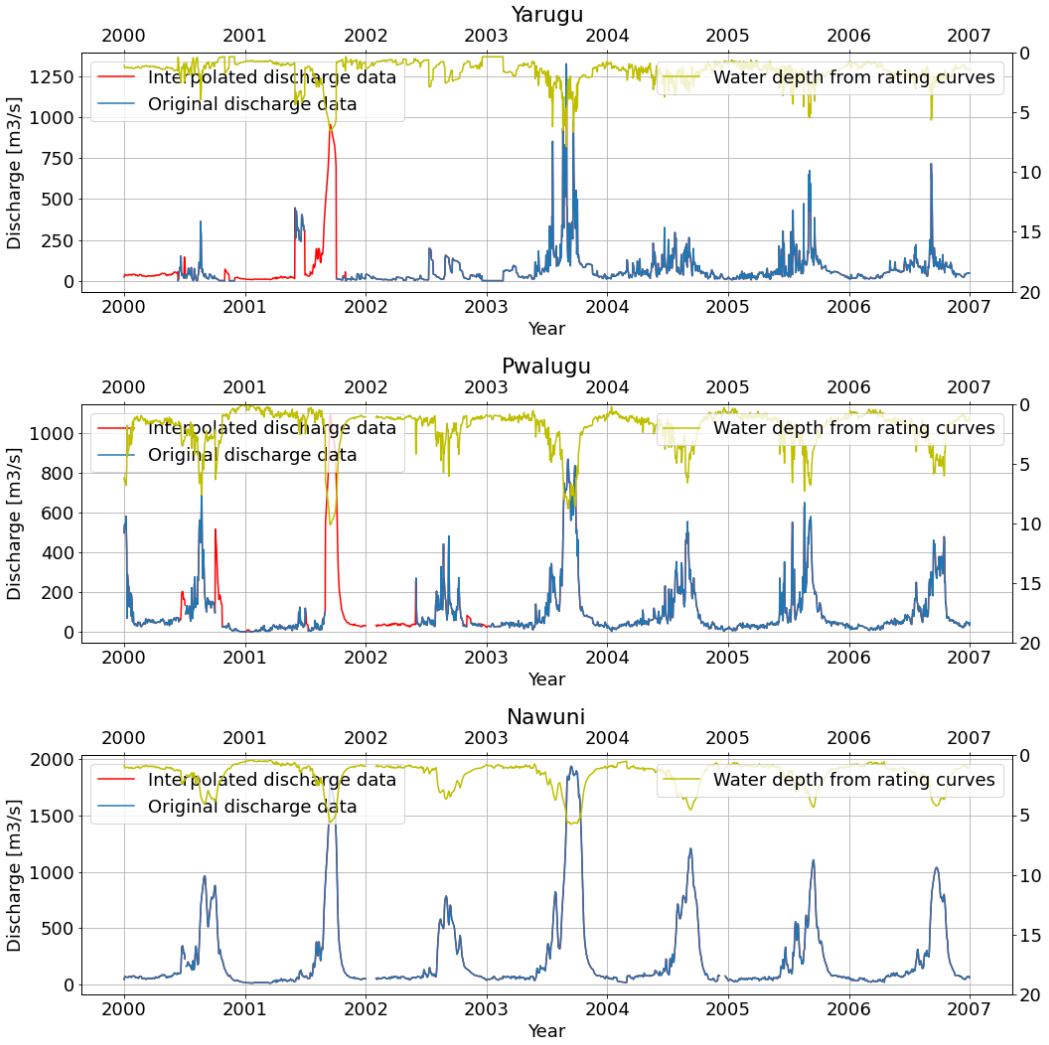

Figure 4.3: Discharge data was given at three stations in the river section. From North to South, the plots show discharge in Yarugu, Pwalugu and Nawuni over the time period between 2001 and 2007.

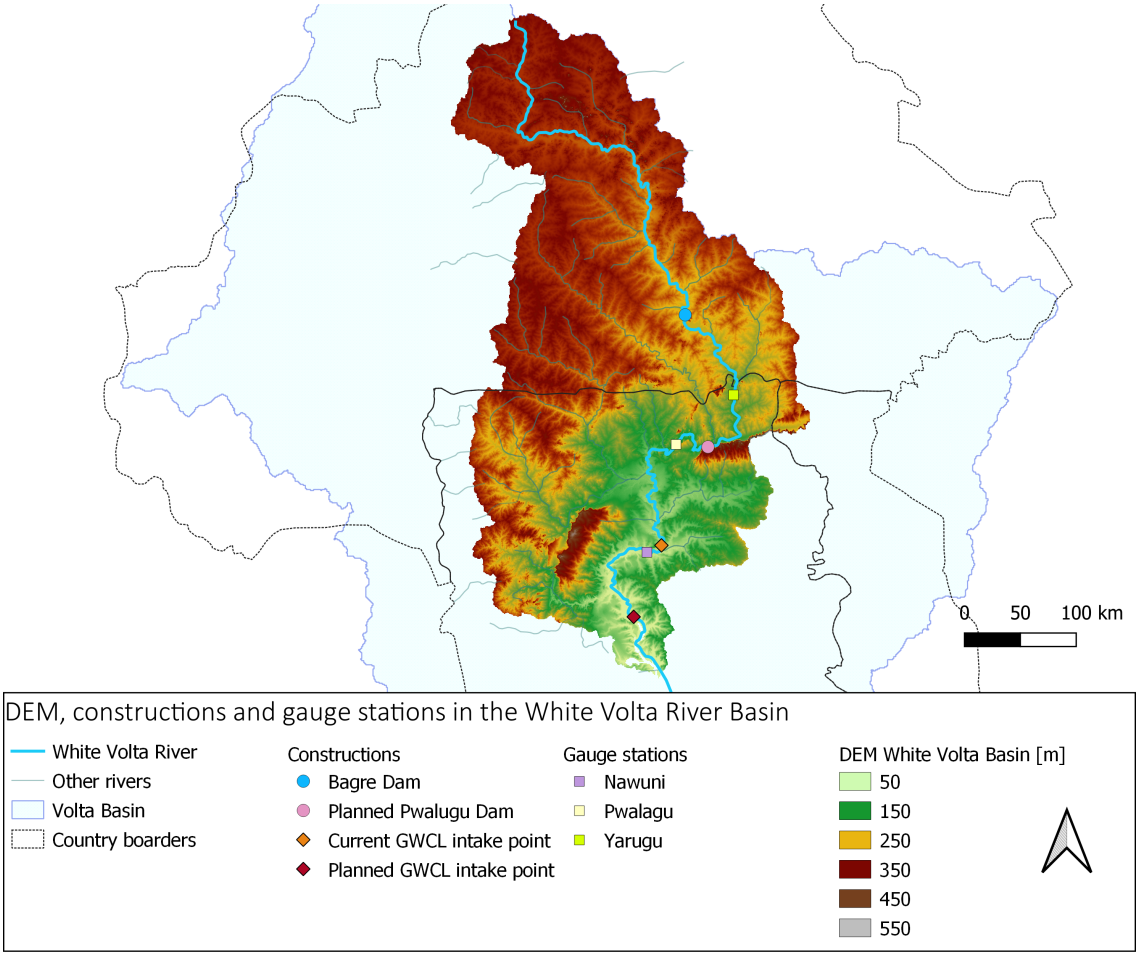

Figure 4.4: Locations where the discharge data is measured and the current and planned constructions in the White Volta River. The Digital Elevation Model (DEM) is displayed over the basin. It becomes clear that the basin does not vary significantly in height, especially in the areas near the river.

The plots in figure 4.3 show the gauge stations starting upstream of the White Volta, moving downstream. During the discharge peak in 2003, it seems like the discharge in the river decreases between Yarugu and Pwalugu station. This is not as expected, considering the fact that one of the largest tributaries of the White Volta, the Red Volta, merge downstream of Yarugu. The amount of extracted water for irrigation or groundwater recharge are unknown. But with this amount in discharge reduction, it can be expected that the rating curves used to calculate the discharge, did not have the right shape parameters. Therefore, it was decided to look into these parameters and convert the discharge data back to water level data.

4.2.2. Water Level Data

The provided discharge data is calculated from water level measurements by rating curves. This transformation formula is shown in equation 4.1.

$$Q = cH - a^p \tag{4.1}$$

in which:
H = measured water depth [m]
a, p, c = shape parameters of the rating curve

The shape parameters of these rating curves are given by the field report of HKV (Udo & Termes,

2011). Table 4.1 shows these parameters for the stations Yarugu, Pwalugu and Nawuni. These shape parameters are used to calculate the originally measured water depth. These are shown in figure 4.3 on the right axes. Because this data is more reliable than the discharge data, it was decided to use the water levels in Yarugu as the upper boundary condition of the hydraulic model. The water level data at the other two stations were used for calibration purposes.

Table 4.1: Shape parameters that were used in the rating curves to convert gauge measurements to discharge data.

Gauging station	c	a	p
Yarugu	53.24835	0.115048	2.029657
Pwalugu	27.82398	0.02857	1.582736
Nawuni	34.55162	-0.20751	1.794556

Hydrolare is the international data centre on the hydrology of lakes and reservoirs. They analyse, process and improve data to make it more easily accessible for projects and research. From this database, the water level data of Lake Volta was extracted.

Another dataset was formally requested by the Volta River Authority and shows the water levels compared to sea level at the Akosombo dam. Both The results are shown in figure 4.5.

Even though it was expected that the satellite data would provide more accurate data as it is based on levels measured over the whole lake, it seems like both data sets give similar water level values. However, the in-situ data, measured at the Akosombo hydropower dam, is more continuous. Therefore, it was decided to continue with this data as the lower boundary condition in the hydraulic model.

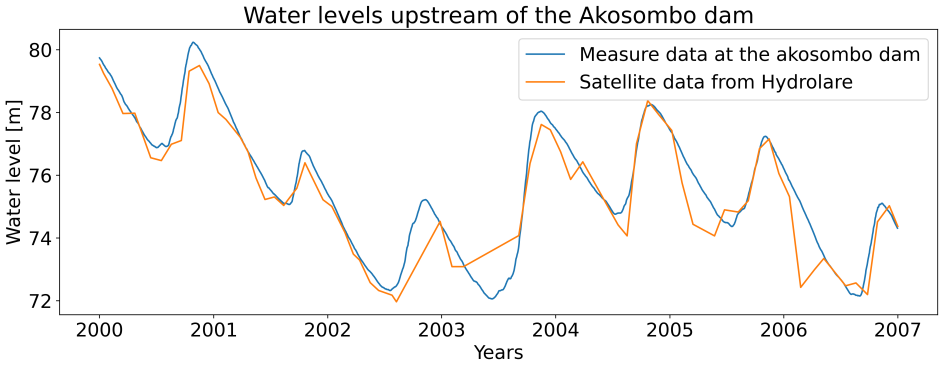

Figure 4.5: Water level data of Lake Volta measured by Hydrolare compared to the in-situ water levels measured at the Akosombo hydropower dam.

.

4.3. Sediment Characteristics

The name of the White Volta river already reveals its characteristic suspended sediment types: fine sand, silt and clay. When suspended in the water, these sediments give the light colour. However, the riverbed itself mainly consists of sand and gravel. The banks of the main channel consist of sand and silt in the upstream reach, and gravel and clay in the downstream reach of the river (Udo & Termes, 2011).

HKV has performed research in the grain size distribution in the White Volta. Table 4.2 shows the results of this research (van der Zwet, 2012).

The density of the bedload in the riverbed is 2650 kg/m^3 (Udo & Termes, 2011) and the porosity of the sand is 0.4. These parameters were needed in the model in order to determine the transport of

bedload that takes place. That is important to know the amount of sedimentation.

Table 4.2: Grain size distribution of the riverbed near Pwalugu (Udo et al., 2011)

River bed section	Av. D16 (mm)	Av. D50 (mm)	Av. D84 (mm)	Av. D90 (mm)
Inner bend	0.27	0.42	0.65	0.75
Middle section	0.40	0.70	1	1.2
Outer bend	0.75	1.4	3	4.5

4.4. GIS Data used for Flood Risk Determination

As explained in chapter 3.3.4, flood risk is determined by a combination of the flood hazard, the exposure of the affected elements and the vulnerabilities of those elements. The flood hazard is based on the return period and the extent of a flood. The exposure is based on the number of people, buildings and agricultural land that is affected by the flood. And the vulnerability is based on the characteristics of the flood and the ability to cope with the situation.

By combining these three different maps (flood extent, exposure, vulnerability) for the known flood in 2003, a base case is created. The model can then be calibrated on this base case. After that, the scenario in which small dams are constructed in the river bed can be compared to the base case in order to map the changes in flood risk.

These flood risk maps were created for seven flood-prone areas near the White Volta river.

4.4.1. Flood Hazard Map

The flood hazard map follows from the 1D2D hydraulic simulations and shows the flood extent and the inundation depth of the flood. The output is based on a combination of surface elevation and hydraulic characteristics. These hydraulic characteristics are influenced mainly by the water level data at the boundaries, the roughness of the river bed and the hydrological input.

A 1D2D hydraulic model can be calibrated on a historical flood by comparing the simulated flood extent of a historical flood to the satellite data in that same year. A satellite that is attractive for these near-time studies, is the MODIS (Moderate Resolution Imaging Spectroradiometer) due to its small temporal resolution of 1 to 2 days. The downside is that it has a spatial resolution of 250 meters. Therefore, if the Landsat satellite or the Sentinel satellite has covered the flood at the right time, these images are preferred (Ahamed, Bolten, Doyle, & Fayne, 2017).

However, for this research, it was not possible to do this calibration as the historical flood occurred during a clouded period. This highly disturbed the images in a way that the surface became invisible.

4.4.2. Exposure Map

As explained in section 3.3.2, the exposed elements taken into account in this research are the number of buildings, the number of people and the area of farmland that is affected by the flood. The exposure map will be created for high-risk places: inhabited places where floods occur. To illustrate, an example is shown in figure 4.6 of the small village Nawuni, located near the White Volta river.

To create these maps, the Open Street Map (OSM) function of QGIS is used from where different elements can be extracted. From there the buildings are extracted as polygons. These polygons were then converted to points in the centre of that polygon (the red dot). Comparing this to a Google Earth Satellite map, showed that not all the buildings were captured by OSM. Therefore, the missed buildings were added by hand (the orange dot). Together these dots show the exposed building in the flood-prone area.

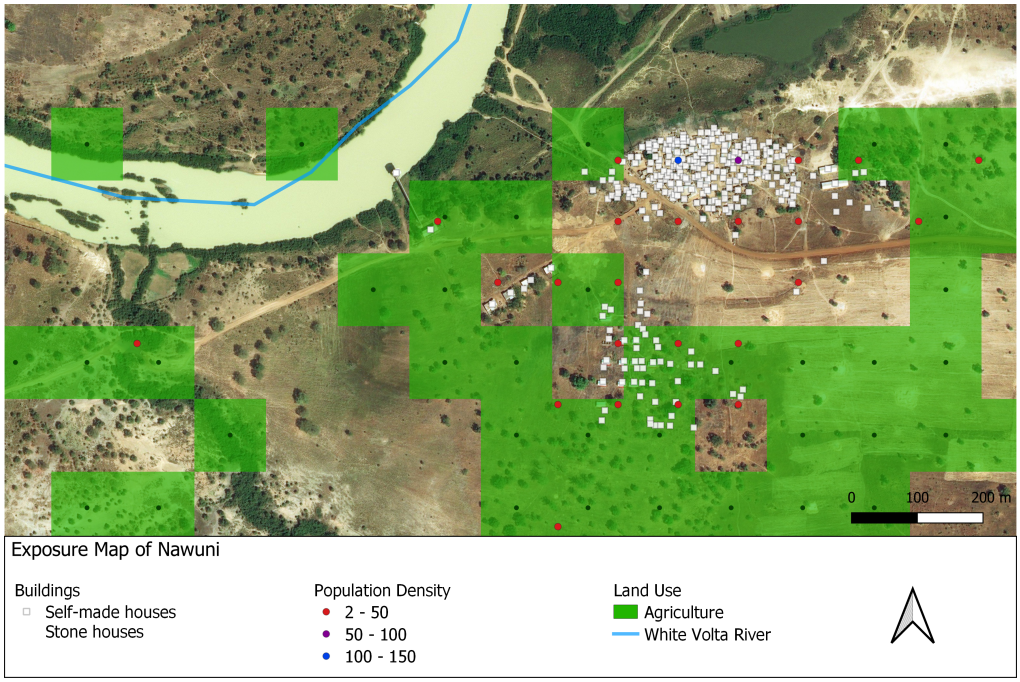

Figure 4.6: Exposure map of Nawuni. The green areas show the agricultural land. These areas are only included once the flood extent passes the centre point, shown by the darker green dot. The population density is also extracted from raster data and grouped in ranges of 50 people per hectare. Lastly, the white cubes show where buildings are located.

Secondly, a population density map of Ghana was added in order to know how many people are affected by the floods. This grid is shown in greyscale and has a resemblance with the building layer. The data was received from the WorldPop Open Population Repository (Leasure, Darin, & Tatem, 2021).

Finally, the land use map was provided from the ESA Globcover Project, led by MEDIAS France/POSTEL (ESA, 2005). The map distinguished between different types of land use, of which the agricultural purposes are extracted. This is shown in the figure as green and brown rasters. These maps show that all the agriculture in the flood-prone areas was rainfed instead of irrigated. This is highly questionable as the land is so close to the river and Ghana experiences periods of drought. However, that fact does is not relevant for the purpose of these maps.

4.4.3. Vulnerability Map

All elements in the exposure map are vulnerable to different aspects of the flood. Therefore the vulnerability map combines the thresholds for the vulnerability of all these elements. For houses, this means the maximum water height, for people the rising velocity of the water and for agriculture the water height in combination with the duration of the flood. The threshold depends on the ability of each element to cope with a flood.

A lot of different crops grow in Ghana. Cereals, roots, legumes, vegetables, fruit and some industrial products are produced all over the country. In northern Ghana, the most widely cultivated crop is maize (FAO, 2004). Many communities in northern Ghana are both for their food supply as for their income largely dependent on maize production. This increases food insecurity when it comes to natural hazards like floods (Mangnus & van Westen, 2018).

The yield loss of maize as a result of a flood depends not only on the flood height and duration but also on the growing stage of the plant. Four rough growing phases can be distinguished: the initial phase, the growing phase, the flowering phase and the maturation phase. In the first phase, only a small flood can already cause the plant to die as it will be completely covered under the water. Then in the middle phases, the resilience against floods is higher, where a flood cause yield reduction from 5

days on, but death only occurs after 8 days. In the final phase, a flood height up to 120 cm does not impact the crop. But above that, yield reduction will occur after 10 days of flooding (Molinari, Rita Scorzini, Gallazzi, & Ballio, 2019). For this research, it is assumed that all crops in northern Ghana are maize in the growing phase, as it represents the most average conditions. Therefore, a flood with a duration of 5 to 8 days reduces the yield by 0 to 100%. The price of different crops in Ghana is shown in figure H.1. Considering the prices of Tamale, it follows that the price of maize is 140 GHS per 100kg. Per hectare land, about 1.5 Mt maize is produced in Ghana (Ragasa, Chapoto, & Kolavalli, 2014). From this, it can be concluded that the profit of maize can be 21 GHS per hectare.

For buildings, the loss of value as a result of floods is often expressed in depth-damage curves. Previous research in Kumasi has made a rough estimation of the flood damage. For residential buildings, the distinction was made between stone houses and self-made houses. The stone houses are built on a foundation and, therefore, have the advantage that a flood up to 20 cm does not impact the house and the household effects, like furniture. Self-made houses are often made of natural materials and are less resilient against floods (Wiersma, 2020). In figure I.1, the depth-damage curves of both types of houses are shown.

Table 4.3: Inundation depths compared to the damage costs.

	Houses		**Maize**		
Inundation depth [cm]	**Stone [GHS]**	**Self made [GHS]**	**6 day flood [GHS]**	**7 day flood [GHS]**	**8 day flood [GHS]**
1- 20	No cost	38	7	14	21
20 - 50	135	76	7	14	21
50 - 100	225	118	7	14	21
100 - 150	345	128	7	14	21
150 - 200	555	150	7	14	21
>200	600	160	7	14	21

Based on satellite pictures of each of the seven villages, it was determined what the building type ratio was (see figure I.2). It was assumed that self-made houses are smaller than stone houses and often have a round or squared shape. Also, the colour of these houses is often darker. The stone houses are assumed to be the larger, lighter buildings that often have a U-shape. Taking these distinctions into account, a rough ratio between the two buildings was determined, shown in table 4.4.

Table 4.4: Ratio stone houses / self-made houses

Ratio stone houses / self-made houses						
Pwalugu	**Duu**	**Janga**	**Dipale**	**Nawuni**	**Daboya**	**Yapei**
0.9/0.1	0.8/0.2	0.9/0.1	0.2/0.8	0.5/0.5	0.6/0.4	0.9/0.1

Calculating flood risk in terms of damage costs becomes more difficult when it comes to human damage. For this research, the population density was included as an indicator of the number of people that suffer from flood damage. But no value is assigned to the damage on the population as a result of for example injuries, trauma or drowning. Furthermore, the population density should be compared to the inundation speed of the flood.

4.4.4. Flood Risk Map

The flood risk map is a combination of all the maps described above. The maps show exactly which places experience the highest flood risk, in terms of money. Floods at places where a lot of elements with high vulnerability are exposed have the highest flood risk. Extreme floods at locations without any elements have a low flood risk, even though the hydraulic characteristics can appear otherwise.

5

Models

This chapter describes the hydrological and hydraulic models that are used to research the impact of the dams on morphology and flood risk in the river. The focus lies on the hydraulic models, as the hydrological model was created as part of the graduation research of another master student (te Witt, 2021).

Three model deliverables are defined: the water depth, the morphological changes and the flood development. These three deliverables all follow from the hydraulic model. The hydrological model is only used as input for overland- and groundwater flow as a result of weather events. D-HYDRO is chosen as the software for the hydraulic model as provides the possibility for both 1D and 1D2D modelling. Data from different gauge stations in the White Volta River and Lake Volta are used to define the boundary conditions and to calibrate the model. Around villages that are located close to the riverbank, the flood development is modelled in 2D.

5.1. Model Deliverables

For this research, a combination of two models was used: a hydrological model and a hydromorphological model. Together, the models can help to answer the research question. Therefore, they have to deliver the following information:

1. The water depth at every location in the river in order to know when and where a flood occurred.
2. The amount of sedimentation and erosion near the dams in order to know how much sand will accumulate upstream of the dam. This information is needed to review the possibility of controlled sand mining upstream of the dam and to know what the downstream effect is on the river bed.
3. The development of a flood in inhabited areas close to the river, in order to know the flood extent and the inundation depth of the flood in a certain area.

5.2. Model Schematization

The model schematization shown in figure 5.1 shows how the hydrological model and the hydraulic model are related to one another. The hydrological model covers the runoff in the whole White Volta Basin, shown as a DEM. As the output of this model, the inflow from the basin into the White Volta river is modelled. This output is then used as input in the hydraulic model where it recharges the river water. The hydraulic model is bounded by the upper gauge station in Yarugu, in the North, and by Lake Volta in the South. In between, the model can be calibrated on the other two gauge stations in Pwalugu and Nawuni. The blue line represents the White Volta river and is used as a shapefile to set up the 1D hydraulic model. The modelled river segment is about 600 km and passes the current and the future drinking water intake points of Tamale. These are points of interest as floods have caused problems in the past for taking in drinking water. Using Google Maps, the inhabited areas near the river stream

were found. These areas were included in the 1D2D model in order to visualize the flood development in those places. Finally, the location of the Pwalugu Dam is shown in the figure, however, the effect of this dam is not included in the model.

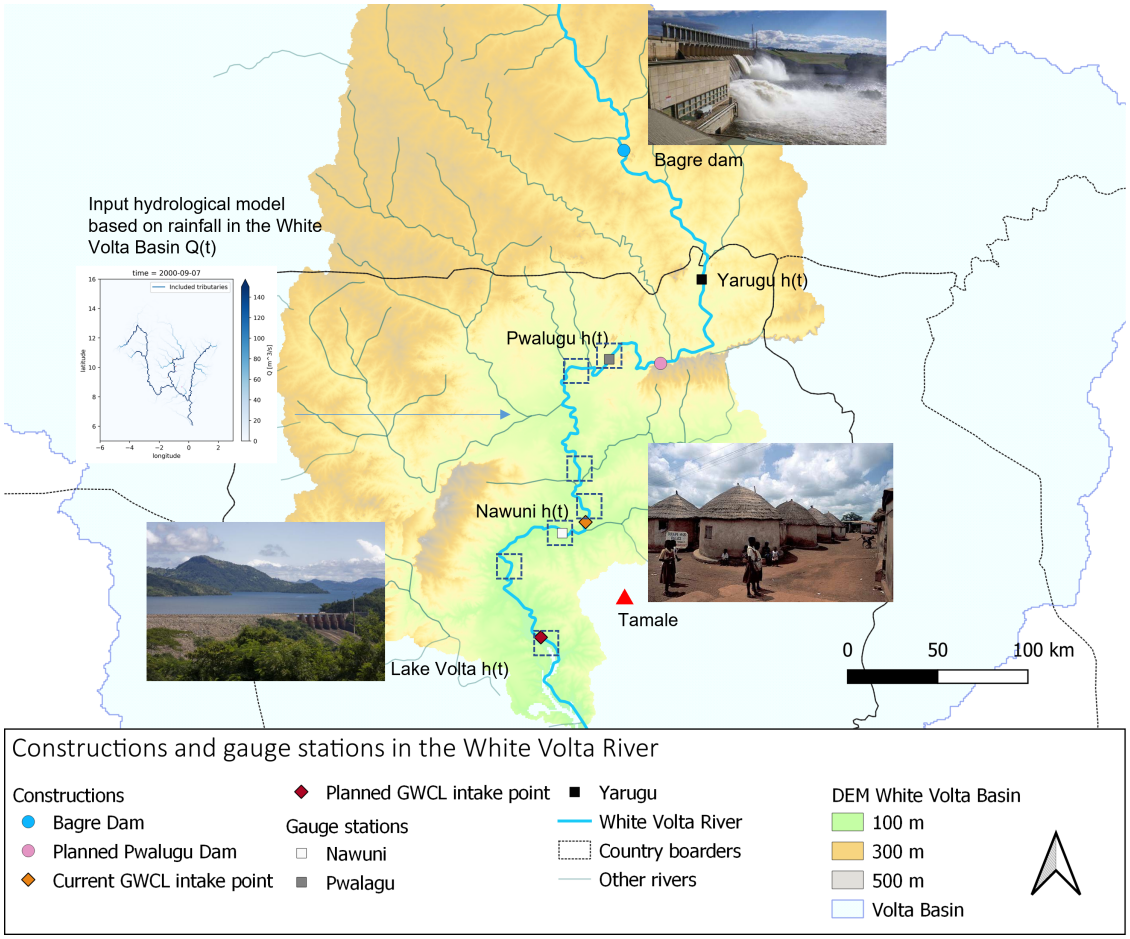

Figure 5.1: Model schematization of the White Volta River. The output of the hydrological model, shown in the graph on the left, will be used as input for the hydraulic model. This hydraulic model is bounded by the water levels in Yarugu and Lake Volta. The dotted squares show the areas that are included in the 2D model. Within these areas, villages are located that have a high risk of being flooded.

5.3. Hydrological Model

The hydrological model was developed by a previous master thesis research (te Witt, 2021). The software W-Flow is used to create the model. The original model runs for the whole Volta Basin. When calibrated on the gauge stations in the White Volta, the model provides maps of the daily mean discharge in the basin. For this research, the model was calibrated on the station in the White Volta River. In figure 5.2a the discharge map for one day is shown. The model can create maps with daily discharge values between 2000 and 2007. The spatial resolution of these maps is 5x5 km.

The daily mean discharge from seven different tributaries was collected and used as input data for the hydraulic model. In figure 5.2a, the locations of these tributaries are shown. Figure 5.2b shows the daily mean discharge over time at the end nodes of each of these tributaries. Especially the Red Volta and the Black Volta can have high discharges during the wet season. However, the impact of the Black Volta on the hydraulic model is minimal, as the tributaries only merge at the inflow of Lake Volta. The output of these seven tributaries was saved and used as input for the lateral flow in the hydraulic model.

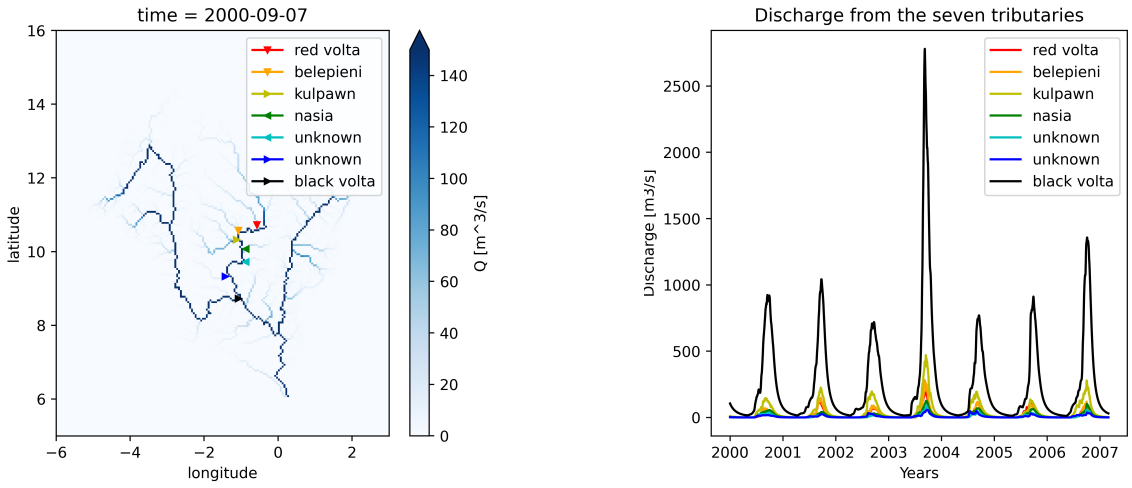

(a) (b)

Figure 5.2: (a). Discharge map from the hydrological model in W-Flow. This map is calibrated on the time period between 2001 and 2007 on the same discharge stations as used in the hydraulic model. The figure shows the data of one day in September 2000. There are maps like these for each day between 2000 and 2007. The red dots show the places from where the discharge data is extracted. (b). Discharge data of the tributaries over time. The data shows the discharge at the inflow locations shown in figure a. between 2000 and 2007

5.4. Hydraulic Model

In this section, the hydraulic model is explained. The schematization of the model is already shown in figure 5.1 with the two boundaries at the Yarugu gauge station and Lake Volta. After that, the considerations to choose D-HYDRO as the most suitable modelling software is explained. Then, the model set-up is discussed and the calibration process is explained. These steps all lead to running different scenario's in which the dams are constructed in the riverbed.

5.4.1. Software Selection

The software Delft3D FM (D-HYDRO) is a currently developed software that builds on older software like Delft 3D Suite, SIMONA, Duflow and SOBEK 2. The software can be used for hydraulic models in all three dimensions. Therefore, it is important to decide beforehand how many dimensions are necessary for this model. A 1D model has a shorter computational time than a 2D model. However, the level of detail is limited for 1D models, so it depends on the required scale of the output and the scale of the input data whether a 1D model gives sufficient information or not.

When it comes to the water level in the river, the first component of the model output, the scale of the model depends on the scale of the input data and the scale of the needed outcome. When detailed data is not available, a detailed model does not improve the outcome a lot because the error is already present in the data. Also, when the impact on the water level spreads out over a large river segment, the computational time of modelling this in detail can become very high. For this research, raster data will not be more detailed than 20x20 meters.

For this research, only the significant backwater effects, that can increase the flood risk were of interest. When looking at comparable projects in the area, backwater effects range in the order of 10 to 50 km (Udo & Termes, 2011). Therefore, detailed 2D models would not add significant value since the scale of the backwater effect is large.

The second component, the morphological changes in the riverbed, is more difficult as it depends on the level of detail that you want to receive on the turbulence near the dam. The goal of doing morphological calculations is to find out how much sedimentation will occur near the dams that can be used for sand mining in the future. Therefore, there is no interest to know the exact movement of the sediment but only the amount of deposition. A 1D model would thus be suitable for the morphological model.

Thirdly, the model needs to provide information on the flood development in the region. To be able to map flood risk, the flood height, extent and duration have to follow from the model. These components require a 2D model that shows the development of the flood.

As the floods only need to be modelled at inhabited places, it was decided to use the D-HYDRO 1D2D software. This software is able to create a 1D model of the river, which enables connections of 2D grids on places of interest. Therefore, the computational time can be reduced in the components that only need a 1D computation, while the flood development can still be determined in a 2D manner. The downside of the software is that only the beta version is available as it was still in development during this research. Therefore, only the basic elements could be set up in the Graphical User Interface (GUI), while the largest part had to be created and run in batch files. Also, some interpolation steps had to be performed in Python and Matlab.

5.4.2. D-HYDRO Model Input

To set up the D-HYDRO model, a model grid was created. The 1D grid was based on the shape of the river between Yarugu and Lake Volta, as shown in figure 5.1. The 2D grid was based on the locations where villages were located close to the river. The step by step approach to creating these grids is explained in appendix D.

By generating computational grid nodes, adding the boundary conditions and initial conditions and refining the shape of the river by defining at least two cross-sections, a first model was created. After running this simple model in the GUI, the model was exported and further developed in text files.

The cross-sections were defined as described in 4.1.3. These river width values were interpolated using Matlab and Python codes. The river depth was interpolated and flattened using the moving average of the raw data from the profile tool in QGIS. By combining these tools, the cross-sections were defined for every computational grid node in the model. Then, the lateral inflows from the hydrological model and the physical parameters were defined, after which the model ran by batch files. This approach was chosen because the software is still in development and the GUI did not perform well enough yet to be used. The detailed steps of how the model was built are described in appendix D.

In order to receive the required model deliverables within the optimal computational time, three slightly different models were created: a 1D model without morphological simulations, a 1D hydromorphological model that can be used in order to simulate the changes in the river bed and a 1D2D coupled hydraulic model for determination of the flood risk. The 1D model has a small computational grid node density in order to accurately model the morphological changes as a result of the dams. The 1D2D model already has a large computational time due to the 2D modelling. Therefore, the morphological output of the 1D model was used as input, after which the model could run without morphological calculations and with a larger distance between the computational grid nodes. This decision comes with the assumption that the 2D component of the model has a limited impact on the morphology.

5.4.3. Model Calibration

As there were three gauge stations in the White Volta river, one used as the upper boundary of the model, there were only two stations on which the model could be calibrated: Pwalugu and Nawuni. Calibration was done by changing the Chézy roughness parameter in order to influence the discharge and water levels in the river.

The first calibration round was needed for the first morphological run in order to find the equilibrium state for the bed level. This calibration was done on the 1D2D model without morphological components to reduce computational time. Appendix F.1 shows the results of the different Chézy value combinations used for this first calibration. It was decided to run the model with a Chézy value of 60 $m^{0.5}/s$ on the part upstream of Pwalugu and a Chézy value of 50 $m^{0.5}/s$ on the downstream part.

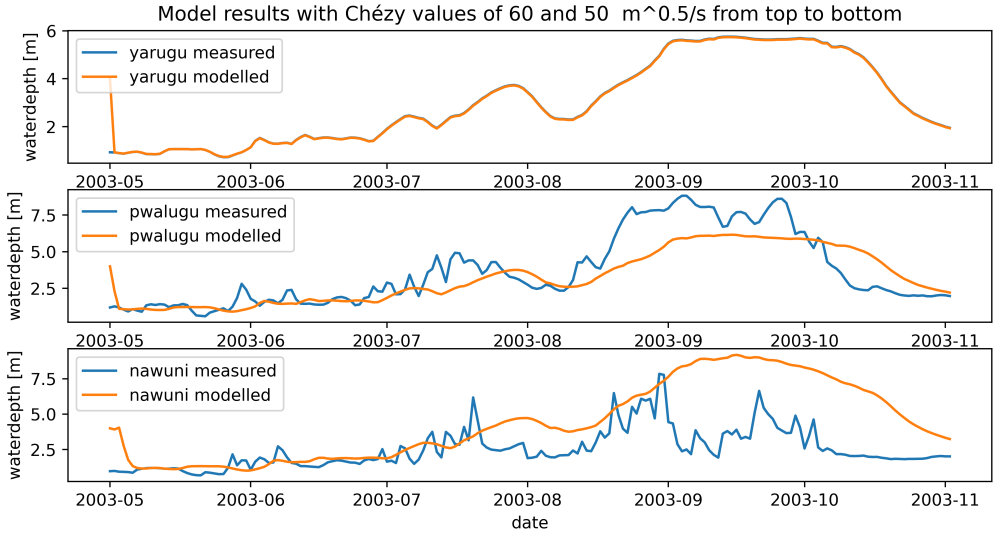

Figure 5.3: Results of the first rough calibration.

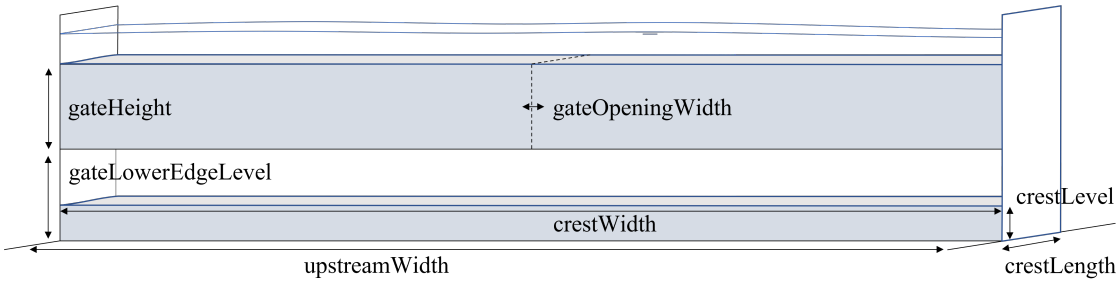

Figure 5.4: The possibilities of the adjustable structure in D-HYDRO. The upper figure is a schematization of the dam as used in this research. The crest is a closed structure that can have any size up to the river bed width. The gate lower edge determines the opening height between the gate and the crest. The gate opening width can be adjusted, so, that there is an opening in the middle of the gate. In this research, the gate is closed. All the other parameters are specified for each dam location.

5.4.4. Implementing Dams near Flood Prone Areas

After calibration of the base case, the scenario in which dams are implemented near the flood-prone areas could be modelled. The D-HYDRO software is able to create different types of structures, like dams, orifices, dams, bridges etc. As explained in section 3.1.1, the dam design in this research contains openings at the bottom in order to maintain the base flow at all times. Therefore, it was decided to create a 'general structure' where you can schematise the structure with pipes near the bottom. In figure 5.4, this basic adjustable structure of D-HYDRO is shown. The gate is able to open up, the crest width can be adjusted within the boundaries of the riverbed width and the space between the gate and the crest can be changed. The goal was to find a design that stores water upstream and mitigates the floods during the wet season while maintaining the base flow during the dry season. By experimenting with different dimensions for every flood location, seven unique structures were created for this research.

The gate- and crest height of the structure is dependent on the location where the structure is placed. Figure 5.5 shows the corresponding dam locations chosen for the model. The locations are about 2 kilometers upstream of the villages. That way, the location is close enough to be used as a sand supplier, but far enough to mitigate the flood onto an uninhabited piece of land.

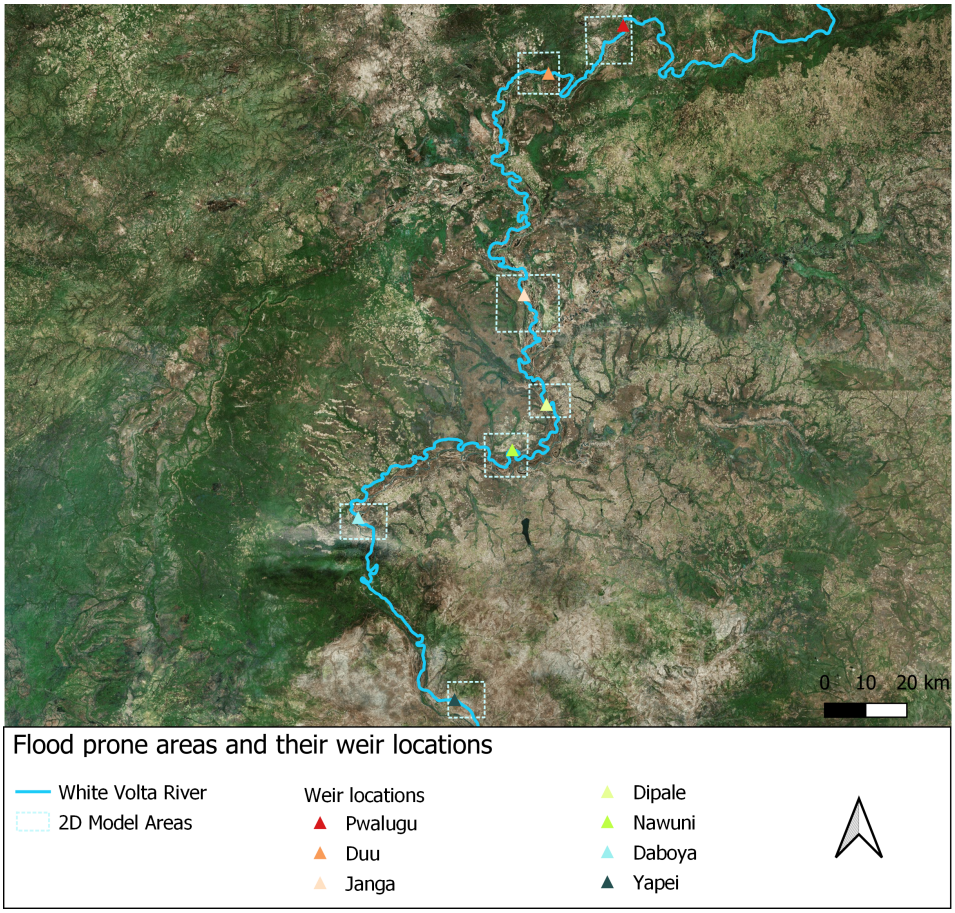

Figure 5.5: The locations where the dams are implemented on the river reach. Each dam is located about 5 km upstream of inhabited areas within the flood-prone regions.

5.4.5. Hydromorphological model

The hydromorphological model includes sediment characteristics and is able to simulate the morphological changes in the bed level. The model was used twice, first in order to find an equilibrium state in the base case, then to simulate the impact of the dams on the bed level. Both model runs are described in this subsection.

After taking the moving average, the bed level data was still very irregular (see figure 4.2). Therefore, in order to create a more realistic bed level, the hydromorphological model was run for 50 years and the final changes in the bed level after that run were used as input for the real model. To do so, the 1D model was adjusted, so that the computational grid size was 50m. In order to make calculations on grid sizes as small as that, the user time interval was reduced to 60 seconds. Then, the morphological scale factor was set to 50, which means that one year of morphological changes is repeated 50 times. This way, a bed level can be imitated that has experienced 50 years of hydraulic forces while only running the model for one year, reducing computational time.

The beginning and final situation of that hydromorphological run is shown in figure 5.6. The output of the morphological run shows a bed level that is in equilibrium. This bed level was used as the initial bed level to run the base case and the scenario including the dams on.

After creating and running the base case. The final hydromorphological model was built. To do so, the sediment and morphological files were added to the master definition file of the model. The characteristics from the field research of HKV were used as input for the sediment file parameters (Udo & Termes, 2011). The morphological scale factor was set to 25 so that the output represents a situation in which the year 2003 has occurred 25 times. Appendix D.2.2 shows the exact parameters used in

the input files.

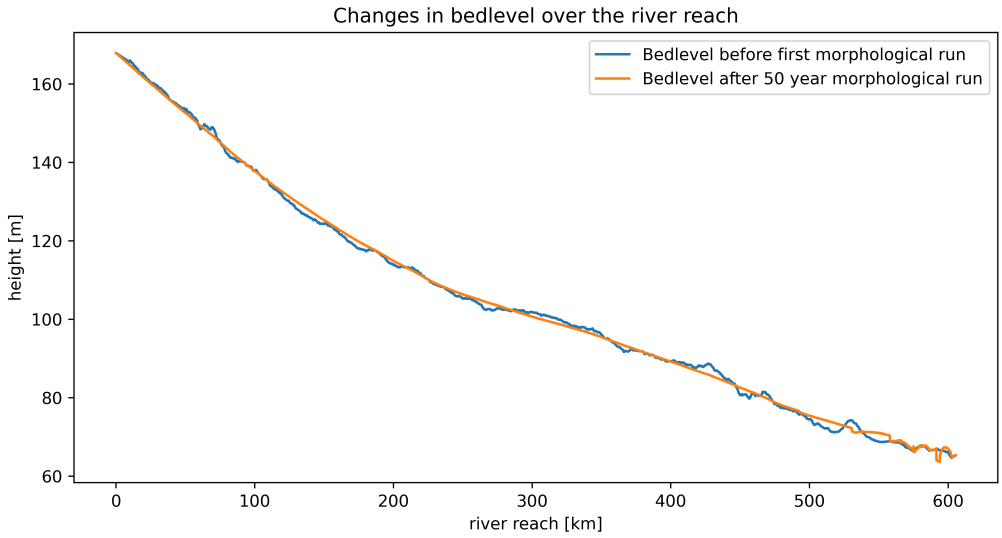

Figure 5.6: The bed level before and after the first morphological run. The blue line shows the bed level after taking the moving average of the DEM data underneath the river. The orange line shows the state of the bed level after the year 2003 was run fifty times in a row. The erosion that has smoothened the bed level, did not move all the way downstream yet. So, for a better result, the model should have run even longer.

5.4.6. 1D2D Hydraulic Model

After finishing the 1D hydraulic model, the model was extended with 2D grids. In order to keep reduce the computational time, the distance between the 1D grid nodes was first increased to 1000 meters. For every flood-prone location, 2D grids were created using the RGFGRID tool. The DEM was then interpolated over these grids in order to simulate the behaviour of the water when it flows out of the river bed. Appendix D.4 elaborates on the exact steps that were taken in order to set up the coupled 1D2D model.

The seven grids all cover areas of about 20 km around a village. They have grid sizes of approximately 200 meters. The model was only able to connect the grid nearest to the 1D computational grid node. As a result, the water is only able to leave the 1D model every 1000 meters. Figure 5.7 shows an example of a flood at three different time steps from the start of the flood up to the fully developed flood. The figure shows clearly the impact of the grid sizes on the flood simulation.

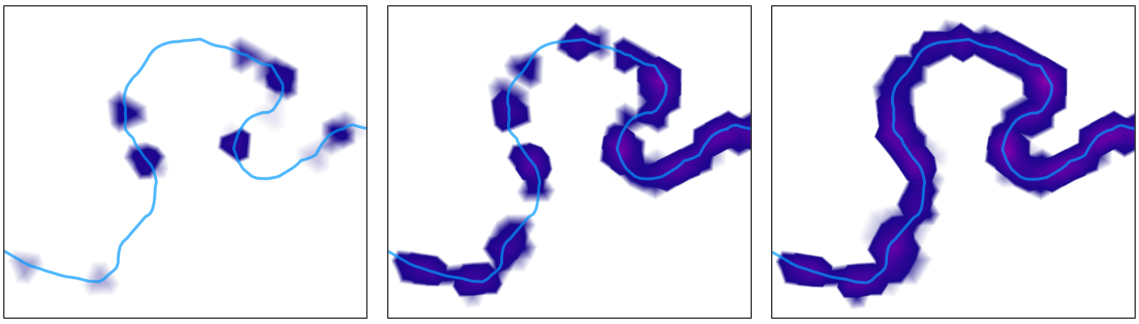

Figure 5.7: Flood development through the 1D2D links. The left figure shows a situation in which a flood is starting to develop. It shows clearly how the river water is only able to spread over the 2D grid from a 1D computational grid node, that is located 1000 meters apart. Moving to the right, the flood develops and the effect of the grid sizes becomes less visible.

6

Results

In this chapter, the model results will be discussed. In the first part, the calibration process is shown that led to a representative base case. The modelled river characteristics during the year 2003 are visualised. Then, based on the results of the base case, the dam dimensions are chosen, so, that the base flow is maintained in the dry season while storing water upstream during the rain season. After that, the impact of the small dams on the river hydraulics and morphology is studied. The results are visualised by flood risk maps for each flood-prone area and calculations on the sediment build-up upstream of the dams.

6.1. The Base Case

The base case was created in order to simulate the river as it is in its current state. To do this, the river characteristics from the literature were used as model input, after which the model was calibrated so that its output fits the measured water depth data.

6.1.1. Calibration Results

The model was calibrated by changing the Chézy parameters over three river segments in the 1D model. As explained in section 3.2.2, the Chézy parameter defines the roughness of the riverbed. The segments on which these values were differentiated are located between Yarugu, Pwalugu, Nawuni and Lake Volta, as those are the locations in the river of which water depth data was available to compare the model to. Figure 6.1 shows the final result after this calibration. The upper graph shows the model boundary and therefore, the input data is the same as the modelled values. This graph is included as it is interesting to see how much of its shape is preserved downstream. A more in-depth description of the calibration process, including a sensitivity analyses of the Chézy parameter, is described in appendix F.2.

From the sensitivity analyses, it became clear that increasing the Chézy parameter has the effect of decreasing the water depth in the upstream region. Therefore, starting downstream, the calibration process was done step by step on the three regions between Yarugu, Pwalugu, Nawuni and Lake Volta. From the calibration, it was found that the model performs best with a parameter set consisting of the Chézy values 30, 40 and 70 $m^{0.5}/s$ respectively from Yarugu moving downstream.

As can be seen in figure 6.1, the model accurately captures the peaks of the water depth. However, moving downstream, a delay in these peaks arises. As the model has to be able to determine flood risk, it was decided that the peaks are more important to capture then the timing of the peaks. Therefore, this parameter set was chosen over sets that did capture the timing aspect but under- or overestimated the peaks.

Looking at Pwalugu, the modelled outcomes are a good approximation of the measured water depth, both in the base flow as in the peaks. However, for Nawuni, the base flow is underestimated. This can

cause unrealistic dry spells in the model after the construction of the dams.

It should be noted that there is no bathymetry available for the White Volta river what makes calibration of the model more difficult. The impact of the river bed has a big influence on the water levels, but these changes in elevation are now almost non-existing. Therefore, the changing water levels are mainly determined by the changing river width and the changes in the roughness of the riverbed, determined by the Chézy parameters. In case a bathymetry would be available, the graphs in figure 6.1 would most likely differentiate more from the boundary condition.

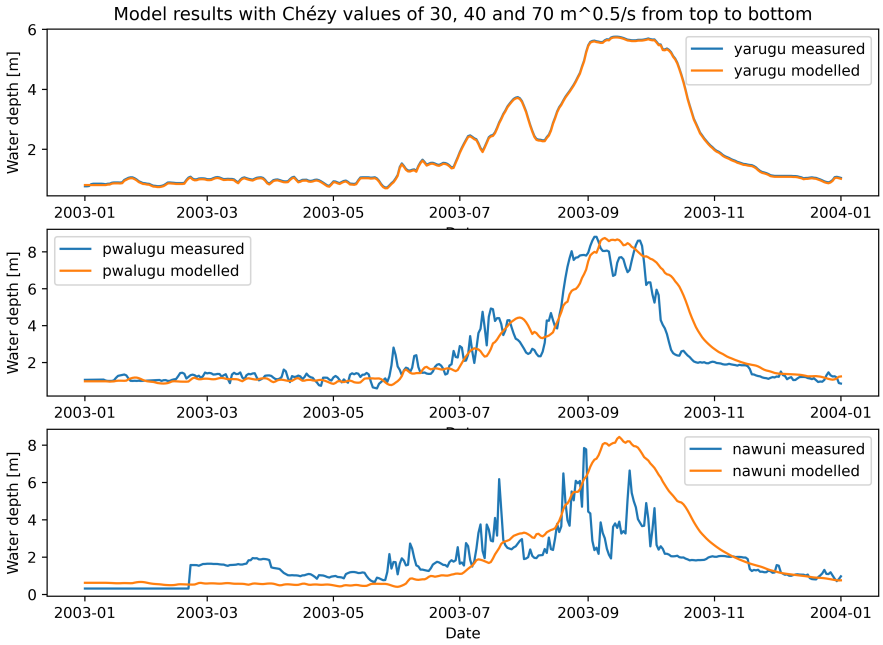

Figure 6.1: Calibration results of the 1D model. At the top, the water levels in Yarugu are shown. As this is the boundary of the model, the measured values and the modelled values are exactly the same. The second graph shows the calibration results in Pwalugu, the first gauge station moving downstream. The third graph shows how the model simulates the water levels in Nawuni, the second gauge station moving downstream in the river. These model results will be used as the base case for the rest of the research.

6.1.2. Water Levels in the Base Case

In figure 6.2, the water levels in the base case are shown for every other week in 2003. As can be seen, the water levels are far below the bank height for almost the whole year. However, the levels rise quickly in September, exceeding the bank height at almost every location in the river. These model results are generated by the 1D2D model. There, where the model is 1 dimensional, infinitely high banks are assumed by the model. Therefore, the model can show clearly where the capacity of the river to store the water is not sufficient. In reality, the water would flow over the banks between the villages as well, and the extreme heights simulated by this model, would not be reached.

Figure 6.2 also shows the places where the tributaries flow into the White Volta River. It can be seen that the Red Volta has a big impact on the water level, even though this tributary does not have the largest discharge, as shown in figure 5.2. Yet, the relative discharge of the Red Volta compared to the White Volta at the place of intake is large which causes the water level to rise this high. From figure 5.2, you might expect the Black Volta to have a large impact on the water level as well. However, the inflow takes place in the delta-like area before Lake Volta, which causes its impact on the water level to be minimal, while the added discharge is high.

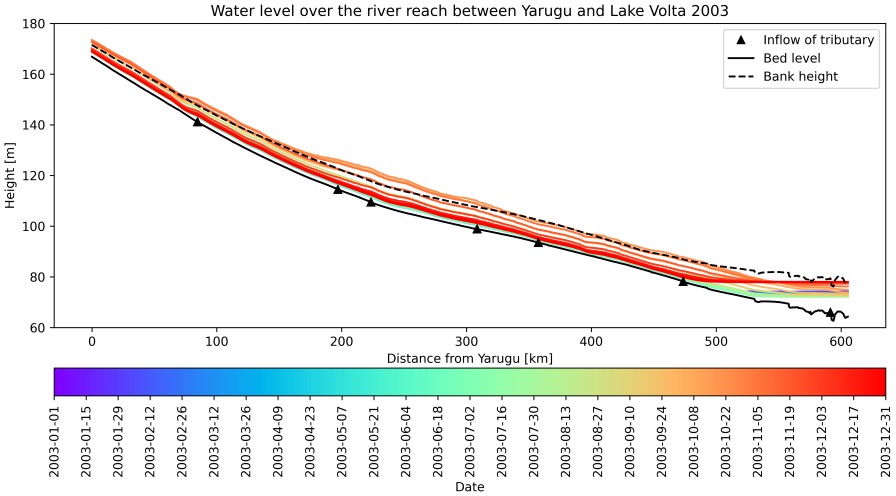

Figure 6.2: Longitudinal view of the water levels between Yarugu and Lake Volta during 2003. These water levels are simulated using the 1D2D flood model. As the largest part of this model is in 1D, it shows in an extreme way the places and the moments where the riverbed is not able to store the amount of water. The triangles in the plot show where the seven tributaries flow into the White Volta. The first and the last tributaries are the Red Volta and the Black Volta respectively.

6.1.3. Flood Maps in the Base Case

As shown in the previous section, the water levels exceed the bank heights at almost every location in the river. To visualize the flood extent and inundation depth as a result of these high water levels, flood maps of the 2D part of the model were made using QGIS. The results show that the maximum flood extent occurred around the 19th of September. In reality, there were temporal differences in the flood peaks over the river reach but as the most extreme flood extent has a duration of about 10 days, these differences were ignored and the 19th of September was chosen as the most extreme flood day for each flood location.

Figure 6.3, shows the flood extent on the peak day for Nawuni, simulated in the base case. The flood maps of the other six villages are shown in Appendix J.1. The water depth and the flood duration were compared to the exposed elements and the estimated value loss was calculated from that, as explained in section 4.4. The amount of affected elements within each inundation range is shown in the table at the bottom of figure 6.3. This amount was used in equation 6.1 to estimate the total costs as a result of value loss after the flood. As the most extreme flood extent in the base case had a duration of about 10 days, the damage factor of maize was 1. That means that all the crops in the agricultural area within the flood extent are considered completely lost.

$$\begin{aligned} \text{Cost Agriculture} &= \text{Agriculture} * \text{Damage Factor} * \text{Price of Maize} \\ \text{Cost Houses} &= \text{Houses} * (\text{Ratio Stone} * \text{Damage Factor} * \text{Price of Stone} \\ &\quad + \text{Ratio Self} * \text{Damage Factor} * \text{Price of Self}) \end{aligned} \tag{6.1}$$

Based on the field experience of Jasper Schakel, it was decided to differentiate between two types of houses for the villages near the White Volta River: the small concrete houses and the small wooden houses from table I.1. The prices of these types of houses were combined with the damage factors for stone- and self-made houses, from the research of Guus Wiersma (Wiersma, 2020), leading to the costs as shown in table 6.1. The total damage from each inundation range, counts up to a value loss of 845423 GHS (about €127.000,-) as a result of the flood in 2003. For the other six flood-prone areas, the flood maps of the base case are shown in appendix J.1. The same calculation was performed for each of the villages. The results of these cost estimations are summarized in table 6.2.

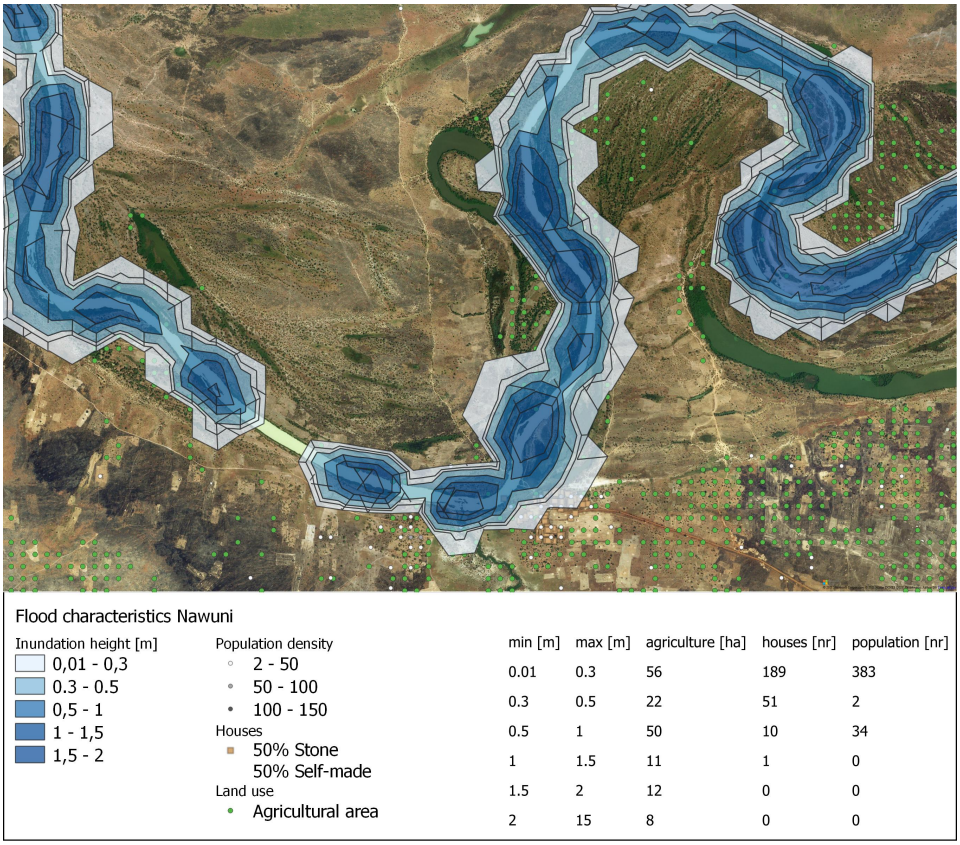

Figure 6.3: Flood map of Nawuni, simulated by the base case. The blue polygons show the flood extent on the 19th of September in 2003. The green dots show the agricultural areas where value loss of crops can be experienced. The greyscale dots give an indication of the population density in this flood-prone area. The brown squares show each house in the village. In the right corner of the figure, the attribute table is added, where the number of elements within the flood extent are counted, per inundation range.

Table 6.1: Flood damage in [GHS] for the base case in Nawuni

	Inundation ranges [m]					
	0.10-0.30	**0.30-0.50**	**0.50-1.00**	**1.00-1.50**	**1.50-2.00**	**>2.00**
Agriculture	1880	720	1680	360	400	280
Price [GHS]	21	21	21	21	21	21
Costs agriculture [GHS]	47376	18144	42336	9072	10080	7056
Affected houses	189	51	10	1	0	0
Stone houses	94,5	25,5	5	0,5	0	0
Price [GHS]	52704	52704	52704	52704	52704	52704
Damage factor	0	0,2	0,3	0,5	0,9	1
Self build Houses	94,5	25,5	5	0,5	0	0
Price [GHS]	12016	12016	12016	12016	12016	12016
Damage factor	0,2	0,4	0,7	0,8	0,9	1
Costs Houses [GHS]	227102	391354	121112	17982	0	0
Total Costs [GHS]	274478	409498	163448	27054	10080	7056

Table 6.2: Total damage for each flood prone area in the base case.

Place	Agriculture Costs [GHS]	Houses Costs [GHS]	Total Costs [GHS]
Pwalugu	11928	0	11928
Duu	7828	0	7828
Janga	6633	0	6633
Dipale	160	0	159
Nawuni	1670	729145	730815
Daboya	844	98907	99751
Yapei	2741	11889	14630
			871748

6.2. Final Design of the Dams

Taking into account the results from the calibration, different dam designs were considered. Because the base flow was underestimated by the base case, it was decided that the pipes that are needed to maintain this base flow should be located on ground level. As a dam with pipes is not an existing structure in D-HYDRO, it had to be imitated by the general structure type. This led to the structure shown in figure 6.4.

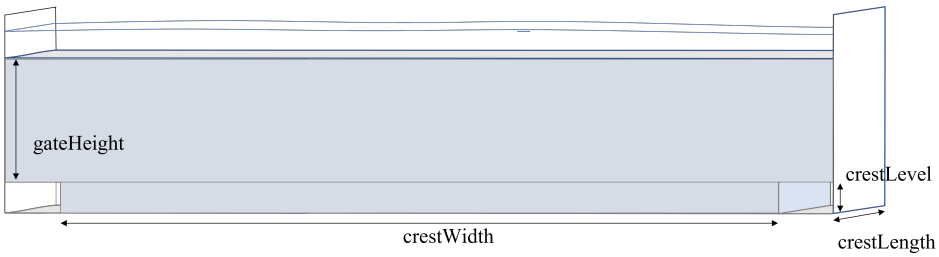

Figure 6.4: Final design of the dam. This general structure has a crest height of 25 cm, and a crest width that is 50 cm smaller than the river width. Adjacent to the crest, a gate is constructed over the whole width of the river bed. This design imitates the real case in which pipes connect the upstream and downstream part of the dam in order to maintain the base flow at all time.

Before deciding on the dam dimensions, a sensitivity analysis was performed in order to study the impact of these dimensions on flood extent, both upstream and downstream of the dam. This was done in two different ways. First, a situation was simulated in which only one dam was constructed, in Daboya. For different crest heights of this dam, the flood extent on the peak day was compared to the flood extent in the base case. Figure 6.5 shows the results of this sensitivity analysis.

What can be learned from the sensitivity analyses is that constructing a dam in this 1D2D model does not decrease the downstream flood extent during the peak flow. The dams with a 5 meter and 7-meter crest height even increased the flood extent in the upstream areas. This shows that the back-water curve as a result of the dam must be studied very carefully, as they can reach the upstream village. However, it should be noted that these results follow from the 1D2D model, where there is only little space for the water to overflow. Therefore, these backwater effects will in reality be less strong as floods occur between the villages as well.

Another sensitivity analysis on the dam dimensions was performed in order to see whether the backwater effects can be mitigated by constructing dams in every flood-prone area. To do so, dams were constructed with crest heights of 25%, 40%, 60% and 80% of the total bed height at the dam location. The results from this analysis in Nawuni are shown in figure 6.6. The results for the other six flood-prone areas are shown in appendix G.1.

In figure 6.6, you can see that in none of the scenarios, the downstream flood extent decreases compared to the base case. In the case of the 80% crest height, the flood extent even increases so

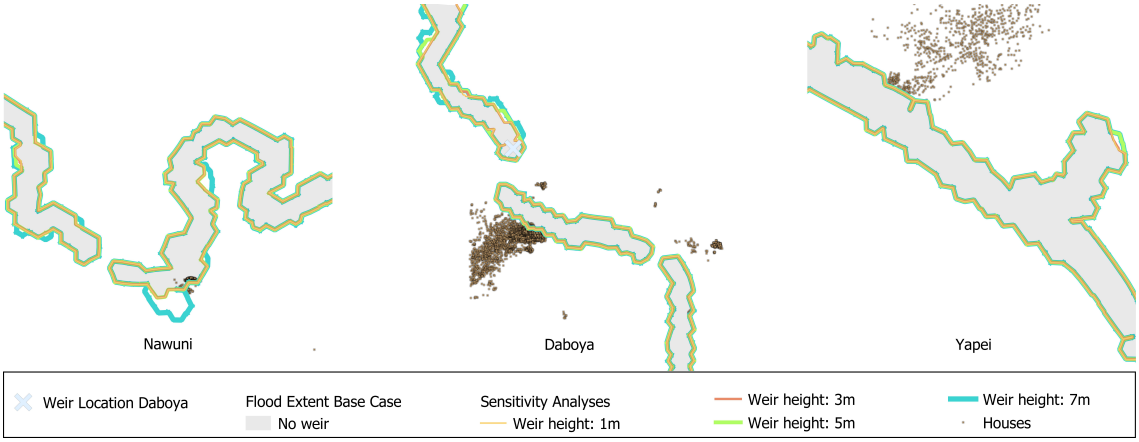

Figure 6.5: Sensitivity analyses of the crest height of a dam in Daboya, on the flood extent. In the left figure the upstream village is shown, in the middle village Daboya itself and on the right the downstream village. For four different crest heights of the dam in Daboya, the flood extent is shown in the three villages. The brown squares show where in the village the houses are located, to give an idea of the impact on the flood risk.

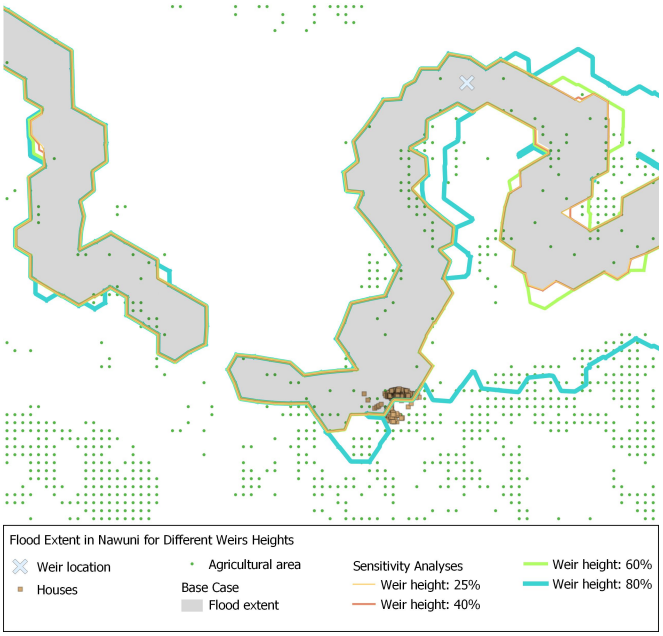

Figure 6.6: Sensitivity analyses of the crest heights of multiple small dams, on the flood risk in Nawuni. The contour lines show the flood extent for the situation in which every village has implemented a small dam with the corresponding relative crest height. The agricultural areas are displayed by the green dots and the houses are shown as the brown squares.

much in the upstream area, that water flows back to the village via overland flow. Besides that, the downstream flood extent has increased as a result of the dam in Daboya, the first downstream village after Nawuni.

Taking the results from both sensitivity analyses into consideration, it was decided to choose the dam design with the highest crest, that does not increase the flood extent near the village. The situation with 40% crest height compared to the bed height was chosen as the best fit. Appendix G.2 shows the exact dimensions of each of these dams.

6.3. Impact of the Dams on the Water Level

This section shows how the water levels are influenced by the implementation of the dams. Figure 6.7 visualises the water levels for every other week during 2003 in the case that every village has a dam with a crest height at 40% of the riverbed height.

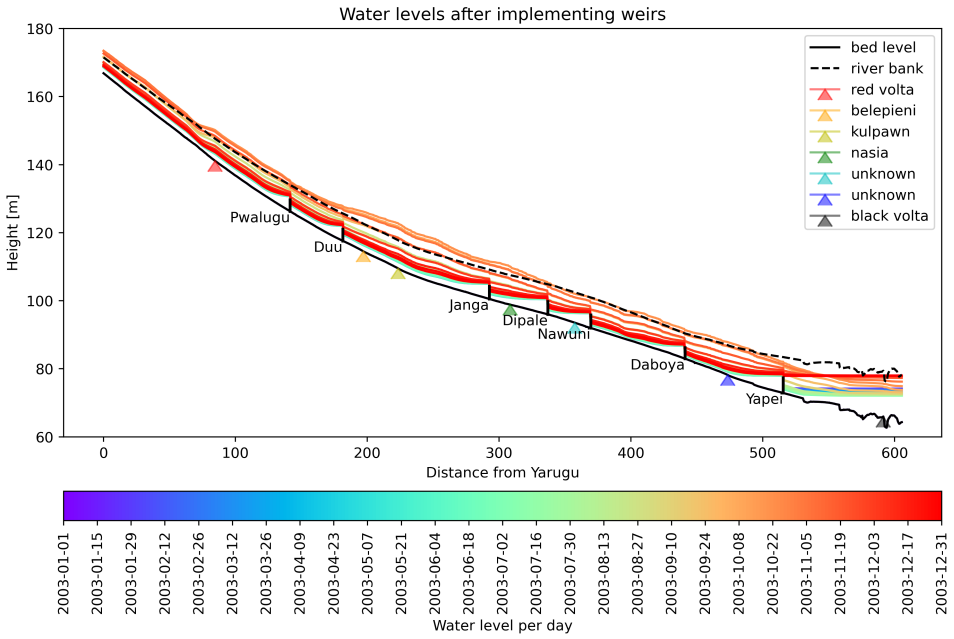

Figure 6.7: Water levels after implementing the seven dams. The triangles show the locations at which the tributaries join the White Volta River. Every line in the graph shows the mean water level during one day, every other week.

During the dry season, the dams have a large impact on the water levels. The backwater is high during these weeks, storing the water in the upstream part of the river. However, as expected from the sensitivity analyses of the dams, during the discharge peaks in the end of September, the storage capacity of the riverbed is not large enough to retain the water or relocate the floods in order to decrease floods occurring in the villages.

Figure 6.8 shows the water level during the peak discharge in the situation with one dam located in Daboya, versus the base case. In that figure, it can be clearly seen how far the backwater curve of a dam reaches. Without creating extra storage, for example in the form of reservoirs, it is not possible to retain this amount of water between each flood-prone area.

6.4. Flood Risk Mapping with 2D Model

As already seen in the sensitivity analyses of the dams, the flood extent can not be reduced by constructing the dams as the river does not have the capacity to store all the river water during the peak discharge. However, the upstream flood extent did increase which means part of the water is retained upstream of the dam. In this section, the effects of constructing the dam on the flood risk are investigated by looking at the damage costs of the floods and comparing them to the base case. By doing this, the impact of possible changes in inundation depth is considered.

Comparing the flood risk for all the cases gives the results of table 6.3. Unfortunately, even though the flood extent looked similar to the base case by eye, some extra elements are exposed to the floods

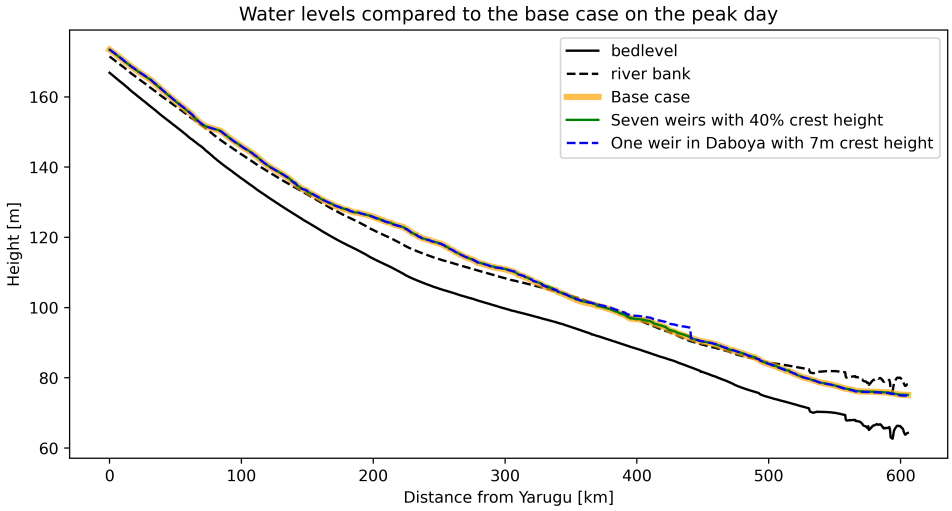

Figure 6.8: Water levels during the peak day in the base case compared to the implementation of seven dams with a crest height of 40% and the implementation of one dam with a crest height of seven meters in Daboya. The figure shows clearly how the backwater curve during the peak discharge can not be distinguished from the base case, while the seven-meter dam shows a backwater curve of about 50 km.

as a result of the dams. Also, some elements are exposed to a higher inundation range, causing more damage. However, as explained before, the backwater effects are most likely exaggerated by the model. Therefore, it is a likely case that in fact, these damage increases are smaller.

Table 6.3: The changes in damage before and after implementing the dams.

Village	Base Case Agriculture Costs [GHS]	Houses Costs [GHS]	Total Costs [GHS]	Dam Scenario Agriculture Costs [GHS]	Houses Costs [GHS]	Total Costs [GHS]	Difference between Dam and Base Case
Pwalugu	11928	0	11928	12096	0	12096	+1,4 %
Duu	7800	0	7800	7800	0	7800	+0,2 %
Janga	6600	0	6600	6600	0	6600	0 %
Dipale	160	0	160	160	0	160	0 %
Nawuni	1700	729000	731000	1700	763900	765600	+4,8 %
Daboya	840	98900	99700	840	108600	109500	+9,8 %
Yapei	2700	11900	14600	290	11900	14700	+0,8 %
			871700			916600	+5,1 %

6.5. Sediment Build-up Upstream of the Dams

Besides storing more water in the river bed upstream of the dams, the goal of implementing the dams was to generate upstream sedimentation that can create a possibility for controlled sand mining in the river bed. Therefore, it is important to determine how much sediment can be collected by constructing the dams.

As morphological calculations take up a lot of computational time, and the floods do not influence the morphological processes much, it was decided to use the 1D model for these calculations. The model simulated the year 2003, with a morphological scale factor of 25, meaning that the outcome shows the morphological changes as if the year 2003 has occurred 25 times, which makes the outcome more stable. To know the deposition in a year, the outcome was divided again by the morphological scale factor.

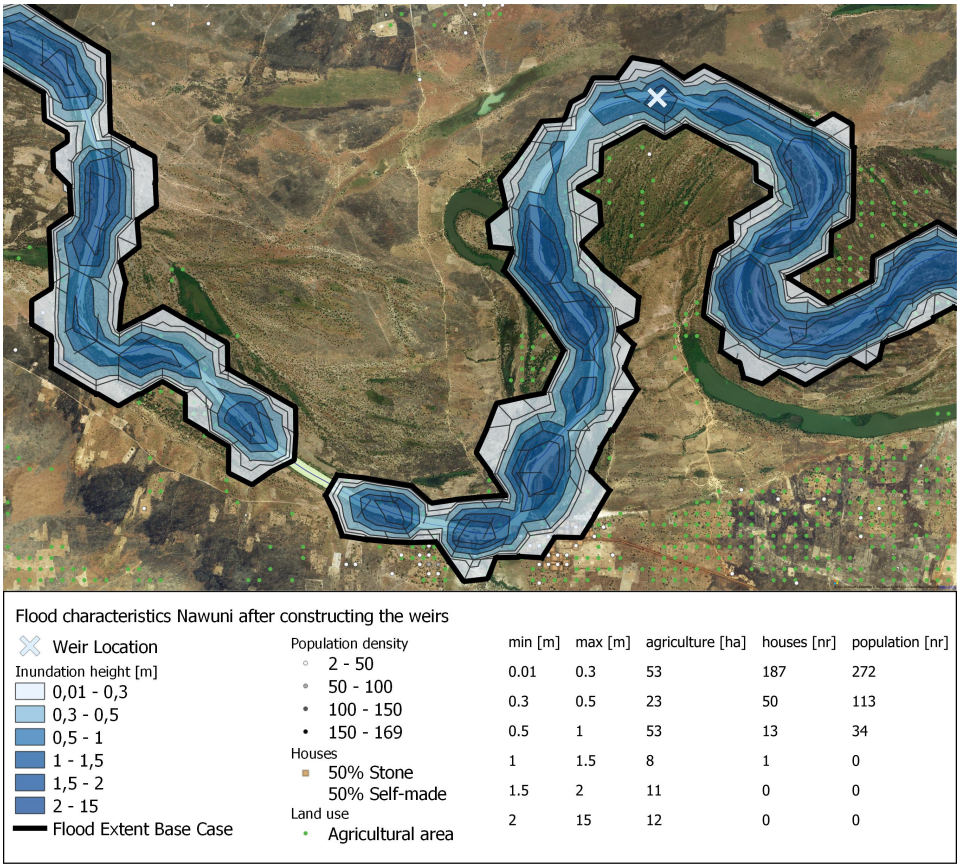

min [m]	max [m]	agriculture [ha]	houses [nr]	population [nr]
0.01	0.3	53	187	272
0.3	0.5	23	50	113
0.5	1	53	13	34
1	1.5	8	1	0
1.5	2	11	0	0
2	15	12	0	0

Figure 6.9: Flood risk in Nawuni after implementing the dams. The black contour lines show the flood extent in the base case and the blue polygons visualize the flood extent that will occur after the dams are placed in every village. The table at the bottom shows the number of elements per inundation range that are affected by the flood. Using this table, the total damage costs can be calculated.

As the distance between grid nodes in the 1D model is 200 m, the sedimentation can be calculated per segment of 200 meters. Figure 6.10 shows the total sedimentation and erosion that occurs in the river stream. For now, the software did not allow to add sediment concentrations to the lateral discharges, therefore, the tributaries are left out of the simulation to avoid dilution of the sediment concentration. For the calculation of the sedimentation, a relative contribution of the laterals will be calculated, assuming their sediment concentration is similar to that of the main flow.

Following the Exner principle, as described in section 3.2.1, the plots can be explained. The Exner principle shows how increasing flow velocities increase the sediment transport capacity of the water, after which more sediment can be suspended in the water, causing a possibility for erosion. Similar, when flow velocities decrease, the sediment transport capacity reduces, and the largest particles start to settle. As the dams not only slow down the velocities but also block the sediment, even more sedimentation occurs.

In figure 6.10, the sedimentation and erosion with respect to the dam locations are compared to the mean velocity and the river bed width over the river reach. Upstream of the dams, the flow velocity decreases and sediment settles. Downstream, the flow velocity increases, and the unexploited sediment transport capacity causes erosion to occur. Furthermore, at places where the river width quickly increases and decreases, the velocity decreases and increases. Also at these places, sedimentation and erosion can be observed. What can be clearly seen in the figure is that most of the sedimentation occurs upstream in the river. Therefore, in order to divide the sediment better over the seven villages, the upstream dams should be adjusted. For example, by decreasing the crest widths of the upstream

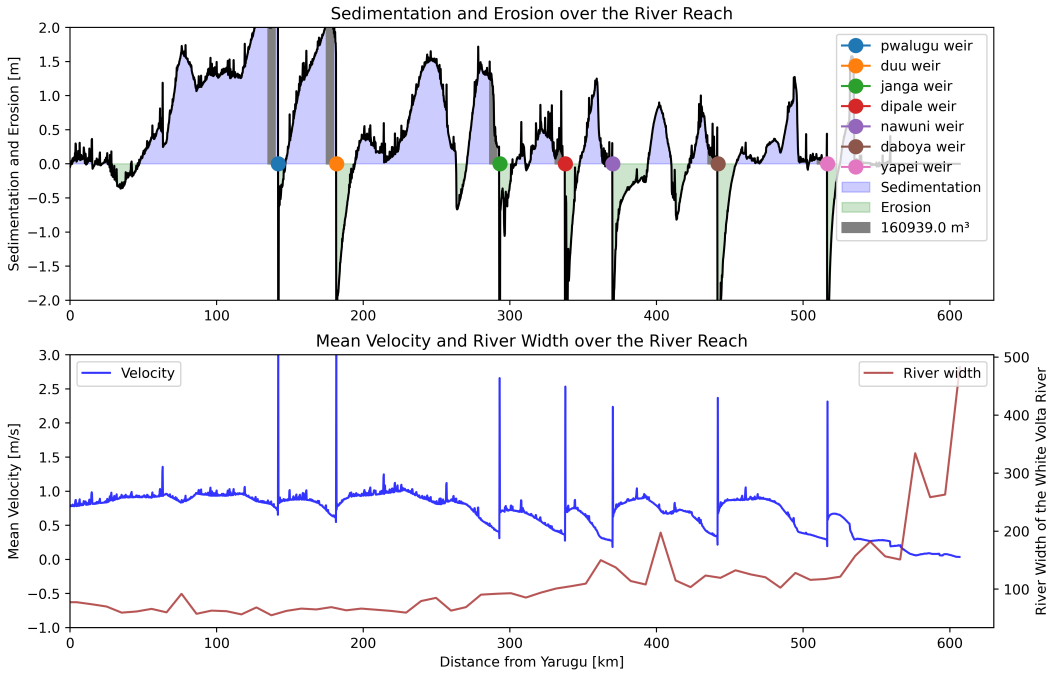

Figure 6.10: Erosion and sedimentation as a result of the dams. The purple areas in the top figure visualize how much sedimentation occurs and the green areas show erosion. The coloured dots show where the dams are going to be placed. Upstream of the dams, over a length of 5 kilometers, the area is highlighted in grey where the sand mining will take place. The legend shows the total amount of sand that can be dredged in a year. The bottom shows the mean velocity and the river width over the river reach and can be used to explain the sedimentation and erosion from the upper graph.

dams, more sediment stays dissolved in the water and is able to be captured at the downstream dams. It was assumed that the sedimentation that occurs over the river segment up to 5 km upstream of the dam, will be used for possible sand mining. Therefore, the sedimentation amount in this area was calculated. The area is marked in grey, in figure 6.10.

As explained before, the sedimentation amount was simulated in the 1D model without including the tributaries. The influence of the tributaries was included by calculating the ratio between discharge with and without the tributaries. The simulated sedimentation amount was then multiplied by this ratio in order to gain a more realistic result. This method is further explained in appendix K.

In order to understand the amount of sediment that can be dredged from the rivers, it was expressed in amount of trucks per day per village. This calculation assumes average trucks that are able to carry 4 m^3 of sand. Table 6.4 shows how many trucks eventually can be filled from the upstream sedimentation. It should be taken into consideration that dredging of the sand from the rivers is only possible during the dry seasons as the water levels will be too high during the rain season to enter the river safely.

Table 6.4: Amount of trucks that can be filled from the upstream sedimentation.

	Pwalugu	**Duu**	**Janga**	**Dipale**	**Nawuni**	**Daboya**	**Yapei**
Sedimentation without laterals [m3]	23500	28600	16300	4900	1500	4100	1500
Ratio	1.18	1.19	1.85	1.98	2.06	2.06	2.51
Final Sedimentation	27800	34000	30100	9756	3178	8522	3803
Amount of trucks per day	19	23	21	7	2	6	3

7

Discussion

This study aimed to explore the impact of constructing multiple small dams on flood risk near inhabited areas and determine the sedimentation upstream of these dams. By using a 1D2D coupled hydraulic model, the impact was quantified. In order to set up this model, assumptions and simplifications were made to fill the knowledge and data gaps of the study.

7.1. Data

The data used to set up the model can be divided into different categories. The geographical data from satellites needed to set up the flood risk maps, the discharge data from the hydrological model and the direct input data to build the hydraulic model. The limitations of these datasets are discussed in this section.

7.1.1. Geographical Data

The geographical data is almost completely satellite-based and comes from different sources, generated at different times. Therefore, it should be noted that not all these geographical datasets correspond perfectly with each other. For example, the exposure map consists of buildings, agriculture and population density. One would expect the population density and the buildings to be located at almost the same places, as most people live in a house. However, it can be seen on the map that there are areas where population density was measured without houses being located. Furthermore, the agricultural areas are determined by FAO in 2019. When viewing this map over the satellite data, you can recognise agricultural places from the pictures that were not detected by that dataset.
Furthermore, in order to calculate the damage of the agricultural areas, the centre points of every 1.2 ha of land were taken and converted to point data. Therefore, when only part of the land was covered by the flood, this was not taken into consideration.

7.1.2. Hydrological Data

The hydrological data came from the hydrological model that was built by another master student (te Witt, 2021). The model was calibrated on the gauge stations in the White Volta. For this calibration, the discharge data, provided by HSD, at the locations of the gauge stations, was used. During the flood of 2003, the discharge data from the three stations in the White Volta River show a large decrease in discharge moving downstream in the river. This is unlikely, as large tributaries join the main river, while the river dimensions do not change a lot. Because of that, it was decided to convert the discharge back to water depth data for the hydraulic model by rating curves, using shape parameters provided by HKV (Udo & Termes, 2011). However, the hydrological model was not adjusted, causing the two models to not fully correspond with one another. Furthermore, from this hydrological model, only the discharge data at the point of inflow from the seven largest tributaries was extracted. The groundwater flow, the

overland flow and the rainfall that falls or flows directly into the river are thereby neglected.

7.1.3. Bathymetry

The bathymetry of the river was based on the assumption that the Google Satellite images were taken at bank-full discharge. This assumption was made after Jasper Schakel paid a field visit to Yapei and compared the water levels at that moment with the extent from the satellite images. However, when assessing these Google Satellite images, it was clear that some places were already flooded on the satellite images. These flooded lands were mainly noticed downstream, near Lake Volta. Therefore, the river width at these places was estimated based on the nearest dry land. Therefore, the downstream river width measurements might be overestimated compared to the real bank-full situation.

Furthermore, the bed level in the bathymetry was based on the DEM and the interpolated values of five measured cross-sections. This method was chosen because satellite images do not penetrate through water and will therefore either measure the water surface or interpolate the data from the nearest land surface. At places where the river is actually bank-full, this method will satisfy. However, at places where the water level is lower than the bank-full situation, or where the data was interpolated over steep floodplains, this method can become imprecise. Also, the used DEM data has a spatial resolution of 30 m, which already causes a lot of variation in the data. This was seen in the output from the Profile Tool.

Because this method for determining the bathymetry lead to a very irregular river shape, a fifty-year morphological run was performed in order to come to a balance in the morphology of the river. The river bed height was also adjusted to this situation, creating a smooth 1D river model to use as a starting point for the rest of the simulations. However, this adjusted river bed did not correspond to the 2D model anymore at every location. Therefore, in order to flow from the 1D model into the 2D grid, there were some extra meters to overcome to match the bank height and the DEM. To solve this, the DEM at every flood-prone area was adjusted by hand to match the bank heights of the bathymetry.

The steps, needed to create a workable bathymetry that collides with the 2D model as well, brought a lot of uncertainty into the model. In order to reduce this uncertainty, it is necessary to add more accurate bathymetry data to the model.

7.2. Hydraulic Model

Both the 1D and the 1D2D models are simplifications of the reality as both water and sediment behave in a three-dimensional manner, under influence of many forces that cannot be included in a model. This section describes some of the limitations of the model that influence the outcome of the simulation.

7.2.1. The River Shape

The 1D model assumes the river as if it were a straight line where water moves in only one direction without the influence of bends or depth. The shapefile from the river was created based on satellite images and shows a very precise route. However, the 1D and the 1D2D model create the river shape from the computational grid nodes at a certain interval in the shapefile. For the 1D model, the river shape is taken from nodes at every 200 m in the shapefile, and for the 1D2D at every 1000 m in the shapefile. This shortens the actual river length, as some of the bends in the river will be missed. This will decrease the storage capacity of the river within each village when compared to the real situation. This limitation can be overcome by decreasing the grid size of the model. Decreasing the grid size overcomes this problem; however, this will result in a longer computational time. For now, the shortening of the river is compensated for by the calibration process.

The river shape is not always in line with the DEM, as the river shape was determined from Sentinel-2 satellite data, based on the reflected colours of the beams. This causes problems when the 1D river stream is coupled to the 2D flood-prone area. After compensating the DEM with the new bed level, as described in the previous subsection, it became clear that this mismatch in DEM and river shape

can cause problems. At some places, the water would overflow from the river into a section of the DEM which was low because it was measured at a place where the riverbed was located. As a result, the water would drain away, during both the dry and the wet season. This effect was relatively small during the wet season compared to the river discharge but should be compensated for when using the 1D2D model in the dry season. Therefore, when simulations were performed with the focus on the dry season, the 1D model was used as that problem then does not occur.

7.2.2. Flood Determination

The 1D2D model is a combination of a 1D grid, coupled with seven 2D grids, covering high-risk flood areas. This means that the water is only able to flow over the river bank whenever a 1D grid point is connected to a 2D grid point. As a result, the water cannot overflow between the flood-prone areas, which increases the backwater effects of the dams all the way up to the upstream villages. This makes the backwater effects of the constructed dam unreliable for 2D areas that are connected by a 1D section. Furthermore, it makes the discharge peaks more pronounced, as the water builds up and only can be released at the 2D regions.

Infiltration of water is ignored in both the 1D and the 2D model parts. Therefore, after the water flows over the river banks, it immediately flows back into the river when the discharge decreases. In practice, part of the water would infiltrate into the soil. This has multiple effects on the flood risk and the discharge peaks. First of all, it would lower the inundation depth as water is released into the ground, decreasing the flood risk. Secondly, because the groundwater flow is a slower process than the overland flow, infiltration would lower the discharge peak. This delay is now compensated for in the calibration process.

As explained, the floods occur at the places where the 1D grid nodes are connected to the 2D grid nodes. As these grid nodes are a kilometer apart in the 1D2D model, there is only one place at every kilometer where the water can be released from the river. In reality, this would be a more continuous process, where there is a connection with the flood plain at every location in the river. Because of this, the results do not always look smooth and some unexpected dry areas between the nodes can be found which in reality would have been flooded as well.

What should be taken into consideration, is that the 1D2D model includes seven inhabited places near the White Volta river downstream of Yarugu. However, when looking closer on Google Maps, some small villages can be found, like Kpasenkpe. These places are now excluded from the flood risk simulation but should be accounted for as well.

Calibration was performed on the flood of 2003. The reason for this decision was that this is the only flood of which both hydrological as hydraulic data is available. However, it would be better to set up the model and calibrate it for a flood after 2013, as new satellite missions were launched from that year, providing more suitable satellites for open water detection. This would make it possible to calibrate the flood extent as well as the gauge measurements. During the rain season in 2003, the atmosphere was too clouded to validate the flood extent by the available open-source satellite images.

7.3. Morphology

A limited amount of data was available for the morphological calculation. Therefore, many assumptions were made concerning the morphological simulations. For example, the chosen bed slope formulation and the Koch & Flockstra parameters were kept in default settings. The impact and options of choosing other methods should be explored. For the sediment characteristics, only one grain size was used, constant over the whole river width. However, different grain sizes are known for the river banks. However, as the manual on implementing morphology in the D-HYDRO model was not completed yet, it was unclear how to implement these different grain sizes.
Another limitation in the model is that it only includes sediment transport of the bedload and neglects the suspended particles. The reason for this is that the model gave errors on when the sediment type was changed and these could not be solved during this research as the manual on implementing morphology was not yet available.

What is discussed in chapter 3.2.4, but not included in the model, is the long term impact of dredging the sediment from the riverbed on the morphology. By introducing dams, upstream sedimentation occurs. By mining this sediment, the total sediment supply along the river continuum is reduced, meaning that less sediment is left to be transported by the river. This accumulation and extraction of sediment will cause over time, an increasing grain size distribution. In a river with larger grain sizes, less sediment is transported, which again reduces the amount of sedimentation upstream of the dams. This feedback loop is not accounted for by the model as only one mean grain size is included.

Currently, a lot of illegal sand mining takes place in the river bed, therefore the morphological equilibrium is already disrupted. However, currently, the sand is mainly dredged from the river banks, where it is most easily accessible. This widens the river, causing lower water levels and more turbidity. The purpose of constructing the dams is to trap sediment to create a possibility for controlled sand mining. However, the quality of the sand trapped by the dam will differ from the quality of the sand in the river bank. The trapped sediment will include organic matter, which makes it more difficult to use the sand for concrete production. More research is needed in order to make sure that the controlled sand mining will actually compete with the illegal sand mining in the river banks.

8

Conclusions and Recommendation

The main objective of this research was to discover how the construction of multiple small dams in the White Volta river impact the magnitude and the occurrence of discharge extremes, sedimentation and flood risks in northern Ghana. This section discusses the main conclusions that can be drawn from the results after which recommendations are given for future research.

8.1. Conclusions

To answer the research questions, literature was used and a hydraulic model was built in which the current situation was compared to a situation in which seven different dams are constructed upstream of the villages. The effects on flood risk and sedimentation were determined from the model outcomes.

The hypothesis of the research was that the construction of the dams would reduce the flood risk and create possibilities for controlled sand mining. By answering all the subquestions, it can be concluded that the dams are not able to reduce the flood risk but will create upstream sedimentation that creates opportunities for controlled sand mining.

What influences the streamflow in the White Volta River and what is the current streamflow of the river?

It can be concluded from the literature that the floods of the White Volta River in northern Ghana, are mainly caused by the spillage of the Bagre Dam in Burkina Faso. The White Volta Basin is a sub-basin of the Volta Basin and spreads out over three different countries, all having a dry savanna climate. Despite its large tributaries like the Red Volta and the Black Volta, the competition for water resources of the White Volta River between the countries is too high. Burkina Faso has increased their share of the water resources by building the Bagre Dam to store irrigation water and generate hydropower. Poor management of this dam results in spillage during the wet season and floods in the White Volta River in northern Ghana. Improved operational management of the Bagre Dam could be the first step in solving these problems. The government of Ghana has decided to solve the problems differently, and made plans to construct its own dam, the Pwalugu Multipurpose Dam. This dam is supposed to have the same effect on Ghana as the Bagre Dam has on Burkina Faso and reduce the risk of floods and drought while generating hydropower. When managed in a sustainable way, this dam can be a good solution. The construction has started but it is not yet clear when this dam will be taken into practice.

Besides the spillage of the Bagre Dam, the streamflow in the White Volta River is influenced by illegal sand mining for construction materials. Especially near Tamale, population growth and urbanisation cause an increasing demand on the sand for mortar and concrete. The sand is often dredged from the river banks, widening the river, and lowering the water levels. Near Nawuni, where the drinking water intake point of Tamale is located, this causes the river to become more turbid, which results in clogging

of the intake pipes.

Constructing multiple small dams upstream of the villages that are located near the White Volta River was researched as a possible solution as it shows potential in reducing the flood risk in these areas, and at the same time, it can create an opportunity for controlled sand mining in the river bed.

What is the impact of constructing dams on river characteristics?

As the Saint-Venant equations describe, placing a dam in a river stream will increase the upstream water levels, called the backwater curve, while lowering the water levels downstream. As the river finds a new balance, in which the discharge stays constant, the velocity of the water upstream of the dam decreases and the velocity downstream of the dam increases. The backwater effect of the dam can create a possibility for water retention in order to flatten the discharge peak in the downstream area.

By simulating the water levels in a 1D hydraulic model, it was found that indeed, the dams have this expected backwater effect on the upstream water levels. However, in the case of the White Volta River, the simulation showed that there is not enough storage capacity in the river bed to retain all the water and prevent floods. Therefore, the dams were designed at locations upstream of the villages with the purpose to relocate the floods from the inhabited areas. Furthermore, this 1D simulation showed that the base flow of the river reduces a lot during the dry season.

Taking the results from the 1D water level simulation into account, the dam design was chosen. The dams were modelled as a general structure with a crest and a joint gate. As the crest was designed slightly smaller than the river width while the gate covered the whole width, a situation was simulated as if two pipes connect the upstream and the downstream sides of the river at the river bottom. The pipes function to maintain the base flow at all times. The maximal crest height was found to be 40 % of the bank height at the location of the dam. This was concluded from a sensitivity analysis on the crest height in which an optimum was found in which as much sediment can be trapped without increasing the backwater curves up to the upstream village.

As a result of the dams, upstream sedimentation and downstream erosion occur. This process was simulated using the 1D hydromorphological model and occurs for two main reasons. First of all, the dams block the sediment flow which causes accumulation of the sediment upstream of the dam. Secondly, the sedimentation and erosion curves can be explained by the Exner principle. Whenever the backwater curve is developed, water upstream of the dams is slowed down. This results in a decrease in sediment transport capacity, causing sedimentation to occur. And consequently, when the water flows over the dam and its velocity increases, the reduced sediment in combination with the increased sediment transport capacity results in erosion. Furthermore, at places where there was a sudden change in the river width, the same results were observed.

The aim of the dams is to use sedimentation as a possibility for controlled sand mining. The extraction of sediment makes it impossible to come to a sediment balance in the river. The sedimentation described above will be compensated for by sand mining. However, the erosion process will never stop as the sediment supply is not sufficient. Therefore, in the long term, erosion will spread out over the whole river stream.

The model results show that in the case of the seven dams that all cover the complete river width, the sedimentation amount reduces quickly downstream as most of the sediment has already settled at the upstream dams. This could be overcome by adjusting the crest width of the dams or increasing the spillway designed to maintain the base flow to find a balance in the sediment share of each village.

How do multiple small dams in the White Volta River change the flood risk?

Flood risk can be quantified by comparing the magnitude of the flood with the exposed elements, their values and their vulnerability against floods. The magnitude parameter was thereby defined as flood extent or inundation depth, depending on the element type. The included exposed elements were

divided into houses, agricultural areas and population. Hereby, a distinction was made between self-made wooden houses or stone houses as these differ in vulnerability. Using depth-damage functions, the value loss of each exposed element as a result of different inundation depths of a flood was determined. By applying this method, flood risk could be expressed as potential value loss.

The flood risk and the inundation depths were simulated by building a 1D2D coupled model with 2D grids over seven different high-risk villages. Flood maps, created from the output of this model, showed that the dams are not able to reduce the flood risk in the villages. Even with the chosen dam design, which did not seem to increase the backwater curves and showed the same flood extent as the base case, the flood risk slightly increased as a result of their implementation. The model showed an increase of the damage costs between 0 and 10% compared to the base case.

However, it should be noted that the 1D2D hydraulic model does exaggerate the backwater curves as it is 1D for the largest part, where the backwater curve cannot be released on the flood plains and therefore builds up until it reaches the upstream village. This can be overcome by increasing the 2D part of the model, or by adding floodplains to the 1D part of the model so that floods are able to occur between the villages as well.

Expert Opinion

These conclusions are based on the model results, which are not a perfect representation of reality. Taking the simplifications by the model into account, and based on the theory, it can be expected that the dams will not increase the flood risk in the upstream village as a result of their backwater curve. The water levels will be reduced by floods that occur between the villages. However, the dams will still unable to reduce the flood risk during peak discharges, as the capacity of the river bed is not large enough to maintain all the water. Therefore, to lower the flood risk in the villages, storage capacity should be increased. A way to achieve that would be by excavating the river bed upstream of the dams in order to create reservoirs.

The Pwalugu Dam will also offer extra storage needed to prevent the floods in northern Ghana. When taken into practice and managed in a sustainable way, the hydropower dam can have a positive influence on the river hydraulics. However, this can only be achieved when the interest of the dam management exceeds the production of hydropower and less water is spilled during the rain season.

8.2. Recommendations

Based on the results and conclusions of this study, some recommendations are made for further research. The biggest improvements can be made within data collection. In order to gain better insight into the effects of the dams on the water levels and flood risk, a detailed bathymetry is necessary. Also, little morphological data was available for this research. Doing field measurements on sediment types and layers would improve the morphological simulation. For example, it would be better if a distinction was made between different layers of sediment. In the current model, a lot of default values had to be used as there was no data for the morphological parameters.

Besides the data collections described above, field research is needed in order to gain a better understanding of the current situation. By paying field visits to the villages near the White Volta River, the wishes and experience of the inhabitants can be involved in the design. For example, the current dam locations are chosen based on QGIS data, without consulting the inhabitants or visiting the location. Also, the amount of the current sand mining from the river bed is unknown which makes it difficult to quantify the impact of the dams.

Furthermore, a longer time range of the gauge data would make it possible to calibrate the model on a different flood. A larger flood during a later year might provide the opportunity to calibrate the model on the flood extent by comparing the model output with satellite data. For the flood in 2003, this was not possible as there were too many clouds in the atmosphere to see the flood extent on the surface.

The 1D2D model could be improved by including floodplains in the 1D sections or by increasing the 2D grids. For now, the 1D part of the model consisted only of the river dimensions, but from the results, it was learned that the extent of the backwater curve, in that case, reaches the upstream village. This might be overcome when there is more space in the model to release water. Also, a larger 2D grid would create more space for the water to drain from the riverbed and lower the flood peaks. However, it is recommended to use a stronger computer in that case, as it would increase the computational time a lot. Search for different modelling software that is more suited to make these calculations might also be a solution.

The seven included villages are the larger villages near the White Volta River. However, when zooming in on Google Maps, some small places can be found where only a little amount of buildings are located near the river banks. These places should also be taken into consideration during future research.

The construction of the Pwalugu Dam was not included in the current model. However, if this dam is taken into practice, it will have a large impact on the hydraulics in the river. Therefore, the dam should be included in the model as well. The dam will affect both the river hydraulics as the sediment flow in the river. When managed in a good way, the dam shows the potential to reduce the flood risk by reducing the peak discharge. However, the dam also might decrease the sediment flow as sedimentation will occur in the upstream research of the dam. This can result in reduced sedimentation amount upstream of the dams.

Finally, this research was performed while the D-HYDRO 1D2D software was still in development. Therefore, not all the manuals were complete and the interface did not work yet. Whenever the software is officially released, it might offer more opportunities for improvement. For example, there was no information to be found on how to add sediment to the inflow of the tributaries. When this can be included in the model, it would improve the morphological outcome a lot.

References

Abass, K. (2020). Rising incidence of urban floods: understanding the causes for flood risk reduction in Kumasi, Ghana. *GeoJournal*. doi: 10.1007/s10708-020-10319-9

Abass, K., Dumedah, G., & Frempong, F. (2019). Understanding the physical and human contexts of fluvial floods in rural Ghana. *International Journal of River Basin Management*. doi: 10.1080/15715124.2019.1653310

Abubakari, S., Dong, X., Su, B., Hu, X., Liu, J., Li, Y., … Xu, S. (2019). Modelling streamflow response to climate change in data-scarce white volta river basin of West Africa using a semi-distributed hydrologic model. *Journal of Water and Climate Change*, *10*(4). doi: 10.2166/wcc.2018.193

Ahamed, A., Bolten, J., Doyle, C., & Fayne, J. (2017). Near Real-Time Flood Monitoring and Impact Assessment Systems.. doi: 10.1007/978-3-319-43744-6{_}6

Amisigo, B. A., McCluskey, A., & Swanson, R. (2015). Modeling impact of climate change on water resources and agriculture demand in the Volta Basin and other basin systems in Ghana. *Sustainability (Switzerland)*, *7*(6). doi: 10.3390/su7066957

Armah, F. A., Odoi, J. O., Yengoh, G. T., Obiri, S., Yawson, D. O., & Afrifa, E. K. (2011). Food security and climate change in drought-sensitive savanna zones of Ghana. *Mitigation and Adaptation Strategies for Global Change*, *16*(3). doi: 10.1007/s11027-010-9263-9

Battjes, J., & Labeur, R. J. (2017). *Unsteady Flow in Open Channels*.

Crosato, A. (2007, 1). *Morphological response at the reach scale* (Tech. Rep.). Delft: UNESCO-IHE.

Deltares. (2020). *D-FLOW Flexible Mesh User Manual* (Tech. Rep.). Delft: Deltares.

Di Baldassarre, G., Montanari, A., Lins, H., Koutsoyiannis, D., Brandimarte, L., & Blschl, G. (2010). Flood fatalities in Africa: From diagnosis to mitigation. *Geophysical Research Letters*, *37*(22). doi: 10.1029/2010GL045467

ESA. (n.d.). *Sentinel-2 Mission.* Retrieved from `https://sentinel.esa.int/web/sentinel/missions/sentinel-2`

ESA. (2005). *ESA Globcover 2005 Project.* Retrieved from `http://due.esrin.esa.int/page_globcover.php`

FAO. (2004). *Principal agricultural crops.* Retrieved from `http://www.fao.org/3/a0013e/a0013e06.htm#bm06.1`

Faure, A. (2003). Improving public information about large hydroelectric dams: Case studies in France and West Africa. *Natural Resources Forum*, *27*(1). doi: 10.1111/1477-8947.00038

GWCL. (2019). *Ghana Water Company Limited.* Retrieved from `https://www.gwcl.com.gh/company-profile/`

Japan Aerospace Exploration Agency. (2021, 3). *ALOS Global Digital Surface Model (DSM)* (Tech. Rep.).

Kankam-Yeboah, K., Obuobie, E., Amisigo, B., & Opoku-Ankomah, Y. (2013). Impact of climate change on streamflow in selected river basins in Ghana. *Hydrological Sciences Journal*, *58*(4). doi: 10.1080/02626667.2013.782101

Komi, K., Amisigo, B. A., Diekkrüger, B., & Hountondji, F. C. (2016). Regional flood frequency analysis in the Volta River Basin, West Africa. *Hydrology*, *3*(1). doi: 10.3390/hydrology3010005

Kron, W. (2005). Flood risk = hazard • values • vulnerability. *Water International*, *30*(1). doi: 10.1080/02508060508691837

Laube, W., Schraven, B., & Awo, M. (2012). Smallholder adaptation to climate change: Dynamics and limits in Northern Ghana. *Climatic Change*, *111*(3). doi: 10.1007/s10584-011-0199-1

Leasure, D., Darin, E., & Tatem, A. (2021, 3). *Bayesian gridded population estimates for Ghana 2019.* Retrieved from `https://wopr.worldpop.org/?GHA/` doi: 10.5258/SOTON/WP00705

Mahe, G., Lienou, G., Descroix, L., Bamba, F., Paturel, J. E., Laraque, A., … Khomsi, K. (2013). The rivers of Africa: Witness of climate change and human impact on the environment. *Hydrological Processes*, *27*(15). doi: 10.1002/hyp.9813

Mangnus, E., & van Westen, A. C. (2018). Roaming through the maze of maize in Northern Ghana. A systems approach to explore the long-term effects of a food security intervention. *Sustainability (Switzerland)*, *10*(10). doi: 10.3390/su10103605

McFeeters, S. K. (1996). The use of the Normalized Difference Water Index (NDWI) in the delineation of open water features. *International Journal of Remote Sensing*, *17*(7). doi: 10.1080/01431169608948714

Molinari, D., Rita Scorzini, A., Gallazzi, A., & Ballio, F. (2019). AGRIDE-c, a conceptual model for the estimation of flood damage to crops: development and implementation. *Natural Hazards and Earth System Sciences*, *19*(11). doi: 10.5194/nhess-19-2565-2019

Musah, B. A. N., & Oloruntoba, A. (2013). Effects of Seasonal Floods on Households' Livelihoods and Food Security in Tolon/Kumbumgu District of the Northern Region, Ghana. *American Journal of Research Communication*, *www*(18).

Ndamani, F., & Watanabe, T. (2015). Farmers' perceptions about adaptation practices to climate change and barriers to adaptation: A micro-level study in Ghana. *Water (Switzerland)*, *7*(9). doi: 10.3390/w7094593

Niang, I., Ruppel, O., Abdrabo, M., Essel, A., Lennard, C., Padgham, J., & Urquhart, P. (2014). Africa. In *Climate change 2014: Impacts, adaptation, and vulnerability. part b: Regional aspects. contribution of working group ii to the fifth assessment report of the intergovernmental panel on climate change* (pp. 1199–1265).

Ragasa, C., Chapoto, A., & Kolavalli, S. (2014). Maize productivity in Ghana. *International Food Policy Research Institute*.

Senzanje, A., Boelee, E., & Rusere, S. (2008). Multiple use of water and water productivity of communal small dams in the Limpopo Basin, Zimbabwe. *Irrigation and Drainage Systems*, *22*(3-4). doi: 10.1007/s10795-008-9053-7

Takouleu, J. M. (2020, 3). *Ghana: Construction of the Pwalugu multipurpose dam will start in April 2020.* Retrieved from `https://www.afrik21.africa/en/ghana-construction-of-the-pwalugu-multipurpose-dam-will-start-in-april-2020/`

te Witt, D. (2021). *Improving the performance of distributed conceptual hydrological models using the spatio-temporal patterns of RS observations* (Unpublished doctoral dissertation). Delft University of Technology, Delft.

The World Bank. (2011). *Climate Risk and Adaptation Country Profile* (Tech. Rep.). Washington.

Udo, J., Klopstra, D., Hartman, M., Andah, W., van de Giessen, N., Termes, P., & Bijkerk, T. (2011, 8). *North Ghana sustainable development, disaster prevention and water resources management. Flood hazard assessment White Volta.* (Tech. Rep.). HKV.

Udo, J., & Termes, P. (2011, 11). *North Ghana sustainable development, disaster prevention and water resources management. Flood hazard assessment White Volta. Field Trip Report and River Characteristics* (Tech. Rep.). HKV.

Unami, K., Yangyuoru, M., & Alam, A. H. M. B. (2012). Rationalization of building micro-dams equipped with fish passages in West African savannas. *Stochastic Environmental Research and Risk Assessment*, *26*(1). doi: 10.1007/s00477-010-0451-7

UNDRR. (2020). *Terminology.* Retrieved from `https://www.undrr.org/terminology`

Van de Giesen, N., Andreini, M., Van Edig, A., & Vlek, P. (2001). Competition for water resources of the Volta basin. *IAHS-AISH Publication*(268).

Van De Giesen, N., Kunstmann, H., Jung, G., Liebe, J., Andreini, M., & Vlek, P. L. G. (2002). The GLOWA Volta project: Integrated assessment of feedback mechanisms between climate, landuse, and hydrology.. doi: 10.1007/0-306-47983-4{_}9

van der Zwet, J. (2012). *The creation of a reservoir in the White Volta River, Ghana: An analysis of the impact on river morphology* (Unpublished doctoral dissertation). TU Delft, Delft.

VRA. (2021, 4). *Volta River Authority .* Retrieved from `https://www.vra.com/about_us/profile.php`

Widiarto, L. A. (2013). *Agricultural Loss Caused by a Flood Event and its Household Impact In Part of Sragen Regency, Indonesia* (Unpublished doctoral dissertation). University of Twente, Enschede.

Wiersma, G. (2020). *Quantifying flood damage* (Unpublished doctoral dissertation). TU Delft, Delft.

Yiran, G. A., & Stringer, L. C. (2016). Spatio-temporal analyses of impacts of multiple climatic hazards in a savannah ecosystem of Ghana. *Climate Risk Management*, *14*. doi: 10.1016/j.crm.2016.09.003

A

Appendix: Literature Review

In this literature review, a range of studies concerning different aspects of the floods and drought in the Volta basin are compared. The papers can be roughly divided based on their focus or research strategy. All the studies are conducted in this century and done by scientists all over the world. The literature review is structured in an introductory part where the research objectives of the studies are discussed. In the second part, the different views on what causes these challenges are compared. Then, the research methods are reviewed and after that, the proposed solutions are compared and discussed. Finally, the research gap that needs to be filled by this study is stated.

The first studies into the possible changes in the hydrology, land use, climate (Van De Giesen et al., 2002) and challenges in water resource management (Van de Giesen et al., 2001) in the Volta basin were conducted during the start of this century. In the following years, the problems increased and research started to focus on finding causes and solutions for the increasing amount of problems. Later on, research was also scoping towards the impact of the hazards on people living in the basin.

Six of the articles in this literature review focus on the impact on communities in the basin, the effect of climate change on the river stream and consequently on their livelihoods: (Musah & Oloruntoba, 2013), (Senzanje, Boelee, & Rusere, 2008), (Abass et al., 2019), (Abass, 2020), (Ndamani & Watanabe, 2015) and (Yiran & Stringer, 2016).

Four other researchers focused on modelling the river streams in the basin and used that to find an explanation of the climatic hazards occurring in the region: (Abubakari et al., 2019), (Kankam-Yeboah, Obuobie, Amisigo, & Opoku-Ankomah, 2013) and (Amisigo et al., 2015). The research (Komi et al., 2016) includes a flood frequency analysis of the basin.

Finally, two studies were added on the positive and negative effects of constructing small dams. The first study looked at the effects of dams on ecology (Unami, Yangyuoru, & Alam, 2012). The second one analyses the impact of existing small dams in Zimbabwe (Senzanje et al., 2008).

A.1. Introduction

From the start of this century, scientists began to address their concerns about water resource management in the Volta Basin (Van De Giesen et al., 2002). The need to identify the causes of floods grew throughout the years (Di Baldassarre et al., 2010) as the flood fatalities kept increasing (Komi et al., 2016). During the last decade, floods and periods of drought are yearly occurring features in parts of northern Ghana (Musah & Oloruntoba, 2013) (Yiran & Stringer, 2016). Both inland and near the river, people struggle with floods (Abass et al., 2019) while drought was historically a problem of the inland communities (Yiran & Stringer, 2016). However, there is strong competition for water resources in the Volta Basin (Van de Giesen et al., 2001). In their research, Amisigo et al. show that the Volta Basin already lacks the surface water quantity to satisfy the three main water demands: hydropower,

agriculture and municipal, while the population keeps increasing. The scope of this research is limited to the impact of floods and drought around the White Volta and therefore the focus lies on the impact on the communities near the river.

The consequences of floods and drought on these communities are widespread. Often, the floods cause damage to crops, housing, bridges, schools, farmlands, animals, health facilities, water supply systems that use river water, irrigation systems, food storage and processing facilities (Musah & Oloruntoba, 2013). Furthermore, fatalities as a result of the floods occur. Fatalities in less developed countries tend to impact the most vulnerable groups as they have limited options of settling in safe places or taking measurements to protect themselves (Abass et al., 2019). This group needs and deserves to be protected from climate hazards and therefore, research and action is needed to find the right solutions.

A.2. Problems concerning the White Volta river

The nature of the problems that cause the floods have received limited attention according to Abass. In 2013, Musah and Oloruntoba performed research into the effects of floods on the livelihoods and food security in northern Ghana. He was the first to include the spilling of excess water by the Bagre dam in Burkina Faso in his research and found it was the main cause of floods in the White Volta River. He claimed that 75% of these floods were caused by the Bagre dam and that only 25% occur as the result of excessive rainfall events. He found that floods occur mainly in August en September and points at poor water management of the Bagre dam in Burkina Faso as the main problem. He states that as the intensity of the rain season increases southwards, Burkina Faso already experiences fewer problems from the rain season and therefore should make sure they manage their dam properly instead of spilling excess water during these months. Abass et al., agree on the reasoning that a combination of heavy rainfall and opening of the Bagre Dam are the main triggers of the flood events.

Only a small amount of studies took the contribution of the water management of the Bagre dam into consideration and, therefore, came to this conclusion. The larger group of studies lays their focus on climate change (Kankam-Yeboah et al., 2013) (Amisigo et al., 2015) and for example mention onset, duration and intensity of the rainfall as the problem of the increasing disasters (Abubakari et al., 2019). These studies do agree with (Musah & Oloruntoba, 2013) that spilling of the Bagre dam is a problem but they do not conclude that poor water management of the dam is the main problem. They state that the water holding capacity of the dam is too limited what causes the dam to spill during the wet season (Kankam-Yeboah et al., 2013) and (Abubakari et al., 2019).

While the cities of northern Ghana lack research into the floodings, Kumasi has been studied more often. Reasons for flooding of the city come down to the rapid expansion of the city with poor spatial planning. As a result, physical development of watercourses and wetland takes place which is dangerous and disrupting for the natural flow regime (Abass, 2020). Kumasi is not representative for this study as it is not located near the White Volta river but it does share the urban evolution as is now visible in Tamale. Therefore, it can be expected that without measurements, the same problems can occur in Tamale.

A.3. Methodologies

As the different studies have different scopes, the methods used also vary a lot. The first studies that were performed give a broad view of the situation and the hydrological cycle Van de Giesen et al.. Changes in land use were noticed and for the first time, the increase in the dam-building activity is called upon as a possible impact on the water resources downstream. These studies combined models from different disciplines in order to gain insight into the hydrology and the water demand of the area.

A lot of the researchers focus on effects on livelihoods and do this by approaching the inhabitants living in the Volta Basin. Musah and Oloruntoba, Abass et al., Ndamani and Watanabe and Yiran and Stringer all used interviews and questionnaires among people from different communities in northern Ghana. Musah and Oloruntoba calculated the relationship between floods and yield loss by using a

chi-square test. Abass et al. analysed the results from his household interviews by using IBM SPSS and following a thematic analytical framework for both of his studies in the area. He refers to the Ghana Meteorological Agency (Gmet) for meteorological data from 1980 onward and uses their temperature and precipitation data in his research. Yiran and Stringer tried to understand the nature of hazards and the impact on livelihoods by focus group discussions and literature research. He analysed the data with the standard precipitation index and crop failure index, for which he used weather data from different stations in Ghana.

The same approaches were followed by Senzanje et al. for his research on small dams in Zimbabwe. He did fieldwork in order to get insight into the volume data of the dams. Also, secondary data from literature was used in his research. Unami et al. looked into the effects of small dams as well, but with ecology as a point of view. A stochastic population model was used for which model values came from literature and field surveys.

The other group of research was model-based and lay their focus on hydraulic modelling of the river stream. Abubakari et al., Kankam-Yeboah et al. and Amisigo et al. used hydraulic models in combination with different climate models (respectively IPCC, ECHAM4/CSIRO and NCAR) in order to get insight in the impact of climate change on the streamflow of the river. Abubakari et al. and Kankam-Yeboah et al. both used SWAT: a process-based model used for hydraulic simulations. Besides the meteorological data, the input consists of land cover, land type and watershed data which were found in literature and by using remote sensing. Finally, sensitivity analyses were used to get an idea of the impact of climate change on the river stream. Meteorological data for the baseline came (in both?) researches from the Ghana Meteorological agency. Lastly, Amisigo et al. used three different models to model the stream flow of the White Volta: CliRun, AquaCrop and WEAP. Komi et al. only performed a flood frequency analyses for disaster risk management in the Volta Basin. He found that the flood frequency of the Volta river can be best described using the generalized extreme value distribution.

A.4. The proposed solutions

Studies that focus on climate change as the main cause for drought and floods in the White Volta, present climate adaptation as the best solution. In 2015, a micro-level study in Ghana found that adaptation measures in the agricultural areas mainly focus on adaptation to long periods of drought while farmers stay poorly prepared for floods. Adaptation measures include changes in crop types, timing of harvest and use of soil moisture conservation techniques (Ndamani & Watanabe, 2015). In urban areas, as one of the problems is the rapid urbanisation and population growth, the amount of development projects increases. City authorities should stimulate sustainable and safe development and increase drainage capacity to cope with floods (Abass et al., 2019).

The studies that took the spilling of the Bagre dam in Burkina Faso into consideration seek for solutions in the management of the dam. The easiest solution mentioned is improved water management of the Bagre Dam. This would call for institutional interventions (Abass et al., 2019). Abass et al. recommends a transboundary water resource management with cooperation from the riparian states to receive this improvement. Others are less critical on the management of the dam and state that the storage capacity of the dam should increase in order to store more water during the wet season that can be released when water is scarce, during the dry season (Kankam-Yeboah et al., 2013) (Abubakari et al., 2019).

Already in 2003, Faure found that communication concerning filling, construction and spillage of the dam was limited and that especially downstream communities where often ignored in this process of information sharing. Early warning systems for the downstream communities would reduce the damage created by floods (Di Baldassarre et al., 2010).

A solution that includes both the problems concerning the dam and the heavy rainfall is to increase the water storage in the White Volta. Mahe et al. concludes that the demand for water will increase as the population grows and land-use changes. He states that the number of dams will increase but

he is concerned that the impact of these structures are underestimated. He argues that not only the positive effects of dams on reducing the discharge peaks, but also the negative impacts on ecology and water availability downstream have to be studied thoroughly (Mahe et al., 2013). Yiran and Stringer suggest constructing small dams in the river stream in order to reduce the streamflow and harvest the rainwater. He argues that this solution will reduce the dependence on rainfed agriculture and therefore cause an increase in the resilience against drought. Unami et al. and Senzanje et al. did research on existing rivers in Zimbabwe where small dams are constructed and agree on the positive impact on water storage. However, there are also concerns that need to be taken into consideration. While small dams create pools of water that can be easily accessed for irrigation and fishery, dams disrupt the natural flow regime which fragments migration routes of fish species (Unami et al., 2012). Furthermore, sediment trapping must be taken considered as the construction of dams can impact the sediment load at sea (Mahe et al., 2013). Finally, in order to equally spread the benefits of the dams, management and conservation need to be well organised, otherwise, the benefits will consist only in the short term.

A.5. Research gap

Uncertainty in the field exists on the contribution of the Bagre Dam and its management on floods in the White Volta. This is important knowledge the difference between a solution that lies in either better water resource management in Burkina Faso or the need for constructions and adaptation in Ghana. More literature research might give answers to this question.

Current research has focused on the second situation, where the solution must be found in Ghana. The possibilities of small dams in rivers are explored. Disagreement exists on whether the hydraulic benefits make up for the loss in ecology and connectivity of the river. A solution that lies in between and could be beneficial for both arguments, is the construction of multiple small dams. This way, the connectivity of the river keeps intact, while water is stored. However, in the current research, this type is construction is not yet explored.

Different models have been used to model the floods in the White Volta River. SWAT is used in two of the studies to model the impact of climate change and land-use changes on the watershed. Deltares has developed a promising new model (D-HYDRO) that can simulate almost in the same way. However, this model can also incorporate the impact of structures in water streams and sediment flow in rivers. As the model is new, it has not yet been used for research in the Volta Basin. The model has high potential as it is based on prominent existing models in the field. Therefore, testing this model for the use of implementing small dams in the White Volta can be a large contribution for further research.

Finally, an important gap in existing research is the possible construction of the Pwalugu dam in Ghana. This project is in development and would impact the flow regime of the river. Implementing this dam in the hydraulic model would give important new insight in the future benefits and possible risks of the communities living near the White Volta river.

B

Erosion Expension Wave

The figure below shows how sandmining of the river bed can result in an erosion expansion wave that quickly grows over the river reach.

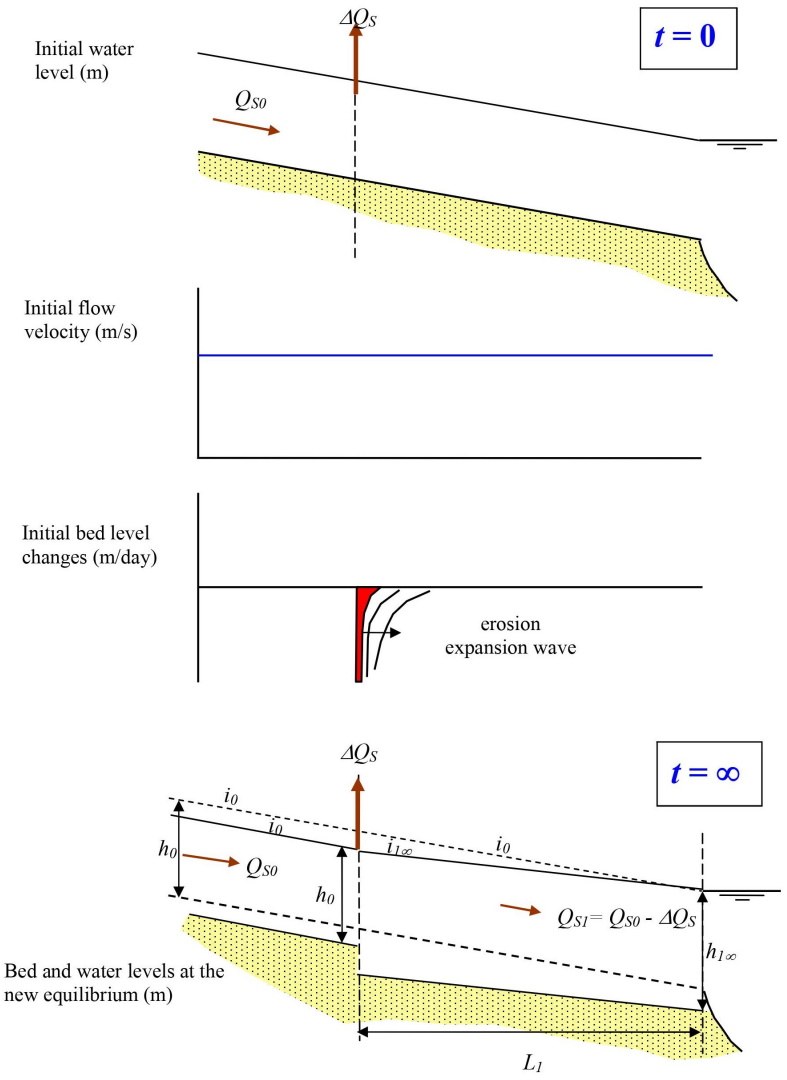

Figure B.1: Erosion expension wave as a result of continuous sand mining in the river bed

C

Appendix: QGIS procedures

C.1. Extraction of the river shape from Sentinel

Figure C.1 shows the conversion from Sentinel-2 raster data to a shapefile. The most common procedure to detect open water is using the Normalized Difference Water Index (NDVI). This method was first used in 1996 by McFeeters, where open water features are delineated from other features by using different wavelengths in remote sensing. The calculation of this NDWI is simple: $NDWI = \frac{GREEN-NIR}{GREEN+NIR}$.

The Sentinel-2 data, shown in the upper corner of figure C.1 shows how the combination of SWIR, vegetation red edge and red, already are able to locate the water. By comparing the reflection in different pixels of the map, it became clear that the SWIR band by itself has great differences in values on the water surfaces compared to the vegetation and land. Therefore, a threshold of 120 was used in QGIS in order to extract the water bodies, as shown in the figure on the right top figure.

In the next step, the raster data was polygonized and only the polygon that is the river was saved. This polygon is shown in the lower right figure. Then, the centerline of the polygon was taken in order to create the river shape, shown in the lower right figure. By comparing the river shape to the Sentinel data, the Landsat data and the Google Maps data, it was concluded that the shape follows almost exactly the river.

Finally, the right balance was found between smoothening the river shape and simplifying it. A very smooth shape creates a lot of nodes very close to one another, which makes calculations in D-HYDRO extremely slow. A simplified river shape can miss some of the finer bends which causes the final river length to become shorter than it in reality was.

C.2. Using OSM to extract elements in flood areas

OSM is a tool in QGIS that is able to detect different elements, like roads, nature, houses and other buildings. This tool is used in order to see what elements are reached by the flood. The combination of the flood characteristics, like water level or rising velocity, will then determine which elements lose value as a result of the flood.

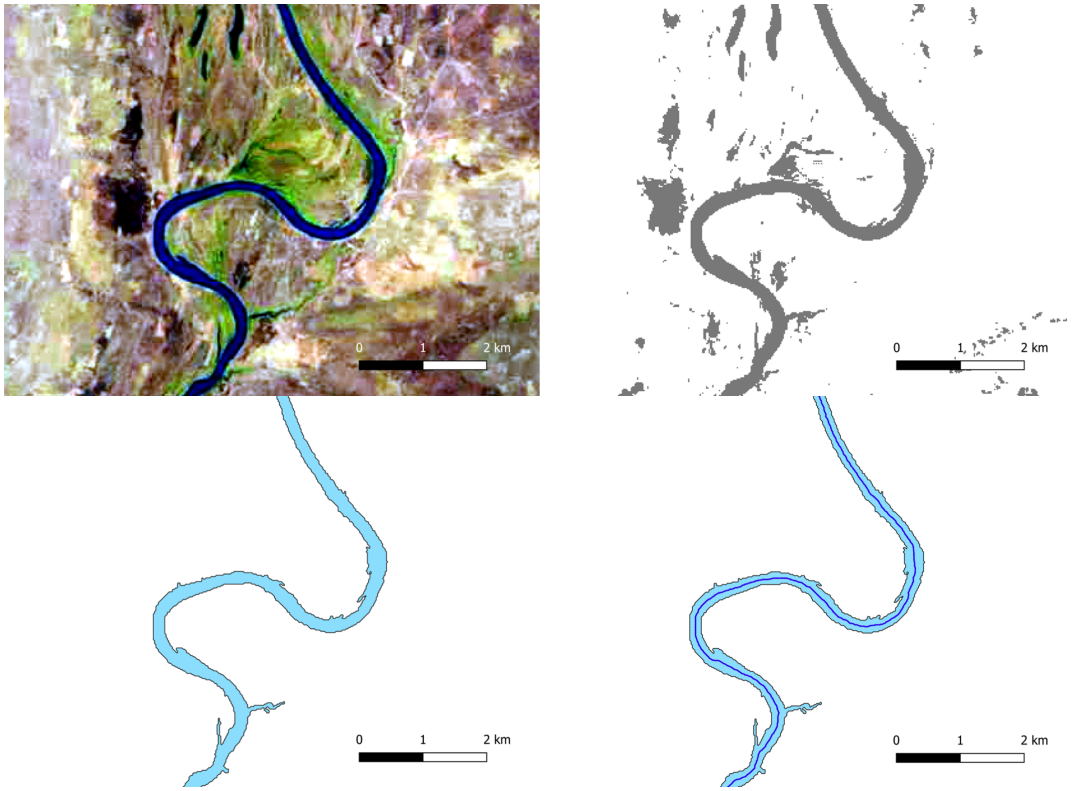

Figure C.1: Stepwise conversion from raw Sentinel data to a vector of the river shape. In the upper left figure, the raw Sentinel map is shown. In the upper-right figure, the Sentinel data is clipped for band1 values lower than 120. These were polygonized, as shown in the grey planes. The lower left figure shows the clipped polygon that is the river stream. And finally, in the lower right figure, the centerline of the polygonized river is created, giving the shape of the river in dark blue.

D

Appendix: D-HYDRO setup

This appendix gives a step-by-step overview of the model setup. It explains how D-HYDRO can be used to create the 1D2D coupled model.

D-HYDRO (Delft3D FM) is software developed by Deltares. The software consists of different modules: D-Flow Flexible Mesh, D-Waves, D-Real Time Control, D-Water Quality, D-Particle Tracking and D-Morphology.

D.1. Creating the White Volta River

When setting up the D-HYDRO model, the first steps can be performed using the GUI. As the GUI is not yet completely finished, it is used as least as possible to prevent error messages.

1. Download D-HYDRO Suite 1D2D (Beta) (0.9.9.52575)
2. Open the program and create a new Flow Flexible Mesh Model
3. Change the grid properties to the coordinate system of the previously create GIS shapefile: WGS84/UTM zone 30N [EPSG:32630]
4. Edit the grid and import the shapefile of the river as a Spline
5. Select the grid and import the selected features to a branch layer, then finish the editing mode. The river stream is now created
6. Click on the nodes and the river stream to change the names
7. Select the stream and generate computational grid nodes. The length between these grid nodes should be larger than the grid size of the 2D model that is going to be coupled later on
8. Change the Initial Conditions of the model, these consist of the initial water level
9. Add the Boundary Conditions for the two outer nodes. In this case, the discharge station in Yarugu and the water levels in Lake Volta were used as the boundary conditions
10. Add cross-sections at the locations where these were measured
11. Run the model and export the dimr configuration to a different folder so that you can continue using batch files

As there were only 4 known cross-sections, these need to be interpolated using Matlab and Python functions. Deltares has developed a tool in Matlab to interpolate the cross-sectional widths. The tool imports the dimr cross-section files, interpolates the cross-sections set by hand and returns the interpolated cross-section for every cell in the model.

These Matlab codes needed to do this, are available via OpenEarth. By using TortoiseSVN, complete folders can be extracted from the OpenEarth repository. Then, the complete folder with Matlab functions was exported to the local drive. The code D3D_interpolate_crossections then needs two inputs: the original D-HYDRO model (mdu) and a similar model folder where the updated cross-sections can be stored (crsdef). After doing this, continue to work on the updated file.

As the Matlab codes only interpolate the bed width and create files for every grid point on the channel, some Python tools were created for this project to interpolate the depth of the riverbed.

The bed levels are derived from the DEM data near the riverbed and then added to the crsloc file by a Python tool, created for this project.

D.2. Model Parameters

The input file for the hydrodynamic simulations is the Master Definition Unstructured (.mdu) file. After exporting the basic model, explained in the first subsection, the mdu file consists 7 different model parts, denoted by square brackets. The sediment part is added by hand as it was not included in the basic file. How to do this is shown in figure D.1. The most important sections of the mdu file are discussed in the paragraphs below.

D.2.1. General

The first part contains basic model information: the used version and the name of the program. This does not need to be changed.

D.2.2. Sediment

To be able to calculate the sedimentation upstream of the dam, the morphodynamics need to be added to the model by hand. To do so, modify the mdu file by adding a sediment characteristics column.

```
[General]
Program                = D-Flow FM
Version                = 1.2.110.68456M
fileType               = modelDef
fileVersion            = 1.09
GuiVersion             = 1.5.0.52560
AutoStart              = 0
PathsRelativeToParent  = 0

[sediment]
MorFile                = mor.mor
SedFile                = sed.sed
Sedimentmodelnr        = 4

[geometry]
NetFile                = FlowFM_net.nc
BathymetryFile         =
DryPointsFile          =
GridEnclosureFile      =
WaterLevIniFile        =
LandBoundaryFile       =
```

Figure D.1: Visualisation of adding the sediment to the MDU text file.

The .mor file and the .sed file are files that consist of parameters about the morphodynamics and sediment transport, they are shown respectively in table D.1 and D.2.

D.2.3. Geometry

The geometry consists of different components. The first file is called $FlowFM_net.nc$ and includes all the information on the 1D and 2D grid of the model. The 1D shapefile determines the shape of the river. Even though the shapefile follows a certain route, the model treats the shape as if it is one straight river without bends. The data is stored as a series of computational grid nodes and internodes with a certain interval. A different file is added to define the cross-section locations and definitions. These are interpolated by the model. For the 2D data, all grid information is stored in the $FlowFM_net.nc$ file as well.

Secondly, a file included in the geometry defines the different structures. In this research, only orifices were places at different locations. Section 5.4.4 elaborates on the parameters of this specific file.

Parameter	Value	Unit	Description
MorFac	25	[-]	Morphological scale factor
MorStt	60.	[min]	Start time for bed updating (in minutes rel. to simulation start time)
Thresh	0.1	[m]	Threshold sediment thickness for reducing sediment exchange
MorUpd	true	[T/F]	Update bathymetry during flow run
CmpUpd	true	[T/F]	Update bed composition during flow run
EqmBc	true	[T/F]	Equilibrium concentration at inflow boundaries
DensIn	false	[T/F]	Include effect of sediment on density gradient
Islope	3	[-]	Bed slope formulation (3 = Koch & Flokstra formulation)
AShld	0.70	[-]	Bed slope parameter Koch & Flokstra
BShld	0.5	[-]	Bed slope parameter Koch & Flokstra
AksFac	0.5	[-]	Van Rijn's reference height (AKSFAC * KS)
RWave	2.0	[-]	Wave related roughness (RWAVE * estimated ripple height. Van Rijn Recommends range 1-3)
Sus	1.0	[-]	Multiplication factor for suspended sediment reference concentration
Bed	1.0	[-]	Multiplication factor for bed-load transport vector magnitude
SusW	0.3	[-]	Wave-related suspended sediment transport factor
BedW	1.0	[-]	Wave-related bedload sediment transport factor
SedThr	0.25	[m]	Minimum water depth for sediment computations
ThetSD	1.0	[-]	Fraction of erosion to assign to adjacent dry cells
Hmaxth	1.e-3	[m]	Max depth for variable ThetSD. Set <SedThr to use global value only
FWFac	1.0	[-]	Vertical mixing distribution according to van Rijn (overrules k-epsilon model)
EpsPar	true	[T/F]	Only for waves in combination with k-epsilon turbulence model TRUE : Van Rijn's parabolic-linear mixing distribution for current-related mixing FALSE: Vertical sediment mixing values from K-epsilon turbulence model
Espir	1.00	[-]	Secondary flow weighting factor for bed load transport
IopKCW	1	[-]	Flag for determining Rc and Rw (Only for Van Rijn (1993)) 1 (default): Rc from flow, Rw=RWAVE*0.025 2 : Rc=RDC and Rw=RDW as read from this file 3 : Rc=Rw determined from mobility
RDC	0.01	[-]	Rc in case IopKCW = 2
RDW	0.02	[-]	Rw in case IopKCW = 2
UpdInf	true	[T/F]	Flag for updating bed at inflow boundaries FALSE (default) : Bed level constant TRUE : Down-wind approach
TraGra	true	[T/F]	Flag for updating bed level with transport gradients
GamMax	0.6	[-]	Maximum ratio Hrms/water depth
Multi	true	[-]	Flag for running parallel conditions

Table D.1: Mor.mor file description

Thirdly, a friction file is included in the geometry. This file defines the friction parameters for the main channel.

Finally, a file including the initial conditions is added. In this file, the initial water depth or water level can be set. The difference between the two is that the water depth uses the bed level as a reference point an the water level uses a constant reference point over the whole river. As the data for this research was measured relative to the river bed, the water depth is used. The initial water depth was randomly set to 3 meters, therefore the model needs startup time to find balance.

Parameter	Value	Unit	Description
[SedimentOverall]			
IopSus	1		If Iopsus=1: susp. sediment size depends on local flow and wave conditions
[Sediment]			
Name	#Sediment1#		Name as specified in NamC in mdf-file
SedTyp	bedload		Must be ”sand”, ”mud” or ”bedload”
SedDia	0.007	[m]	Median sediment diameter (D50)
CDryB	1.60e+03	[kg/m3]	Soil Reference density for hindered settling (dry bed density)
RhoSol	2.65e+003	[kg/m3]	Specific density
IniSedThick	3	[m]	Initial sediment layer thickness at bed (uniform value or filename)
TraFrm	4	[-]	General formula (written like Meyer-Peter Mueller)
ACal	8.0	[-]	Calibration factor
PowerB	0.0	[-]	B Power
PowerC	1.5	[-]	C Power
RipFac	0.7	[-]	Ripple factor
ThetaC	0.047	[-]	Dimensionless critical shear stress parameter

Table D.2: Sed.sed file description

In tabel D.3, the rest of the geometry input parameters are shown.

D.2.4. Numerics

The numerics section was left in default mode. This part includes choices for calculation methods like solver types. Furthermore, thresholds are given for parameters like the threshold water depth for wetting and drying. All values can be found in the Master Definition File chapter of the User Manual (Deltares, 2020).

D.2.5. Physics

The physics section of the mdu file includes the physical parameters that influence the river flow. For example the friction, the water density adn the temperature are defined in this section. All the included parameters are shown in table D.4.

D.2.6. Time

The time section defines all the time parameters. For example, the reference date, the time intervals and the timezone are specified here. In this research the reference date is always 01/01/2000 as that is the date from where the data availability good enough. These values were changed for different runs. When runs cover multiple years, the computational time can be reduced by increasing the time interval.

D.2.7. External forcing

The external forcing section includes only the directory to the boundary conditions file. This file includes the boundary conditions at Yarugu (Q-t) and Lake Volta (h-t), as well as the inflow (Q-t) from the eight larges tributaries of the White Volta river.

D.2.8. Output

In the output section of the .mdu file, the types of output files are assigned. These are stored in the history file or in the map file. The water levels and velocity data was saved for both the historical and map files. Besides that, the history file includes structure settings of the orifice and the map files includes lateral sources and discharges.

Another important parameter in the Output section is the HisInterval. This is the interval in seconds,

Table D.3: Geometry input in the .mdu file

Parameter	Value	Unit	Description
WaterLevIni	0	[m]	Initial water level (overwritten by IniFieldFile)
Bedlevuni	-5		Uniform bed level, (only if bedlevtype>=3, used at missing z values in netfile)
Bedslope	0	[-]	Bedslope inclination, sets zk = bedlevuni + x*bedslope and sets zbndz = xbndz*bedslope
BedlevType	1		1: at cell center (tiles xz,yz,bl,bob=max(bl))
Blmeanbelow	-999		below this level the cell centre bed level is the mean of surrouding netnodes
Blminabove	-999		above this level the cell centre bed level is the min of surrouding netnodes
AngLat	0		Angle of latitude S-N (deg), 0 means there is no Coriolis effect
AngLon	0		Angle of longitude E-W (deg), 0 means Greenwich Mean Time
Conveyance2D	-1		-1:R=HU, 0:R=H, 1:R=A/P, 2:K=analytic-1D conv,3:K=analytic-2D conv
Nonlin1D	1		Non-linear 1D volumes, applicable for models with closed cross sections. 1 =treat closed sections as partially open by using a Preissmann slot
Nonlin2D	0		Non-linear 2D volumes, only i.c.m. ibedlevtype = 3 and Conveyance2D>=1
dxDoubleAt1DEndNodes	0		Extend endnodes with half Δx.
Slotw2D	0		
Slotw1D	0.005		
Dxmin1D	1		
Makeorthocenters	0		1=yes, 0=no switch from circumcentres to orthocentres in geominit
Dcenterinside	1		limit cell center; 1.0:in cell <->0.0:on c/g
Bamin	1E-06		Minimum grid cell area, i.c.m. cutcells
OpenBoundaryTolerance	3	cell size	Search tolerance factor between boundary polyline and grid cells.
RenumberFlowNodes	1		Renumber the flow nodes (1: yes, 0: no)
Kmx	0		Number of vertical layers
Layertype	1		1= sigma-layers, 2 = z-layers, 3 = use VertplizFile
Numtopsig	0		0 Number of sigma-layers on top of z-layers
SigmaGrowthFactor	1		layer thickness growth factor from bed up
AllowBndAtBifurcation	1		Extend endnodes with half Δx
UseCaching	1		Use caching for geometrical/network-related items (0:no, 1: yes)

on which the calculated values are saved. This value was specified for each different run. When runs cover multiple years, this value was increased in order to reduce the data size. For intervals in the order of 300 seconds, the data size increased to an order of 20 GB.

D.3. Calculate the water height

The water levels are calculated using the Saint-Venant equations. When the model runs, the water levels are saved for each node, on each time step. The data is stored in the output folder under FlowFM_his.nc.

Table D.4: Physical parameters in the mdu file

Parameter	Value	Unit	Description
UnifFrictCoef	40	[m^0.5/s]	Uniform friction coefficient, 0=no friction
UnifFrictType	0		0=Chezy, 1=Manning, 2=White-Colebrook, 3=WhiteColebrook of WAQUA
UnifFrictCoef1D	40	[m^0.5/s]	Uniform friction coefficient in 1D links, 0=no friction
UnifFrictCoefLin	0	[m/s]	0. Uniform linear friction coefficient for ocean models , 0=no
Umodlin	0		linear friction umod , only for ifrctyp=4,5,6
Vicouv	1	[m2/s]	Uniform horizontal eddy viscosity
Dicouv	1	[m2/s]	Uniform horizontal eddy diffusivity
Vicoww	5E-05	[m2/s]	Uniform vertical eddy viscosity
Dicoww	5E-05	[m2/s]	Uniform vertical eddy diffusivity
Vicwminb	0	[m2/s]	Minimum viscosity in production and buoyancy term
Smagorinsky	0		Add Smagorinsky horizontal turbulence : vicu = vicu + ((Smagorinsky*dx)**2)*S
Elder	0		Add Elder contribution : vicu = vicu + Elder*kappa*ustar*H/6); e.g. 1.0
Irov	0		Wall friction, 0=free slip, 1 = partial slip using wall_ks
wall_ks	0		Nikuradse roughness for side walls, wall_z0=wall_ks/30
Rhomean	1000	[kg/m3]	Average water density
Idensform	2		1=Eckart, 2=UNESCO
Ag	9.81	[m/s2]	Gravitational acceleration
TidalForcing	0		(0=no, 1=yes) (only for jsferic == 1)
Doodsonstart	55.565		TRIWAQ = 55.565D0 , D3D = 57.555D0
Doodsonstop	375.575		TRIWAQ = 375.575D0 , D3D = 275.555D0
Doodsoneps	0		TRIWAQ = 0.0 400 cmps , D3D = 0.03 60 cmps
Salinity	0		Include salinity, (0=no, 1=yes)
InitialSalinity	0	[ppt]	Inital salinity concentration
Sal0abovezlev	-999	[m]	Salinity 0 above level
Backgroundsalinity	30	[ppt]	Background salinity concentration
InitialTemperature	6	[degC]	Inital temperature
Secchidepth	2	[m]	Water clarity parameter
Stanton	-1		Coefficient for convective heat flux ( ), if negative, then Cd wind is used
Dalton	-1		Coefficient for evaporative heat flux ( ), if negative, then Cd wind is used
SecondaryFlow	0		Secondary flow (0=no, 1=yes)
BetaSpiral	0		Coefficient for secondary flow
Temperature	0		Include temperature, (0=no, 1=only transport, 5=heat flux model (5) of D3D), 3=excess model of D3D

D.4. Couple to 1D2D model

The created 1D model considers the river as given by the cross-sectional parameters. The outer points of the riverbank are considered to be infinitely high so that water will always stay in the river bed. In order to model what will happen once the water level exceeds the riverbank, a 2D grid needs to be added at these flood locations.

A 2D grid can be generated using the Delft3D RGFGRID software. The following steps should be taken in order to create the grid.

1. Determine the locations on the 1D model where the water depth exceeds the riverbank height.

Table D.5: Time parameters in the mdu file

Parameter	Value	Unit	Description
RefDate	20000101	[yyyymmdd]	Reference date
Tzone	0		Data Sources in GMT are interrogated with time in minutes since refdat-Tzone*60
DtUser	300	[s]	User timestep in seconds (interval for external forcing update & his/map output)
DtNodal		[s]	Time interval for updating nodal factors in astronomical boundary conditions [Dd HH:MM:SS.ZZZ]
DtMax	30	[s]	Max timestep
DtInit	1	[s]	Initial timestep in seconds
UpdateRoughnessInterval	86400	[s]	Update interval for time dependent roughness parameters
Tunit	S	[D/H/M/S]	Time units in MDU
TStart	115689600	[Tunit]	Start time w.r.t. RefDate
TStop	118195200	[Tunit]	Stop time w.r.t. RefDate

Find the exact coordinates of these flood locations.

2. Open QGIS and cut out a polygon of the DEM at the flood location. In order to limit the computational time, this polygon should not be larger then 2 km to start with. Save this polygon as .xyz file using the GRASS tool *r.out.xyz*
3. Open the RGFGRID tool of Delft3D and click on import attributes. Import the samples (.xyz) created in the previous step.
4. Click on Edit - Polygon - New and create a polygon within the samples. Then refine the polygon so, that there are about 80 points, close to one another.
5. When enough points are created on the polygon, go to Operations - Grow Grid from Polygons. This will create the 2D grid.
6. Delete the samples and export the grid as UGRID. This format is needed for the D-Flow module of the D-HYDRO.
7. Open the GUI of Delft 3D where the 1D model is already defined. Click on Spatial operations - Import and import the cropped DEM (.xyz) files of the flood area.
8. Then import the 2D grid by clicking with the right mouse button on Grid and import the 2D unstructured grid.
9. Click on Copy to Spatial data and then interpolate the selected set on the 2D grid. The result will look like figure D.2
10. Finally, make links between the 1D and the 2D grid by clicking on Map - Generate links and draw a polygon around the whole model. Every 1D grid point will now create a link with the nearest center of one of the 2D grid cells.

Due to a limitation in the method for determining the bathymetry, the 1D and 2D grid did not completely fit. As a result of the underestimated bed level of the river, a bank-full situation in the model did not drain towards the 2D grid immediately but needed a couple more meters at some places. To compensate for this, every 2D grid was adjusted slightly, to make sure the riverbank of the 1D model corresponds to the boundary of the floodplain of the 2D model.

D.5. Model the flood risk

By running the previously generated 1D2D model, outcomes for the 1D as well as for the 2D grid were generated. When opening these .nc files in QGIS, different parameters could be reviewed, for each day of interest. The data of multiple consecutive days with high water levels were compared to the Open Street Map of the underlying villages. Buildings and agricultural areas were selected and the

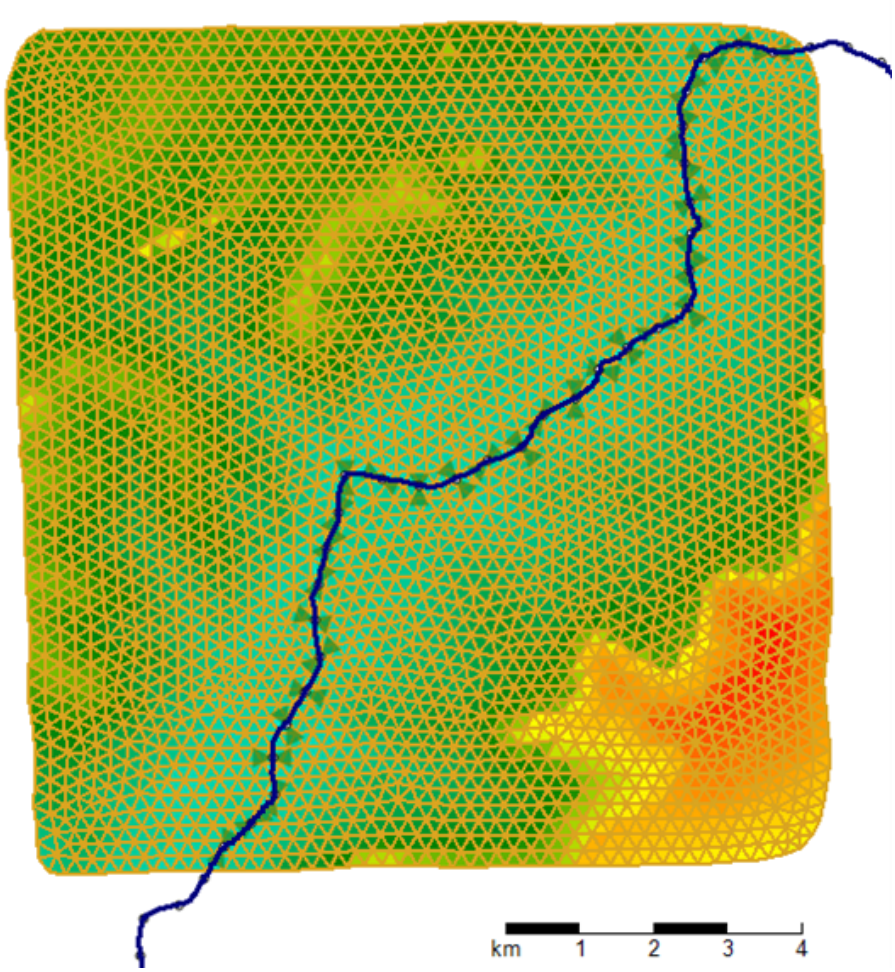

Figure D.2: 2D interpolated grid

Table D.6: 2D Grid adjustment values

	Pwalugu	Duu	Janga	Dipale	Nawuni	Daboya	Yapei
Bed level [m]	124.13	117.13	100.13	95.75	91.67	83.53	72.51
Freeboard at t=0 [m]	7.90	8.07	8.62	8.84	8.98	7.41	10.68
DEM [0]	137	129	114	108	103	94	88
2D Grid adjustment [m]	-4.97	-3.8	-5.25	-3.41	-4.35	-3.06	-4.81

water levels and flood duration were coupled to these areas. By doing that, flood risk for the situation with and without the dams could be compared.

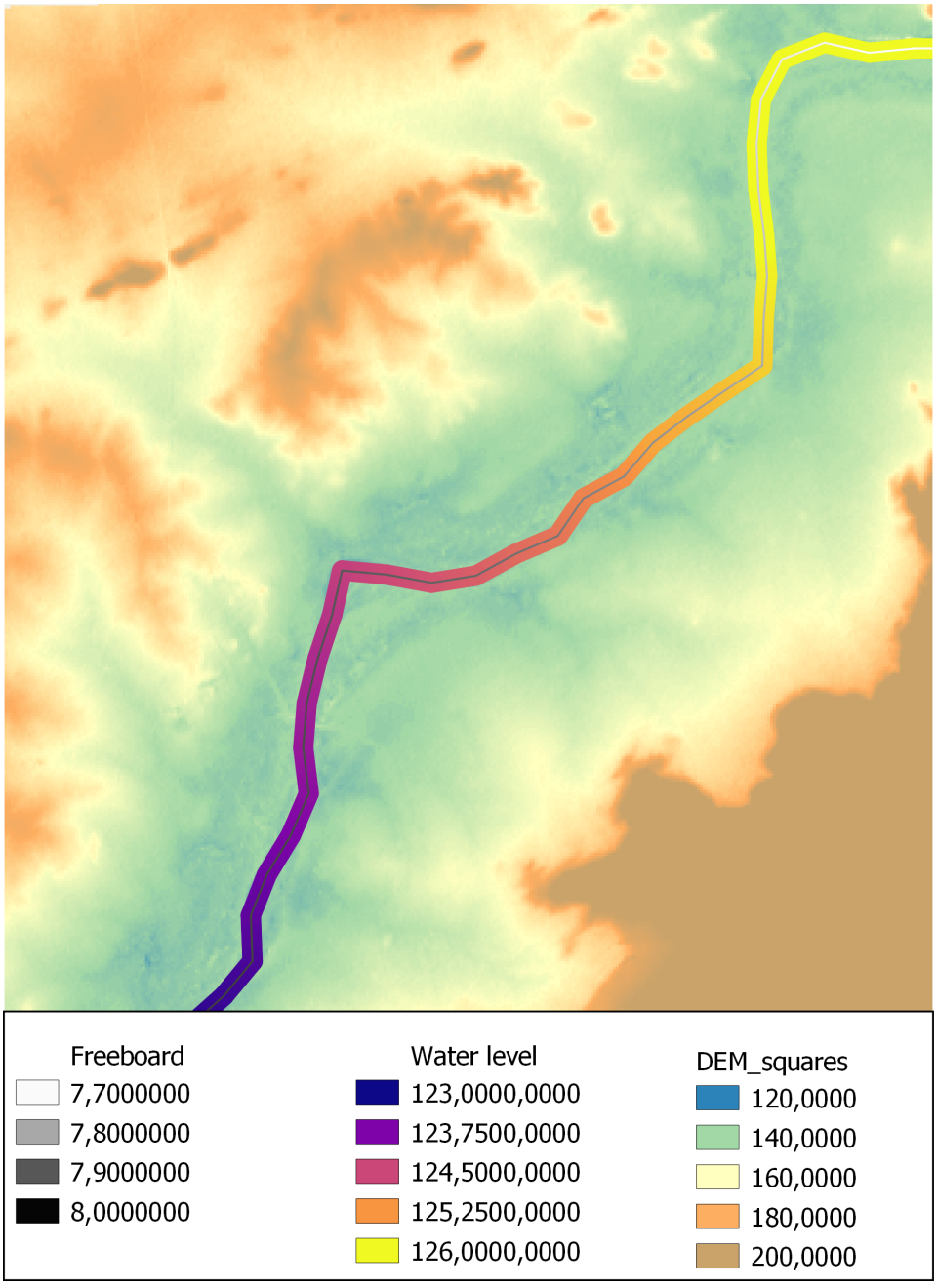

Figure D.3: Adjustment of the 2D grid to comply with the bed level.

E

Derivation of the Saint-Venant equations

This appendix shows the more in-depth derivation of the Saint-Venant equations discussed in section 3.1.2.

E.1. Continuity equation

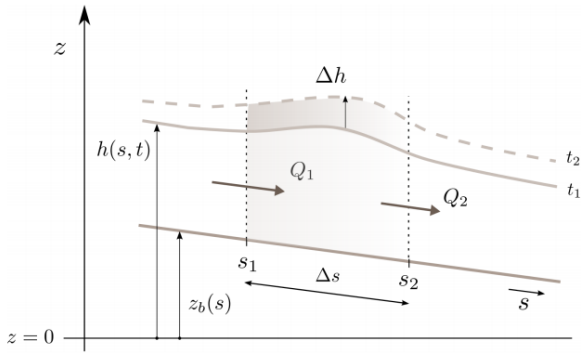

Figure E.1: Longitudinal cross-section of a river reach (Battjes & Labeur, 2017)to visualize the volume balance when a wave occurs. This theory can be applied to calculate the backwater effects.

Figure E.1 illustrates a schematic cross-section of a river reach at two time steps t_1 and t_2. When you consider the control volume between s_1 and s_2 you can set up the mass balance. Because the river has a free surface and a limited depth, the pressure variation over the height is small and the density can be considered homogeneous. This means that the water is incompressible which reduces the mass balance to a volume balance, see equation E.1.

$$(Q_1 - Q_2) * \Delta t = -\Delta Q * \Delta t \tag{E.1}$$

The volume balance states that the incoming discharge minus the outgoing discharge over a time period Δt is equal to the change of water volume that is stored in the control volume over that same time period. When these are positive, it means that the volume of water between s_1 and s_2 has increased, as is the case in the example of figure E.1. The change in stored volume can also be substituted by ΔV and expressed in terms of cross-section change ΔA and the control length Δs as shown in equation E.2.

$$\begin{aligned} \Delta V &= -\Delta Q * \Delta t \\ \Delta A * \Delta s &= -\Delta Q * \Delta t \\ \frac{\Delta A}{\Delta t} &= \frac{-\Delta Q}{\Delta s} \end{aligned} \tag{E.2}$$

Taking the limit for time and space equation E.2 to zero and substituting the width of the free surface (B) of the river is the final step to derive the continuity equation (3.2).

E.2. Momentum Balance

As explained in equation 3.3, momentum of water the mass of that water times the velocity of that mass.

Newton's second law couples the change of the velocity in time (acceleration) of an object, with mass m, with the forces acting on that object by $F = m * a$. When rewriting the second law of Newton we receive equation E.3. Important to remember from this, is that the forcing per unit mass equals the momentum.

$$\begin{aligned} \vec{a} &= \frac{dv}{dt} \\ \vec{F} &= m * a \\ \vec{F} &= m\frac{d\vec{v}}{dt} = \frac{d\vec{p}}{dt} \end{aligned} \tag{E.3}$$

As shown in equation 3.3 and E.3, there are a lot of vectors involved in momentum and force. This means that the values have three directional components: the streamwise direction s; the normal direction n in the plane of the flow; and the bi-normal coordinate pointed in the vertical direction (Battjes & Labeur, 2017).

Equation E.4 shows the three-dimensional Euler equations.

$$\begin{aligned} \frac{\mathrm{D}u_s}{\mathrm{D}t} &= \frac{\partial u_s}{\partial t} + u_s\frac{\partial u_s}{\partial s} = -g\frac{\partial(z+p/\rho g)}{\partial s} \\ \frac{\mathrm{D}u_n}{\mathrm{D}t} &= \frac{\partial u_n}{\partial t} + \frac{u_s^2}{r} = -g\frac{\partial(z+p/\rho g)}{\partial n} \\ \frac{\mathrm{D}u_z}{\mathrm{D}t} &= \frac{\partial u_z}{\partial t} = -g\frac{\partial(z+p/\rho g)}{\partial z} \end{aligned} \tag{E.4}$$

The right terms in these equations represent the forcing per unit mass, mentioned in the previous part. For now, this forcing consists of gravity and pressure gradients. This combination is often expressed as the gradient of the piezometric head h_p. The piezometric head can be calculated by equation E.5.

$$h_p = z + \frac{p}{\rho * g} \tag{E.5}$$

When considering long waves, some assumption can be applied on these Euler equations:

1. Vertical accelerations are neglected. This causes the term $\frac{\mathrm{D}u_z}{\mathrm{D}t}$ to be zero.
2. The water is shallow with a hydrostatic vertical pressure distribution. This means that the weight on top of the bottom water does not affect the density of this water. Therefore, the change in vertical pressure is also set to zero. This eliminates the whole third Euler equation.
3. At the free surface, the piezometric head is calculated with the atmospheric pressure and the height h above the reference level $z = 0$. Considering that the vertical change in pressure is zero, the right hand term can always be calculated using this boundary condition.

These assumptions lead to equation E.6 (Battjes & Labeur, 2017).

$$\begin{aligned} \frac{\partial u_s}{\partial t} + u_s \frac{\partial u_s}{\partial s} &= -g \frac{\partial h}{\partial s} \\ \frac{\partial u_n}{\partial t} + \frac{u_s^2}{r} &= -g \frac{\partial h}{\partial n} \end{aligned} \tag{E.6}$$

For one dimensional use, it is assumed that the particle acceleration is the same over the whole cross-section. Therefore, the average flow can be used which simplifies the equations even more, to the form of equation E.7.

$$\frac{\mathrm{D}U}{\mathrm{D}t} = \frac{\partial U}{\partial t} + U \frac{\partial U}{\partial s} = -g \frac{\partial h}{\partial s} \tag{E.7}$$

Up to this point, the only forcing included is gravity and pressure. However, the river bed will cause for flow resistance which plays a large role in the acceleration of the particles. This flow resistance is expressed per unit mass as $\frac{\tau}{\rho * R}$, where R is the hydraulic radius which, in shallow rivers, can be approximated by the water depth d. Adding this to the simplified Euler equation leads to equation E.8.

$$\frac{\partial U}{\partial t} + U \frac{\partial U}{\partial s} + g \frac{\partial h}{\partial s} + \frac{\tau}{\rho R} = 0 \tag{E.8}$$

The last step is to relate the resistance to the flow velocity and then express the equation in terms of discharge. It is assumed that, for flows with high Reynolds numbers, the resistance varies with the flow velocity as expressed in equation E.9. Here, c_f is the dimensionless resistance coefficient. Also, it is assumed that the resistance is evenly distributed over the river bed.

$$\tau_b = c_f \rho |U| U \tag{E.9}$$

The flow velocity can be expressed as the discharge divided by the conveyance cross-section. Substituting equation E.9 and the discharge, gives the second shallow-water equation: the momentum balance (see equation 3.4).

F

Calibration

This appendix elaborates on the calibration methods used in order to come to the final model and shows the results when using different parameters.

F.1. Calibration of the first morphological run

Before running the first morphological model, a rough calibration was performed. Several combinations of Chézy values were tested in order to come to model output that corresponds with the measured water depths at Pwalugu and Nawuni.

One value was assigned to the river segment before Pwalugu and a second value was assigned to the segment after Pwalugu. Figure F.1 shows the results of several combinations of these Chézy values. The results were not yet acceptable for the final model but were good enough for this first rough run. By the eye, it was chosen to start off with a Chézy value of 60 $m^{0.5}/s$ on the first segment and 50 $m^{0.5}/s$ on the second segment.

F.2. Calibration of the final model

With the Chézy values of the previous section, a rough estimation of the morphological impact on the riverbed was made. This was used as a starting point of the final models, of which the 1D model was calibrated in a more extensive way.

For this calibration, three river sections with different Chézy values were defined: Yarugu - Pwalugu, Pwalugu - Nawuni, Nawuni - Lake Volta. To gain better insight in the impact of the Chézy value, a small sensitivity analysis was performed. The model ran between May and November of 2003, for different combinations of Chézy values. Figure F.2 shows the model output with different combinations of Chézy parameters. On the right side, the Chézy value of the first segment ranges between 30 and 60 $m^0.5/s$. Towards the right, the figures show differentiation in the Chézy parameters for the second and the third segments respectively.

What becomes clear from these plots is that the first Chézy parameter has an overall impact on the height of the water depth, both in Pwalugu as in Nawuni. Increasing the chézy value causes a decrease in the water depth and the other way around. The second Chézy value has mainly an effect on the water depth in Pwalugu, while the third Chézy value affects the water depth in Nawuni.

From the results of the sensitivity analyses, different possible Chézy combinations were tested in order to find out what the best fit was. The process was trial and error based, adjusting every time the parameters and running the model again. From this calibration process, the best parameter set was found when the first, second and third segments have the Chézy values of 30 40 and 60 $m^0.5/s$ respectively. The results of this calibration process are shown in figure F.3.

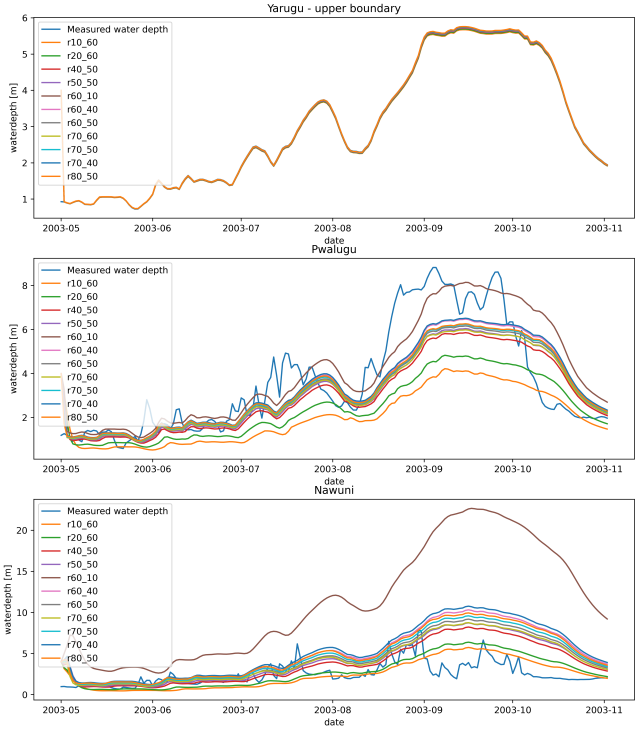

Figure F.1: First rough model calibration.

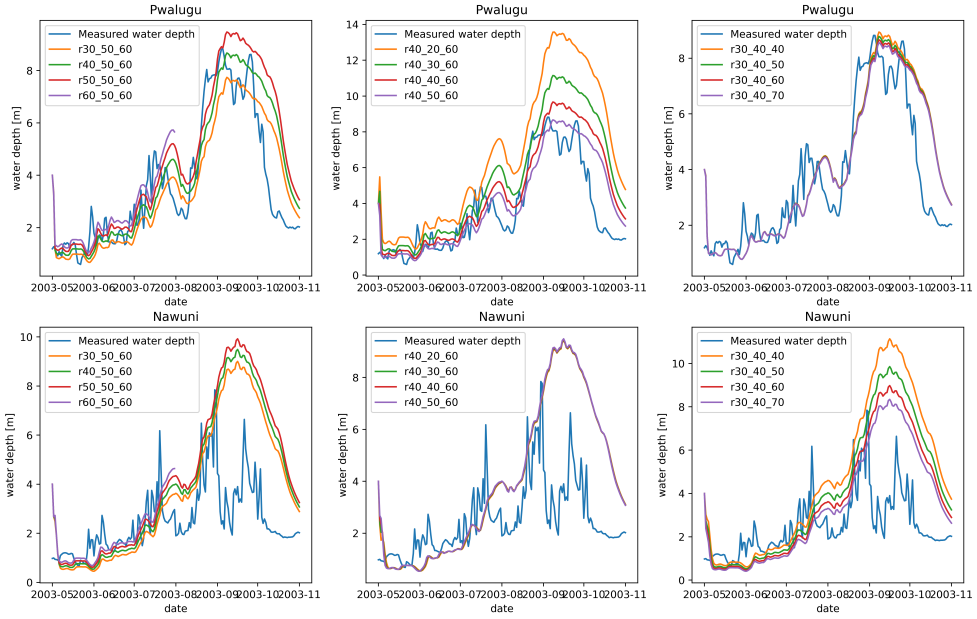

Figure F.2: Sensitivity analyses of the Chézy value.

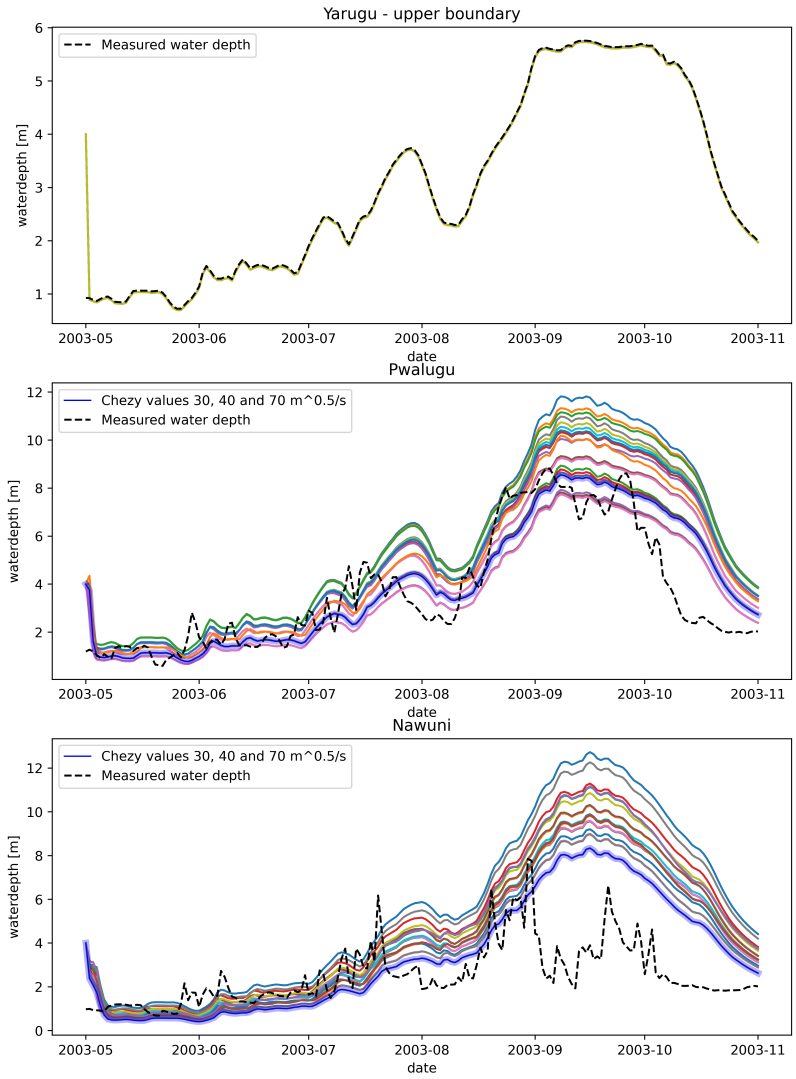

Figure F.3: Final calibration of the 1D model

G

Dam design

G.1. Results from the Sensitivity Analyses of the Dams

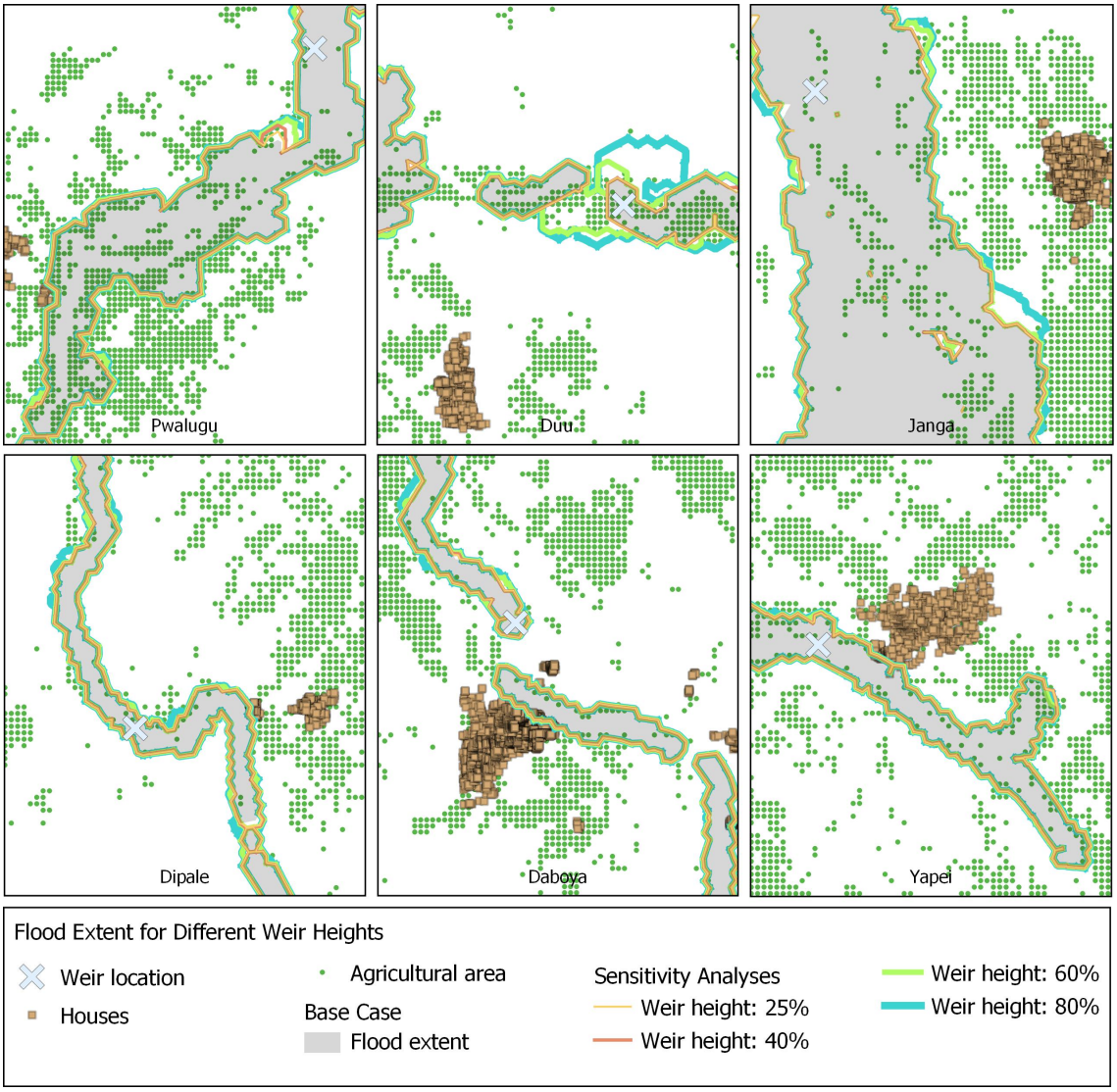

Figure G.1: Sensitivity analyses of Pwalugu, Duu, Janga, Dipale, Daboya and Yapei, for increasing crest heights.

G.2. Final Dam Designs for Each Flood-Prone Area

In this appendix the dam dimensions of each of the seven dams are shown.

	pwalugu	**duu**	**janga**	**dipale**	**nawuni**	**daboya**	**yapei**
upstream1Width	38.18	46.79	72.01	83.28	119.65	99.89	97.83
upstream1Level	126.21	117.59	100.52	95.97	91.97	82.93	72.84
crestWidth	38.18	46.79	72.01	83.28	119.65	99.89	97.83
crestLevel	126.46	117.84	100.77	96.22	92.22	83.18	73.09
crestLength	3	3	3	3	3	3	3
downstream1Width	38.18	46.79	72.01	83.28	119.65	99.89	97.83
downstream1Level	126.21	117.59	100.52	95.97	91.97	82.93	72.84
gateLowerEdgeLevel	126.46	117.84	100.77	96.22	92.22	83.18	73.09
gateHeight	2.23	2.30	2.13	2.05	2.00	1.80	2.59
gateOpeningWidth	0	0	0	0	0	0	0

Table G.1: Structure dimensions

H

Prices of Crops in Ghana

			Wholesale Prices (GH¢)							Average		
Commodity	Unit	Weight	Accra	Bawku	Dambai	Kumasi	Takoradi	Tamale	Techiman	This month	Last month	% Change
Cassava (Fresh Tubers)	Bag	91kg	173.00	N/A	65.00	120.00	187.50	147.00	150.00	140.42	141.83	-1.00
Gari	Bag	68kg	257.00	230.00	300.00	145.00	350.00	180.00	265.50	246.79	231.57	6.57
Cowpea (White)	Bag	109kg	480.00	444.00	480.00	512.00	460.00	549.00	352.40	468.20	477.14	-1.87
Groundnut (shelled)	Bag	82kg	590.00	592.40	480.00	590.00	600.00	422.00	417.00	527.34	544.43	-3.14
Maize (white, grain)	Bag	100kg	170.00	118.20	200.00	145.00	180.00	140.00	126.00	154.17	153.86	0.20
Millet (grain)	Bag	93kg	300.00	230.00	370.00	250.00	349.00	340.00	340.00	311.29	263.71	18.04
Rice (imported)	Bag	50kg	380.00	N/A	N/A	480.00	359.00	N/A	384.00	400.75	412.75	-2.91
Rice (local-white)	Bag	100kg	363.00	430.00	500.00	330.00	290.00	404.00	395.00	387.43	375.14	3.27
Soya Beans	Bag	109kg	325.00	230.00	340.00	230.00	381.00	351.00	337.00	313.43	294.57	6.40
Tomato (cooking)	Crate	72kg	358.00	N/A	263.00	150.00	380.00	278.50	333.00	293.75	348.17	-15.63
Wheat (Grain)	Bag	50kg	400.00	N/A	N/A	210.00	300.00	257.00	260.00	285.40	285.60	-0.07
Yam (pona-medium)	100 tubers	250kg	1050.00	N/A	565.00	800.00	972.00	809.00	529.00	787.50	742.83	6.01

Figure H.1: Maize prices in different cities of Ghana.

Flood damage

Figure I.1 shows the depth-damage curves of stone houses and self-made houses that were used in order to calculate the percentage of value decrease as a result of the floods for the self-made houses and for the stone houses.

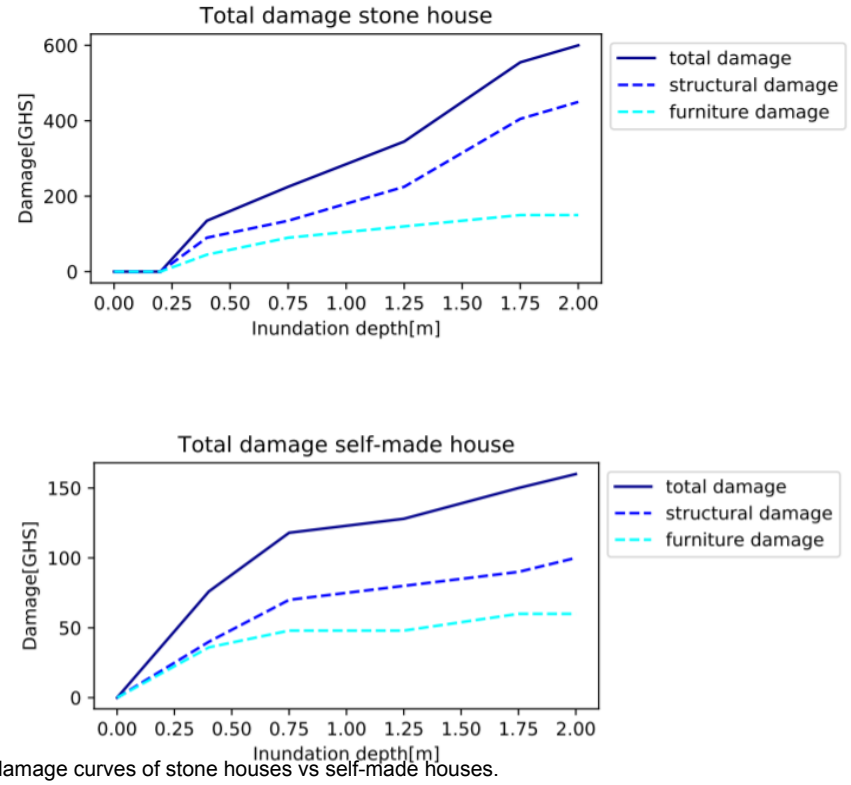

Figure I.1: Depth damage curves of stone houses vs self-made houses.

To determine whether a village has self-made or stone houses, Google satellite images were used and estimation was made of the ratio between the two types of houses. Figure I.2 shows these satellite images. It was assumed that the larger, U-shaped white houses are made of stone and that the smaller, often round and brown buildings are the safe made houses.

Figure I.2: Houses

Table I.1 shows the local prices of building materials and contractors needed to build a house in Ghana.

		Concrete House Small 1 level	Concrete House Small 2 levels	Concrete House Medium 2 levels	Concrete House Large 2 levels	Steel House Small 1 level	Wooden House small 1 level
Volume Concrete Slaps	**Quantity**	19,5	39	66	207	-	-
	Unit price (USD)	153,00	153,00	153,00	153,00	-	-
	Total amount (USD)	2983.50	5967.00	10.098,00	31.671,00	-	-
Steel for concrete Slaps	**Quantity**	2143,05	4,28	7,25	22,74	-	-
	Unit price (USD)	1100,00	1100,00	1100,00	1100,00	-	-
	Total amount (USD)	2357,36	4714,71	7978,74	25.024,23	-	-
Formwork Slaps	**Quantity**	120	271	419	963	-	145
	Unit price (USD)	12	12	12	12	-	12
	Total amount (USD)	1440,00	3252,00	5028,00	11.556,00	-	1740,00
Contractors / workforce	**Quantity**	90	180	300	600	-	-
	Unit price (USD)	5	5	5	5	-	-
	Total amount (USD)	450	900	1500	3000	-	-
Roof	**Quantity**	25	25	50	225	170	25
	Unit price (USD)	6,2	6,2	6,2	6,2	6,2	6,2
	Total amount (USD)	155	155	310	1395	1054	155

Table I.1: Prices for construction materials in Ghana

From I.1, in combination with the mean house sizes observed near the White Volta river, the total prices of a house were determined. Table I.2 shows the total costs of constructing each type of house.

From field visits by Jasper Schakel, is was assumed that the villages near the White Volta river mainly consists of the first and the last type of houses. Therefore, in these types are the ones on which the flood damage was based.

	Concrete House Small 1 level	**Concrete House Small 2 levels**	**Concrete House Medium 2 levels**	**Concrete House Large 2 levels**	**Steel House Small 1 level**	**Wooden House small 1 level**
Width [m]	5	5	10	15	5	5
Length [m]	5	5	5	15	5	5
Height 1 level [m]	3	3	3	3	3	3
Thickness wall [m]	0.2	0.2	0.2	0.2	-	-
Thickness floor level [m]	0.3	0.3	0.3	0.3	-	-
surface [m²]	40	40	150	300	30	30
Levels	1	2	2	2	1	1
Price [dollars]	8711	17.726	43.168	86.336	1116	1986
Price [GHC]	52.703	107.246	261.167	522.334	6751	12.015

Table I.2: Prices of six types of houses

J

Flood risk maps

In this section, the flood maps will be shown for each village, first for the base case and then also for the case in which the dams are implemented.

J.1. Flood Risk Before and After Implementing the Dams

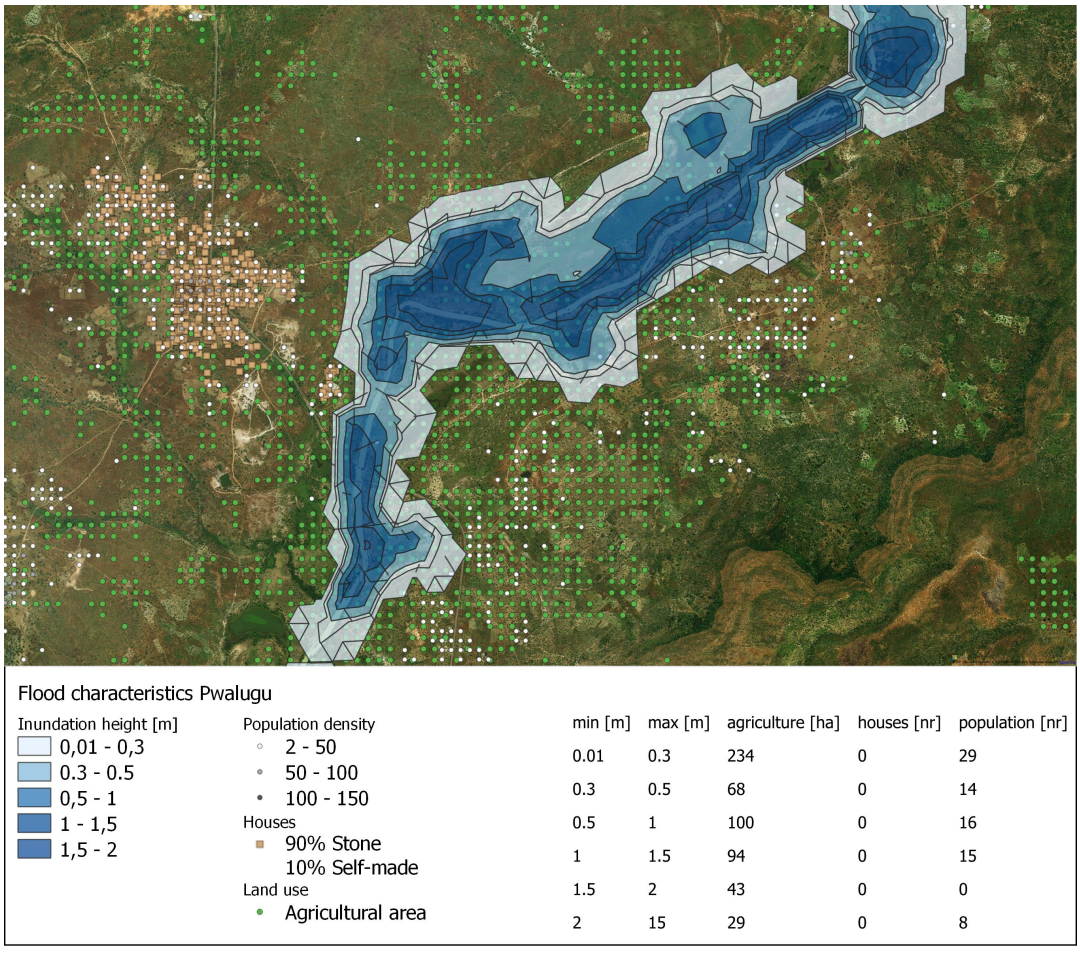

Figure J.1: The flood map of Pwalugu simulated by the base case.

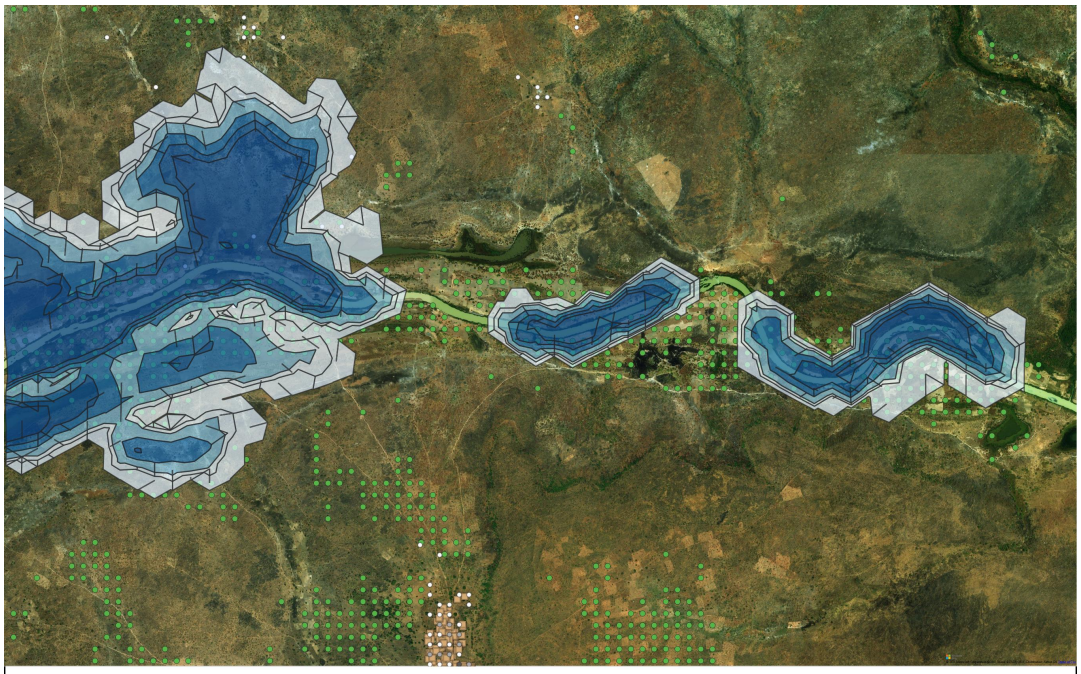

Flood characteristics Duu

Inundation height [m]
- 0,01 - 0,3
- 0.3 - 0.5
- 0,5 - 1
- 1 - 1,5
- 1,5 - 2

Population density
- 2 - 50
- 50 - 100
- 100 - 150

Houses
- 80% Stone
- 20% Self-made

Land use
- Agricultural area

min [m]	max [m]	agriculture [ha]	houses [nr]	population [nr]
0.01	0.3	83	0	18
0.3	0.5	43	0	3
0.5	1	103	0	0
1	1.5	88	0	0
1.5	2	43	0	0
2	15	106	0	9

Figure J.2: The flood map of Duu simulated by the base case.

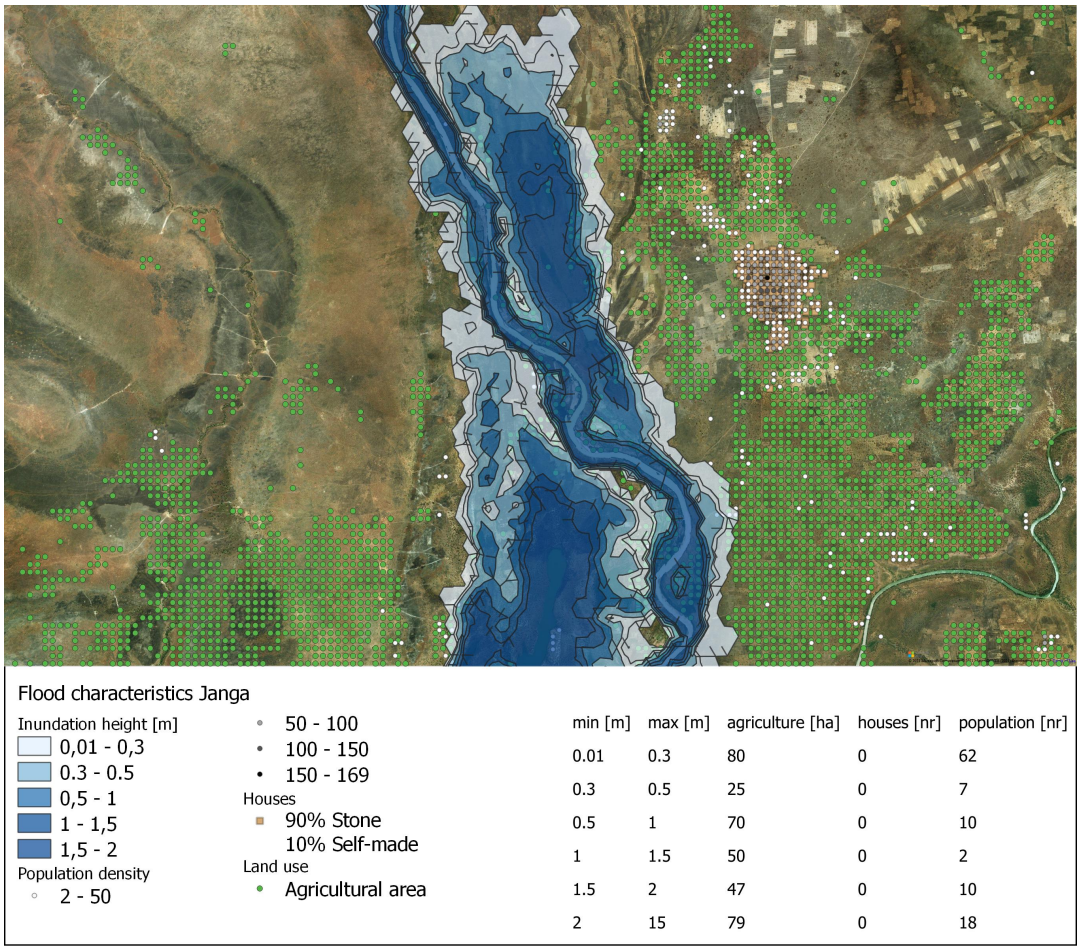

min [m]	max [m]	agriculture [ha]	houses [nr]	population [nr]
0.01	0.3	80	0	62
0.3	0.5	25	0	7
0.5	1	70	0	10
1	1.5	50	0	2
1.5	2	47	0	10
2	15	79	0	18

Figure J.3: The flood map of Janga simulated by the base case.

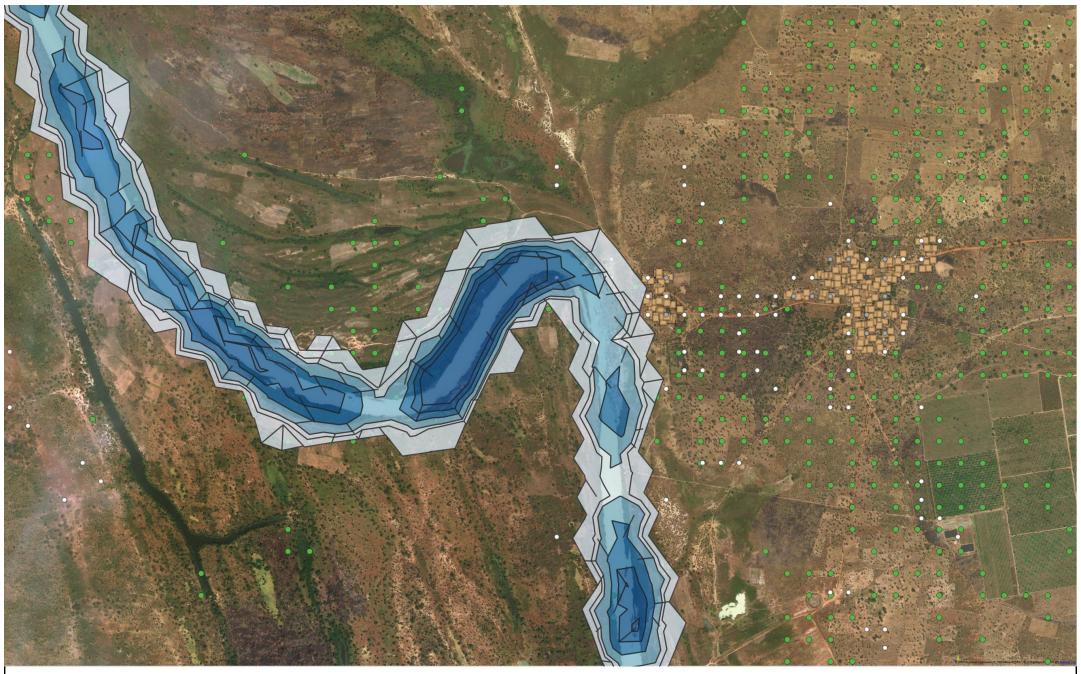

min [m]	max [m]	agriculture [ha]	houses [nr]	population [nr]
0.01	0.3	24	0	19
0.3	0.5	2	0	6
0.5	1	5	0	2
1	1.5	7	0	0
1.5	2	0	0	3
2	15	0	0	0

Figure J.4: The flood map of Dipale simulated by the base case.

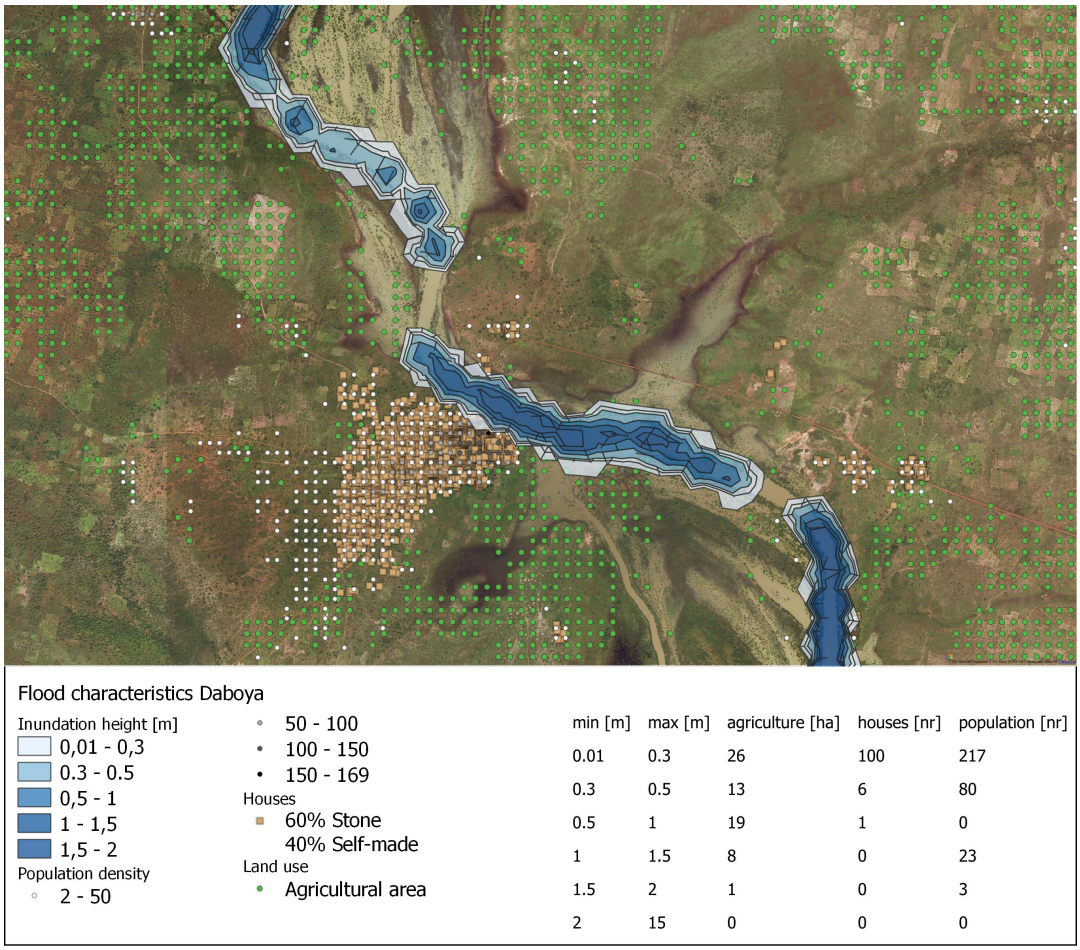

min [m]	max [m]	agriculture [ha]	houses [nr]	population [nr]
0.01	0.3	26	100	217
0.3	0.5	13	6	80
0.5	1	19	1	0
1	1.5	8	0	23
1.5	2	1	0	3
2	15	0	0	0

Figure J.5: The flood map of Daboya simulated by the base case.

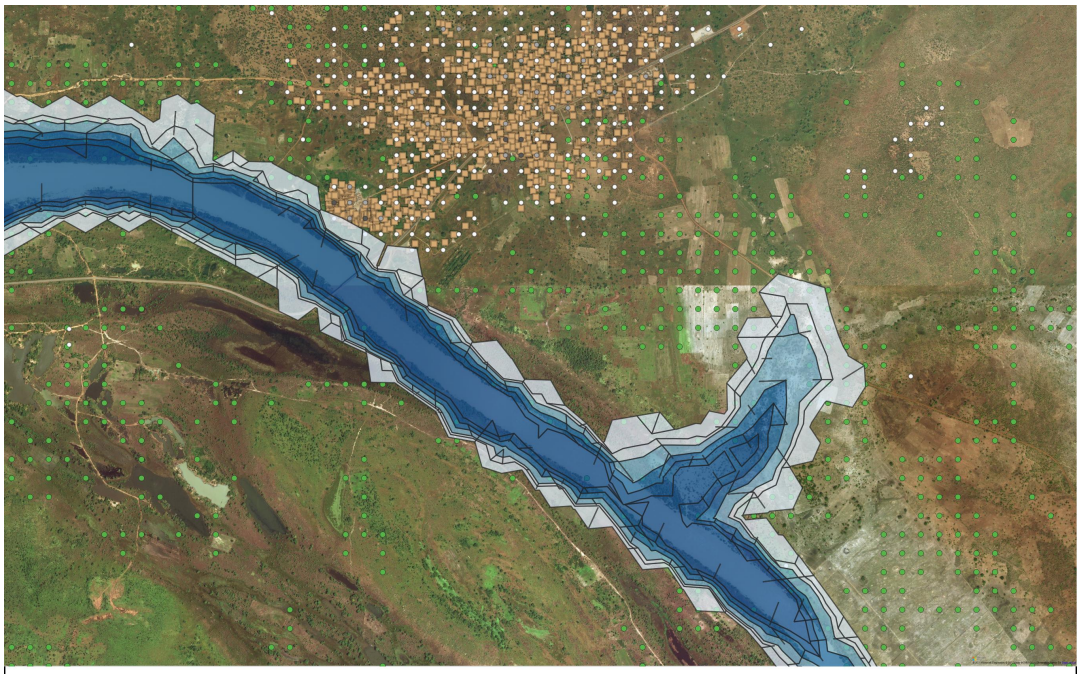

Flood characteristics Yapei

Inundation height [m]
- 0,01 - 0,3
- 0.3 - 0.5
- 0,5 - 1
- 1 - 1,5
- 1,5 - 2

Population density
- 2 - 50
- 50 - 100
- 100 - 150

Houses
- 90% Stone
- 10% Self-made

Land use
- Agricultural area

min [m]	max [m]	agriculture [ha]	houses [nr]	population [nr]
0.01	0.3	55	8	56
0.3	0.5	16	1	9
0.5	1	28	0	4
1	1.5	20	0	2
1.5	2	13	0	0
2	15	13	0	0

Figure J.6: The flood map of Yapei simulated by the base case.

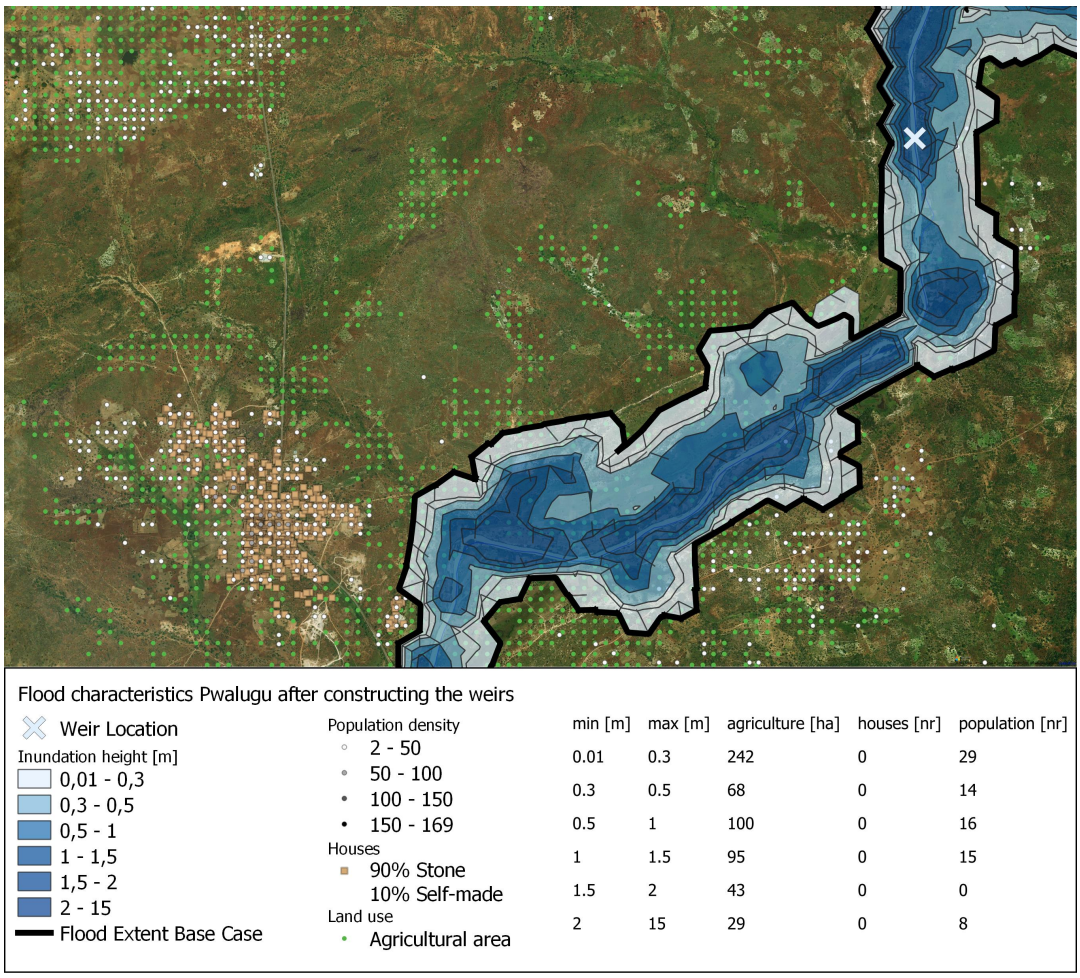

min [m]	max [m]	agriculture [ha]	houses [nr]	population [nr]
0.01	0.3	242	0	29
0.3	0.5	68	0	14
0.5	1	100	0	16
1	1.5	95	0	15
1.5	2	43	0	0
2	15	29	0	8

Figure J.7: The flood map of Pwalugu after Implementing the Dams.

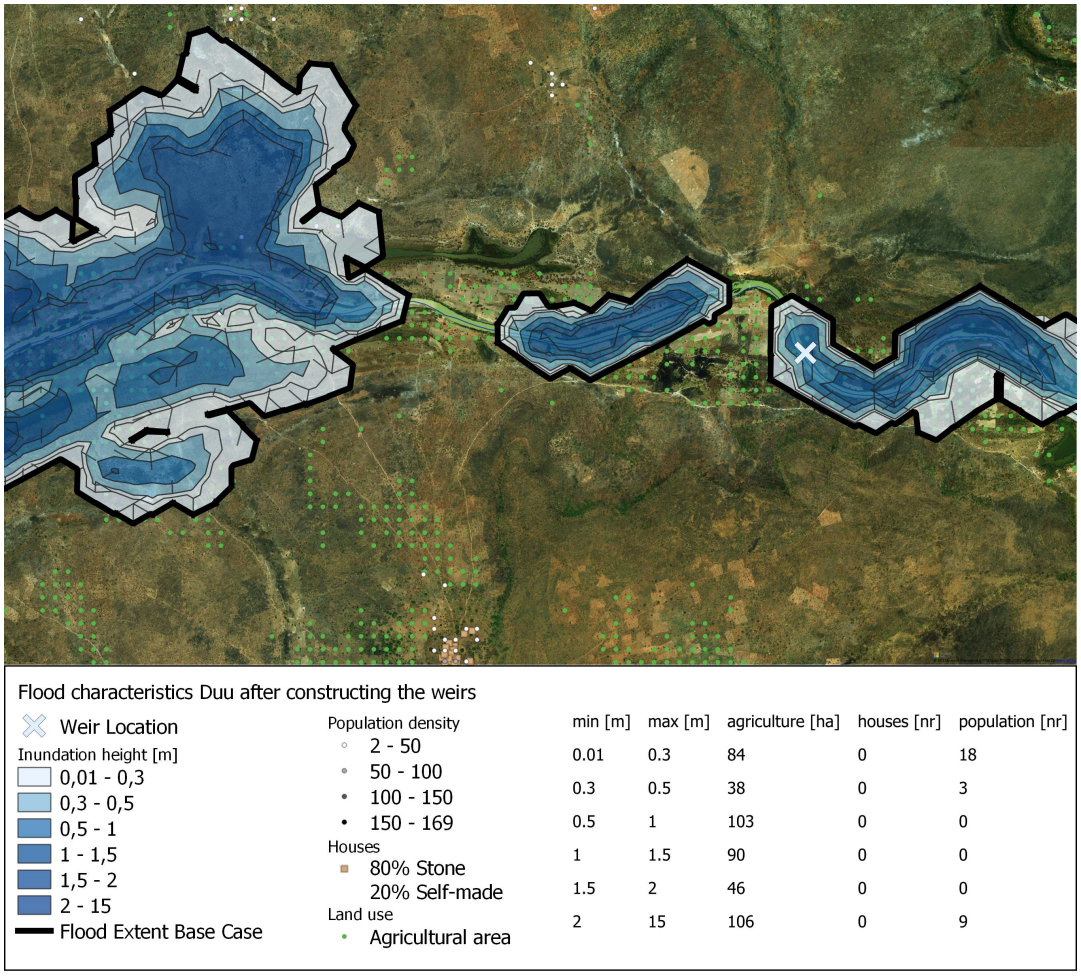

Figure J.8: The flood map of Duu after Implementing the Dams.

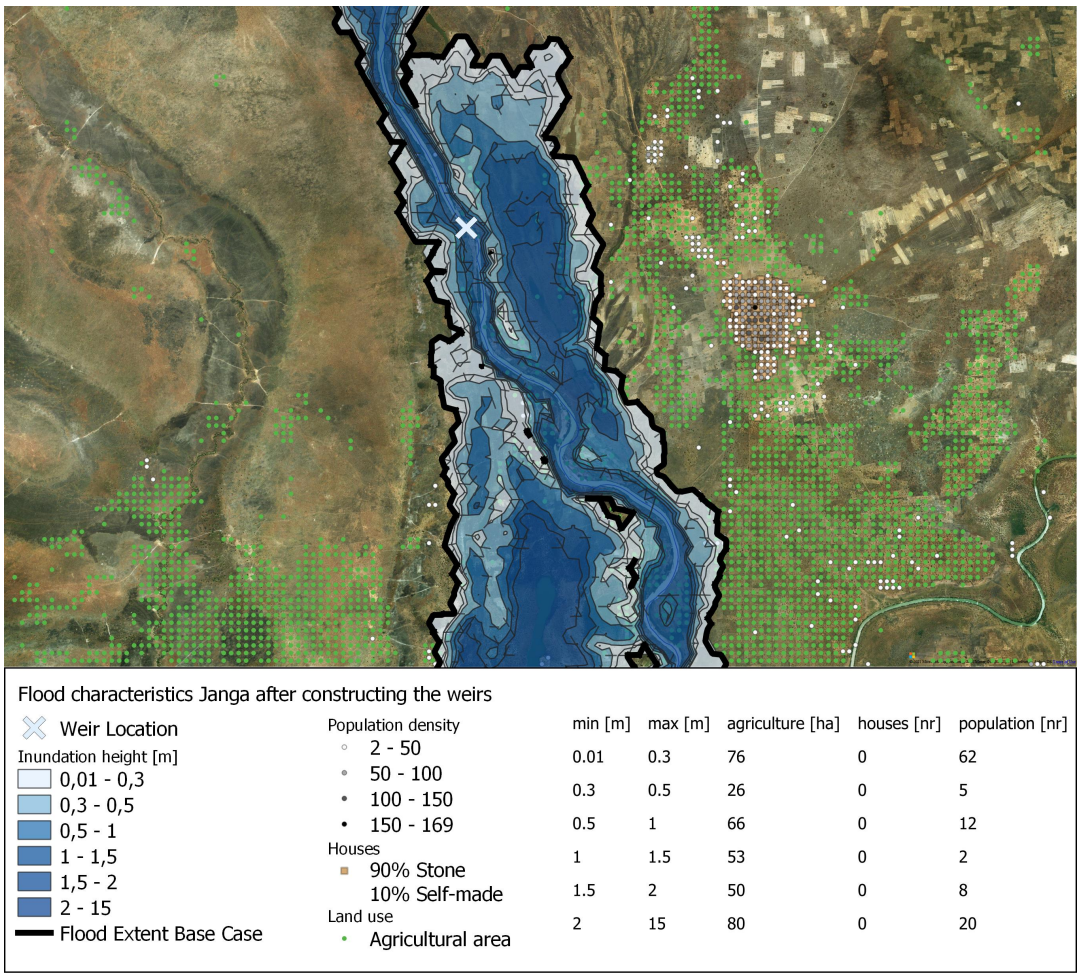

min [m]	max [m]	agriculture [ha]	houses [nr]	population [nr]
0.01	0.3	76	0	62
0.3	0.5	26	0	5
0.5	1	66	0	12
1	1.5	53	0	2
1.5	2	50	0	8
2	15	80	0	20

Figure J.9: The flood map of Janga after Implementing the Dams.

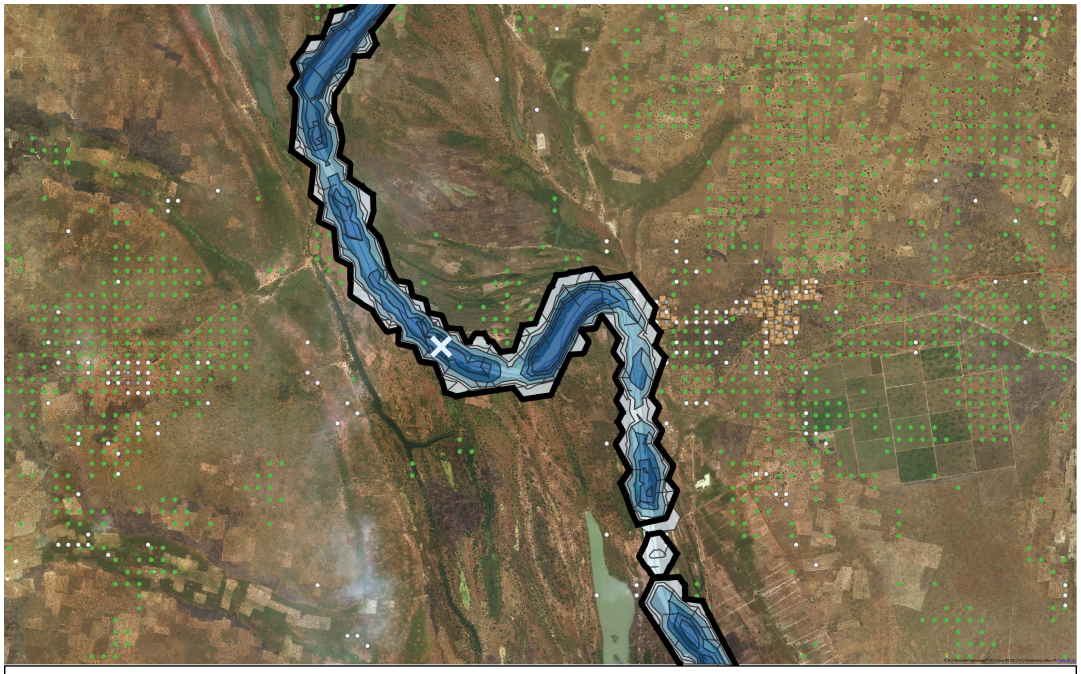

min [m]	max [m]	agriculture [ha]	houses [nr]	population [nr]
0.01	0.3	24	0	19
0.3	0.5	2.4	0	6
0.5	1	4.8	0	2
1	1.5	7	0	0
1.5	2	0	0	3
2	15	0	0	0

Figure J.10: The flood map of Dipale after Implementing the Dams.

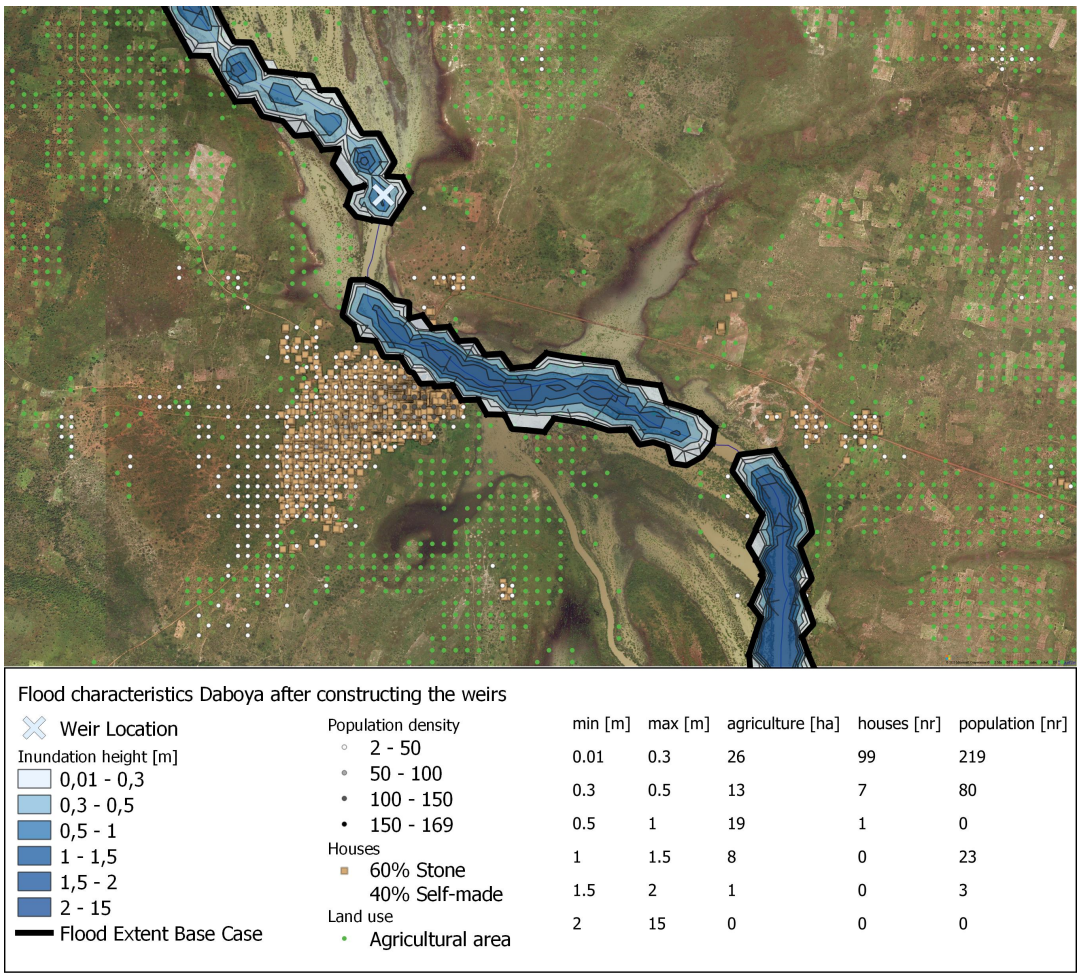

min [m]	max [m]	agriculture [ha]	houses [nr]	population [nr]
0.01	0.3	26	99	219
0.3	0.5	13	7	80
0.5	1	19	1	0
1	1.5	8	0	23
1.5	2	1	0	3
2	15	0	0	0

Figure J.11: The flood map of Daboya after Implementing the Dams.

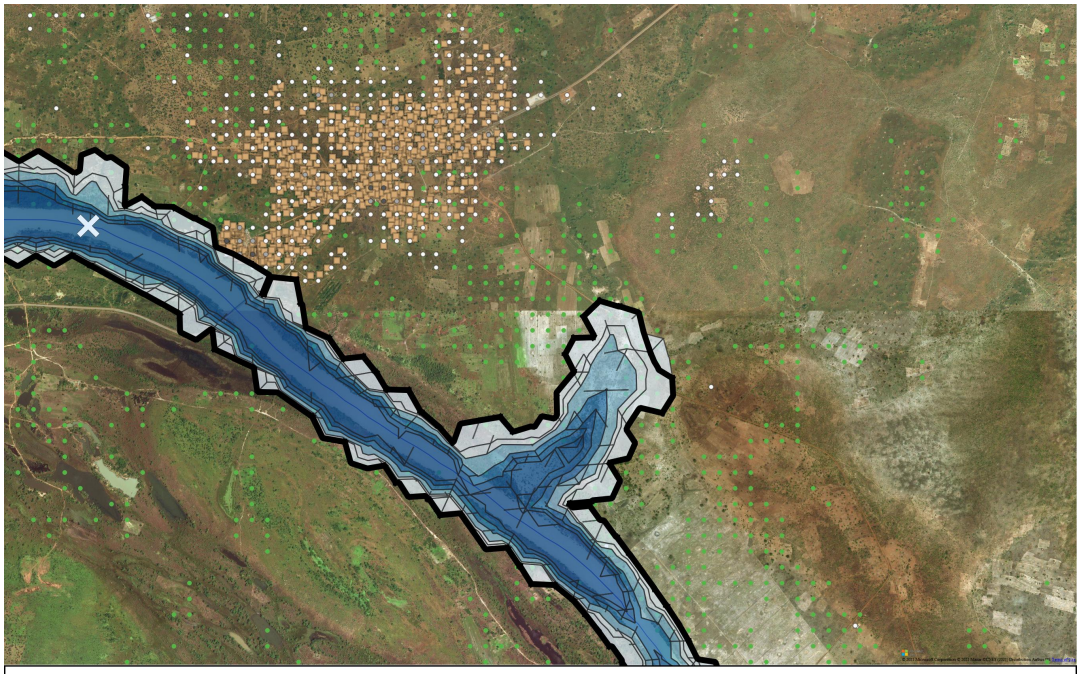

min [m]	max [m]	agriculture [ha]	houses [nr]	population [nr]
0.01	0.3	55	8	56
0.3	0.5	19	1	7
0.5	1	29	0	5
1	1.5	16	0	2
1.5	2	16	0	0
2	15	16	0	0

Figure J.12: The flood map of Yapei after Implementing the Dams.

K

Sedimentation by the Tributaries

Figure K.1 shows the ratios of water levels in the case that tributaries are included, compared to the base case. In the bottom figure, the ratios of these discharge at every location in the river is calculated. These ratios are used as a multiplier for the calculation of the sedimentation amount.

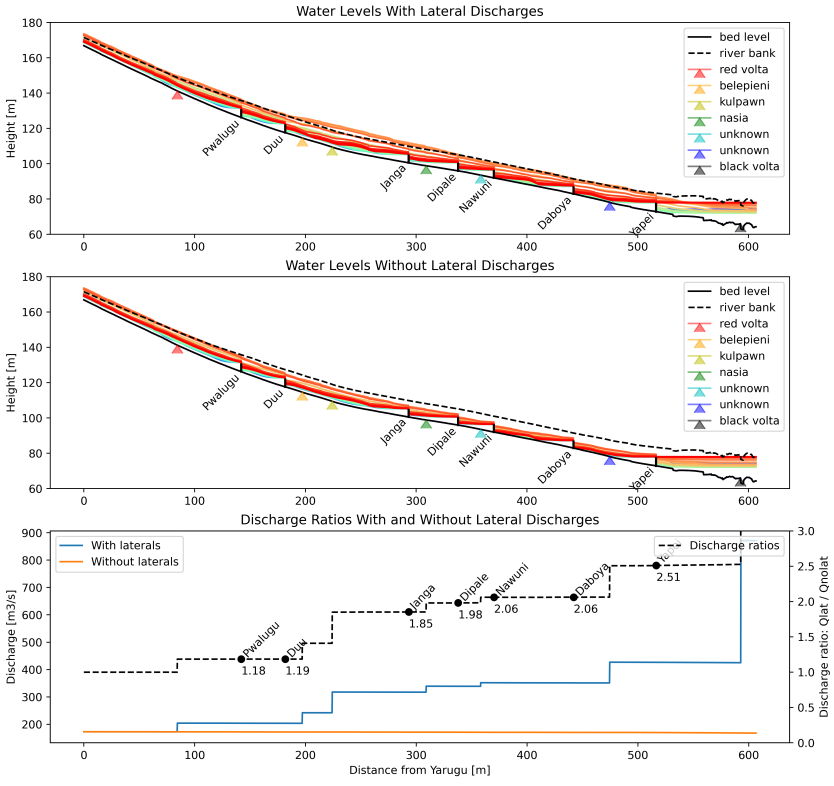

Figure K.1: Erosion and sedimentation as a result of the dams.